MASTER

Room in room acoustics

the influence of direct and diffuse sound fields in recording rooms on the perceived acoustics in listening rooms

Reijnders, W.B.

Award date:
2018

ROOM IN ROOM ACOUSTICS

The influence of direct and diffuse sound fields in recording rooms

on the perceived acoustics in listening rooms

Wouter Reijnders

Room in room acoustics
The influence of direct and diffuse sound fields in recording rooms
on the perceived acoustics in listening rooms

Master Thesis

Wouter Reijnders

Supervisors:
ir. C.C.J.M. Hak
dr. ir. M.C.J. Hornikx
ir. R.H.C. Wenmaekers

Paris, October 2017

Abstract

Over the last ten years, research performed on room in room acoustics has been done at the Eindhoven University of Technology. Room in room acoustics is the study of the effects of room acoustics on the intended (perceived) acoustics of reproduced sound. The effects occur most notably when a recording made in a reverberant environment is reproduced in a similar environment, the case where the playback environment is more reverberant is not taken into account. This follows after conclusions in the literature that a sound field can only be reproduced in a less reverberant environment.

The primary focus of earlier publications and reports is on effects the reproduction has on signals recorded under diffuse field conditions. Little is known when the recorded signal is measured with a certain amount of direct sound. The most notable literature conclusions are that the effects of room in room acoustics can be decreased with two methods. The first is decreasing the reverberation time in the listening room; the second is increasing the direct sound level in the listening room.

The study presented in this thesis aims to give insight on the combined effects of direct sound levels and diffuse sound fields in both recording room and listening room. Specifically, room acoustical parameter deviations were investigated. An analytical presentation of the impulse response is proposed to find these deviations. An extensive set of measurements was conducted to successfully validate the model (within bounds of its application). With this analytical impulse response, acoustical parameters and their deviations as a result of the room in room acoustics scenario are collected.

By convolving two room impulse responses a room in room impulse response is created. The two impulse responses used to create this response represent the recording and listening room. Contrary to the literature, measurements indicate that calculating reverberation time from the room in room impulse response can be done equally accurate as from a single room impulse response. This conclusion is reached after comparing the Curvature Parameter[1] of room in room impulse responses with single room impulse responses.

Parameters calculated from the analytical model show that reproducing reverberation times within an accuracy of the just noticeable difference can be done when the reverberation time in the listening room is 1.2 times lower than that in the recording room. The Initial Drop[2] in the room in room scenario was found to be an energetic subtraction of the initial drop in the recording and listening room. This drop can never be larger than the lower of the two involved initial drops. Because the direct sound level indicated by the Initial Drop is an energetic subtraction, reproduction within 1 dB accuracy is achieved when the Initial Drop in the listening room is at least 6 dB higher than in the recording room.

Furthermore, it is shown that reproduction of the Reverberation Time is primarily dependent on the ratio of the reverberation times in listening and recording rooms. For Clarity, the deviations are primarily depending on the difference of direct sound levels, with the little notion that for higher C_{80} the deviations are also higher. Centre time deviations are found to be depending on both the reverberation time ratio and difference of direct sound level.

---

[1] The curvature parameter can be found in the ISO-3382-2:2008(E) Annex B and is a measure for the curvature of the energy decay curve based on the ratio between T_{20} and T_{30} see section 4.3.4

[2] The initial drop is an indication for the strength of the direct sound field, and will be further explained throughout the thesis and specifically in section 4.3.3

Acknowledgements

I came to the Eindhoven University of Technology four years ago. I found myself struggling and faced with a challenge to which there was no easy way through. It was probably the first time that had happened to me. Initially, I came to Eindhoven to learn about acoustics and so that is what I did. Here I would like to thank those that have actively or passively contributed to my study.

First I would like to thank the people that have helped me develop in the acoustic field, my supervisor for this thesis and a driving inspiration Constant Hak. I would also like to thank Maarten Hornikx for sharing his knowledge and input in the project. Then I would like to thank Remy Wenmaekers and Raúl Pagán Muñoz for their contribution to my development. Special thanks go out to Wouter Wittebol for discussions on the contents of this research and Dennis Pennings for proofreading. I owe some gratitude to the people working in the laboratory of acoustics and from level acoustics for their hospitality and a place to work and not in the last place the enormous amount of cups of coffee I consumed.

Next, to studying acoustics, I have also been the chairman of the study association Mollier, while this did not always mean good news for my study, I managed to learn a many things and meet many people. Especially, I wish to thank my fellow board members for the amazing year we had.

Thank you to my family and friends who have supported me from the beginning to the end. And finally, I would love to express my gratitude for Clémence Valade for mental support and proofreading this thesis.

Wouter Reijnders
Paris 2017

Table of contents

List of symbols

A	Equivalent absorption area	[m²]
c	Speed of sound in air	[m/s]
C	Curvature parameter	[%]
C_{80}	Clarity	[dB]
D_{50}	Definition	[-]
DI	Directivity index	[dB]
ETC	Energy time curve	[dB]
f	Frequency	[Hz]
f_s	Sampling frequency	[Hz]
f_S	Schroeder frequency	[Hz]
ID	Initial drop	[dB]
ID_1	Initial drop in the recording room	[dB]
ID_2	Initial drop in the listening room	[dB]
$ID_{c;d}$	Diffuse field compensation for the initial drop	[dB]
INR	Impulse response to noise ratio	[dB]
j	Imaginary unit	[-]
P	Parameter	[-]
P_x	Source power	[W]
p	Sound pressure	[Pa]
p_b	Backwards integrated sound pressure	[-]
Q	Directivity factor	[-]
r	Source-receiver distance	[m]
r_c	Critical distance	[m]
T *[3]	Reverberation time	[s]
T_1	Reverberation time in the recording room	[s]
T_2	Reverberation time in the listening room	[s]
T_{20}	reverberation time with an evaluation range between -5 dB and -25 dB on the decay curve	[s]
T_{30}	reverberation time with an evaluation range between -5 dB and -35 dB on the decay curve	[s]
RV	Random variable	[-]
S	Schroeder decay curve	[dB]
t	Time	[s]
T_s	Centre time	[ms]
V	Volume	[m³]
w	Sound energy density	[J/m³]
wgn	White Gaussian noise	[-]
ϑ	Start point	[s]
$\delta(t)$	Dirac delta function	[-]
δ	Decay constant	[-]
a	Decay constant	[-]
x	Decay term reverberant field 3*ln(10)/T	[1/s]
θ	Angle of incidence	[°]

---

[3] T refers to the parameter for reverberation time, in the text RT is used as abbreviation of reverberation time as a decay process.

μ	Mean	[-]
σ	Standard deviation	[-]
τ	Time window	[s]
ω	Angular frequency	[Hz]
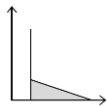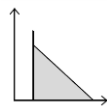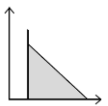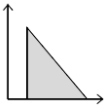
1 Introduction

Every recording in a room contains influences the room has on the sound. This is a result of the acoustics of the room, the source characteristics and the receiver characteristics (e.g. placement and directivity) in this room. If this recording is then played back in another room the acoustics of this second room will again have an influence, this process is called room in room (RinR) acoustics.

RinR acoustics happens when reproducing a recording, one can imagine this in the broadest sense. For every played back recording, given that the recording is played back in a reverberant room, RinR acoustics is relevant. For example acoustic demonstration, concert registration or sound in movies.

As a result of sound production, there will be a sound field. A sound field is the distribution of sound in any given environment. It can be described by a direct proportion and a diffuse proportion. In the direct proportion the sound characteristics of the source are dominant, and in the diffuse proportion, the influence of the room is dominant. In table 1.1 shows examples of room in room acoustics depending on the sound fields of the listening and recording rooms. The indication direct/diffuse means that neither proportion is dominant.

Table 1.1 *Overview of room in room acoustic occurrences*

		Listening room		
		Direct*	**Direct/diffuse**	**Diffuse***
Recording room	**Direct***	Phone call	Acoustic demonstration in an auditorium listened to close to the source	Pop/rock concert playback in a movie theatre
	Direct / diffuse	Live recording in a chamber music hall with an overhead microphone, listened to with headphones	Church recording played back in a church (when the preacher speaks)	Documentary including speech in cave systems listened to in the cinema
	Diffuse*	Auralisation of outdoor sound with many reflections (canyons, caves)	Church recording played back in a church (when the people sing)	Lecturer demonstrating the difference between two concert halls in a large auditorium

Direct holds that the position is within the reverberant radius, diffuse holds that the position is outside the reverberant radius

To quantify the effects of RinR acoustics a comparison is made between the recording room and the RinR scenario using room acoustical parameters. The parameters in the recording room can be obtained by calculations on the impulse response (IR_{rec}). The parameters from the RinR are

obtained from the room in room impulse response (IR_{RinR}). The IR_{RinR} is fundamentally different from the IR [1], [2], most notably for the decay curve not being exponential.

To compare the room acoustics the deviations of the parameters can then be calculated. To collect data for the determination of these deviations; measurements were performed at the acoustic laboratory of the Eindhoven University of Technology (Echo building).

The next step is finding causes to explain the deviation. In studies by Hill [1]; Hak and Wenmaekers [2], [3]; Haeussler, Grosse and Van de Par [4], [5]; Svensson and Zidan [6], it is found that with decreasing reverberation time (RT) the deviation between the acoustics in the recording room and the perceived acoustics in the listening room decrease. A similar trend is found with increased direct sound level [7], [8]. The study from Hak and Wenmaekers [7] proposes a parameter to describe the direct field based on the first 'drop' in the Schroeder decay curve[4] as a scale to express parameter deviation; this parameter is called the initial drop (ID).

1.1 Problem statement

The reduction of parameter deviation for decreasing the reverberation time in the listening room is well described in the literature. Missing, however, is a method of determining the reverberation time for an IR_{RinR}. This is caused because decay curves in the RinR scenario are said to have a concave shape[5]. ISO-3382-2:2008(E) Annex B [9] describes the evaluation of nonlinear (non-exponential) decay curves. However, in this annex only convex shaped decay curves are noted.

The ID is a relatively new parameter, the calculation method used is still coarse since the level difference over the first 50 ms of the Schroeder curve is used [7]. This parameter appears to be a good indication of the direct sound level and can be used to express deviations as a result of room in room. A better, robust definition has to be found for the ID. In the studies that use the ID as a scale for parameter deviations, the value in the listening room is given. The deviations in the diffuse field are expressed on a scale of reverberation ratio. Using only the ID in the listening room results in different threshold values for the deviation when different recordings are used.

Besides this definition, there is also need for a better predictive model linking the reverberant to the direct field in predicting parameter deviations, for both the recording room and the listening room.

1.2 Research question

In this report, the relation between the influence of the direct field and the reverberant field within the room in room acoustics scenario is sought. The central research question is:

> *"What is the influence of direct and diffuse sound fields in recording rooms on the perceived acoustics in listening rooms?"*

The interpretation of the question is as follows. Given two IRs, one measured at a recording position, and one measured at a listening position, can it be predicted what the deviation will be if the recording is played at the listening position?

---

[4] The Schroeder decay curve is representative of the ensemble average of the energy decay, obtained after backwards integration of the squared impulse response

[5] In the discussion section 7.2 discusses that this is not always the case

A study was started in October 2016 to answer this question. The steps are given in figure 1.1. Starting with a literature review, and the analysis of pre-existing measurement sets used in earlier stages of the research. From this analysis, an experiment for the laboratory was designed. The goal of the measurement is to provide data to validate an analytical model that can be used to explain deviations for RinR scenarios. The analytical model is used to produce results for a numerical study. At last, the conclusions are drawn from the analysis of the numerical study.

The research is part of a broader research aiming to create a relatively complete yet straightforward method of determining the acoustical quality of a (listening)room. The work in this report describes an essential bridge between the two most important principles that reduce deviations as a result of room in room. These are reducing the reverberation time in the listening room or increasing the direct sound level in the listening room.

1.3 Applied methods

The study includes an extensive measurement, in which two sources are placed in 5 absorptive scenarios. For each scenario 16 different source-receiver distances are measured. This is done to validate the numerical results from an analytical model. The model is set up in Matlab and should be able to give insight to deviation as caused by specific parameters. These parameters have to be derivable from the IR.
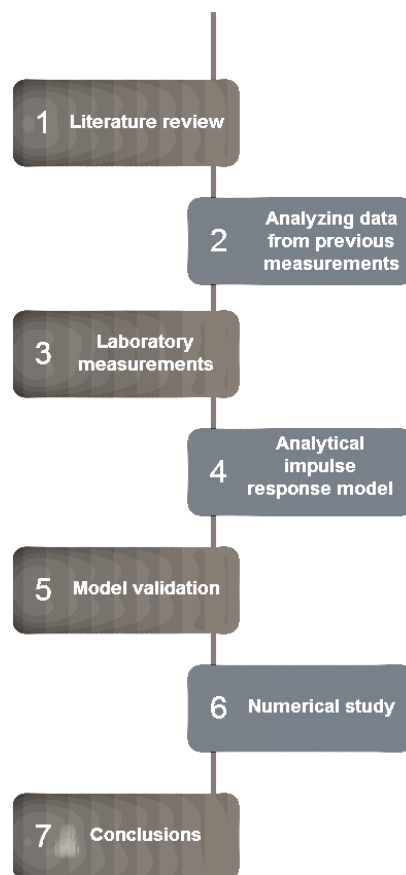
Figure 1.1 steps taken in the research

1.4 Thesis structure

The literature study is spread over chapters 2 and 3; chapter 2 focusses to a greater extent on results and papers published on the subject. Chapter 3 gives an overview of the used analytical IR models in the RinR studies, alongside the theory about the IR. Chapter 4 is about the measurements performed in the laboratory. Chapters 5 and 6 describe the model that is proposed to use in this study, where in Chapter 5 the proposed model is presented and in chapter 6 the validation is discussed. Chapter 7 gives the results following the model and compares these to the measurements. The conclusions are reported in chapter 8. After chapter 8 the reference list and appendices are added. The appendices contain information on the derivation of an analytical impulse response equation, Matlab scripts and list results from the measurements.

2 Literature

This chapter summarises the publications on room in room acoustics research, starting with the history and different research areas, followed by the reported consequences in the temporal and frequency domains. The next section gives information about the direct and diffuse parts of an impulse response. Finally, the results for deviation of acoustical parameters as a result of RinR are summarised.

2.1 State of the research

A. Hill's paper on *'Combined Reverberation Time of electrically Coupled Rooms'* dated 1932 [1] is the earliest notion of the study into room in room acoustics. As one might see in the title of the paper by Hill, he calls the phenomenon electrically coupled rooms. Interesting conclusions from his research were: the combined reverberation time of two rooms is longer than the reverberation time in a single room, the magnitude of the difference is dependent on the difference between the RTs in the listening and recording rooms. Figure 2.1 shows the measurement set-up as used by A. Hill.

FIG. 1. *Arrangement of equipment for measurement of electrically coupled rooms.*
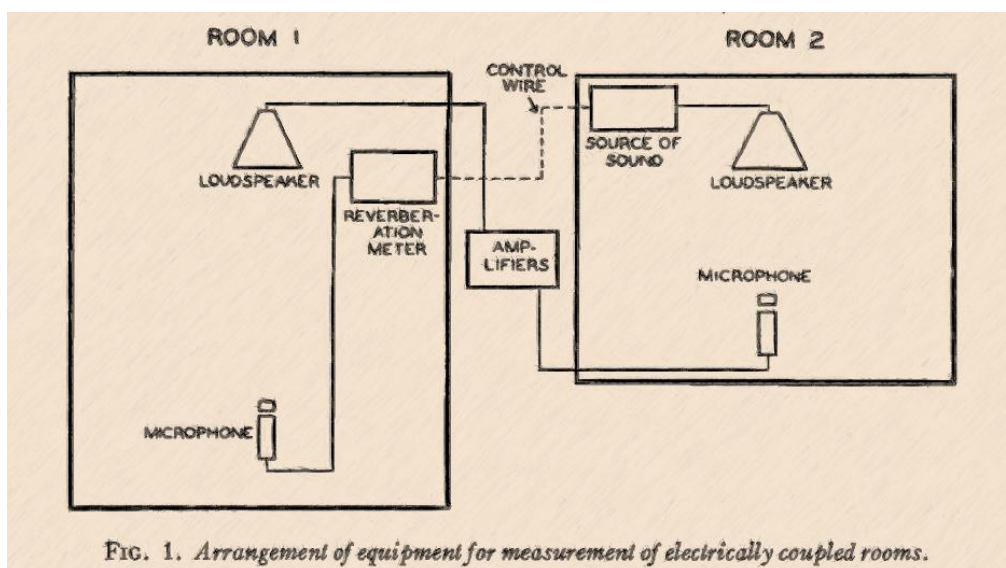
Figure 2.1 *the measurement set-up used by A. Hill in 1932 [1]*

Presently, several research groups are working on similar subjects, the study in this report is a part of the research done at the Eindhoven University of Technology (the Netherlands). The research revolves around the deviation between parameters calculated from the room in room impulse responses (IR_{RinR}) and parameters calculated from single room IRs. To find these deviations, measurements were performed in 11 rooms that are selected to have a broad range of reverberation times (ranging between 0.2s and 5.3s). The next step is finding methods to reduce the deviation. Studies show that this can be done by either decreasing the reverberation time in the listening room [2], [10], [11] or increase the direct sound level in the listening room [7], [12], [13].

In Oldenburg (Germany) a research group lead by van de Par is researching room in room acoustics focussed on perception [4], [5], [14], [15]. One publication, in particular, is closely related

to the work in this thesis "Spectral and perceptual properties of a transfer chain of two rooms" by Haeussler and Van de Par. In this paper, it is argued that the standard deviation of the logarithmic magnitude spectrum increases under the influence of room in room acoustics. This increase leads to a noticeable change in the timbre; this is confirmed by a listening test.

In another research, by Grosse and Van de Par, they created a model that reproduces sound (fields) naturally, they call it: "perceptually accurate reproduction of recorded sound fields". By splitting the reproduced signal into an early and a late part (reverb tail), the perceived decay of the played back signal can be altered to match the perceived decay of the playback room. This splitting means that the playback happens over multiple channels. Contrary to [1] and [2], a listening test proved that the perceived decay of the recording room could be similar to the playback room for the same perceptual accuracy [15]. However, if the listening room has a longer reverberation time than the recording room this does not work.

Analytical research on the effect of convolution is done by Svensson and Zidan (Norway) [6], [8], [16]. The goal of the research is to create a model to predict room acoustical parameters in case of an IR_{RinR}. Much like Barrons' revised theory [17] for a single room. In the study to the parameters in connected rooms, they managed to capture trends agreeing with measurements. However, since the model is theoretical, it does not take flutter echoes and other peculiarities into account causing it to lack in accuracy for single source-receiver configurations [8].

2.2 Reported effects of room in room acoustics

The literature reports effects caused by RinR acoustics in the time and frequency domains.

2.2.1 Effects in the time domain

If the reverberation time in the recording room (RT_{rec}) is shorter than the reverberation time in the listening room (RT_{list}), the RT_{rec} is not reproducible in RT_{list} [1]. Another changing property of the IR_{RinR} is the shape of the reverberation tail. Contrary to single room decay curves, which are linear, the IR_{RinR} has a concave decay curve. A consequence is that the different evaluation ranges on the decay curve will result in different reverberation time values, see section 7.2 for a discussion about this.

Because the shape of the decay curve is different, the shape of the IR_{RinR} is different as well. This can be explained by the increase in the number of reflections [8], figure 2.2 shows a cepstrum of an IR_{RinR}. It can be seen that some reflections add up to one reflection with larger amplitude or that reflections in the IR_{RinR} are the result of reflections in one of the two IRs.

The onset of an IR has to be determined to calculate any parameter involving early to late ratios. The ISO 3382 [9] is not evident in its terminology surrounding this subject. The standard states: the starting point of the measured IR should be determined from the broadband IR and defined as the point where the signal level rises significantly above the noise floor but is more than 20 dB below the maximum. Defrance et al. [18] is a letter written to the Acoustical Society of America expressing their concern on the matter. In the letter, they report a dozen automatic onset detection methods and their significant differences, especially in energetic and statistic acoustical indices. Determining the onset for an IR_{RinR} is more complicated because the rise time increases. The rise time is the time between the impulse response onset and the maximum value.
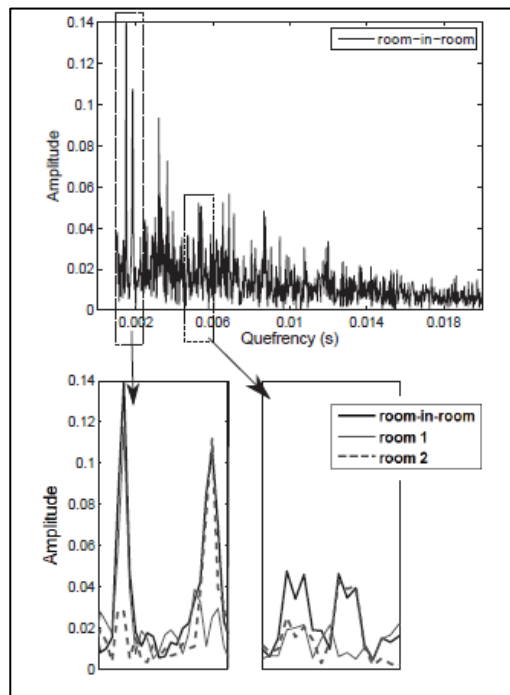
Figure 2.2 *Cepstrum of the IR$_{RinR}$ with enlargements, the figure is taken from [4].*

2.2.2 Effects in the frequency domain

When the IR$_{RinR}$ is compared to the single room IR, an increase in spectral fluctuation strength can be observed. The standard deviation of the logarithmic spectral magnitude increases by a factor of √2 causing perceivable colouration [4].

The modulation transfer function (MTF) is used to determine the speech transmission index (STI) and is closely related to the speech intelligibility [19]. MTF is lower for the IR$_{RinR}$ than for the single IR's [6].

2.3 Impulse response

A room impulse response (IR) is the room's reaction when excited by an impulse. The IR can function as a transfer function. A significant amount of information about a room can be determined by its impulse response. One way to utilise the IR is by auralisation; this is for sound what visualisation is for light. In literature, the IR is divided into three parts [17], direct sound, early reflections and late reflections. The mathematical definition of the IR can be found in chapter 3.

The room IR has many applications in acoustics, for example, an IR can be modified to display the energy distribution, reflection density, and spectral properties of the source, room and receiver [20]. The energy distribution is usually defined in two parts, direct and diffuse. In the direct part, the source characteristics are the dominant feature while in the diffuse part the effects of the room are the dominant feature [21]. The division of the two parts is done by using the reverberation radius, which is defined as the distance from the source where the direct and diffuse fields have equal intensities, e.g. [21], [22]. In the report, the direct part is referred to as direct field, direct sound level or initial drop.

2.4 Impulse response parameter deviations

Specifically studies by Hak and Wenmaekers report about deviations in room acoustical parameters [2], [3], [7], [11]. The deviations are separated between diffuse field conditions and direct field conditions. All reported values are valid for the reproduction of an IR that was measured (or made) under diffuse field conditions.

2.4.1 Diffuse field conditions

It is indicated that to reproduce acoustical parameters a specific ratio of the reverberation time between the recording room and the listening room is needed [2], [3]. Reproduction should be within the just noticeable difference (JND). Deviations reported in this section are valid for scenarios where IR_{rec} and IR_{list} are obtained in a diffuse field.

Hak and Wenmaekers [2] found that RT_{list} should be at least two times shorter than RT_{rec} for reproduction of the reverberation time. The parameter used to reach this conclusion is the T_{20} according to ISO-3382 [9].

RT_{list} should be at least four times shorter than RT_{rec} to reproduce energy modulations [2], the parameter used to reach this conclusion is the Modulation Transfer Index. It is reported that the RT ratio should be at least 10 to reproduce clarity measures, [3], it is thus argued that reproduction of such parameters (i.e. energy ratios) is only possible in a direct sound field.

2.4.2 Direct field conditions

As hinted to before many of the effects of RinR decrease in magnitude when the direct sound level increases, e.g. the reproducibility of centre time improves as the direct sound component increases [11]. Other studies have found similar results, the directivity of the microphones and used loudspeaker set-ups influence the clarity and other energy ratio's [6]. Haeussler & Par found the increase in spectral fluctuation is less present within the reverberation radius [4], i.e. closer to the source.

Several parameters are defined to describe the early to late arriving energy ratio due to the result of room acoustics, for example, definition, clarity, centre time and early and late sound strength. The early-late ratio influences the reverberation time [15], as it is, for a large part, dependent on the late arriving energy. In the research by Hak and Wenmaekers [7] the early arriving energy is studied for its effect in RinR. The parameter used for the indication of the direct sound strength is called the Initial Drop (ID). The ID can be determined from the decay curve. An almost vertical drop indicates the initial drop, see figure 2.3.
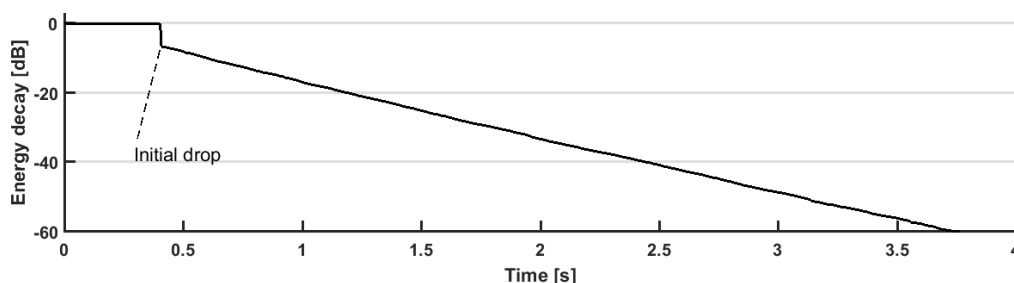
Figure 2.3 *Decay curve within the critical distance at 0.25m from a single source loudspeaker, measured in the reverberation chamber at the Echo building at the Eindhoven University of Technology. The vertical part at the start of the curve is the initial drop.*

Hak and Wenmaekers made a start to quantify threshold values for the direct sound level needed to reproduce parameters [7], [11]. The direct sound level is indicated by the initial drop in the listening room and the reproduction of parameters should be within JND. A series of measurements in large halls and numerical research with synthetic impulse responses lead to the following conclusions.

A minimum ID of 20 dB is needed, to reproduce parameter T_{20}. For the Clarity 15 dB and for the Centre Time an ID of 20 dB is required [7]. These values for ID were found for a scenario where the ratio of reverberation times between the recording and listening room was 1.

It must be noted that the determination of T_{20} and T_{30} when the peak in the IR is 20 dB is not following the ISO 3382 [9] procedure for calculating reverberation time. In this case, the reverberation time is (re)produced within the peak, in other words: the evaluation decay range 'fits' entirely in the peak. The peak is uninfluenced by the room and therefore is an almost 'perfect reproduction', see section 7.3 and figure 7.8 for more about this.

2.4.3   Initial Drop as scale to express parameter deviations

Master projects at the TU/e within the Room in Room acoustics study reached different conclusions with respect to ID threshold values in the listening room. After comparison of the conclusions in [12], [13] it became clear that only a value for ID in the listening room is insufficient to predict parameter deviations. Just like the reverberation ratio for diffuse field conditions, some kind of ratio between the direct sound in the recording room and the listening room should be found.

Literature

3 Theory

This chapter provides the explanation of the mathematical process from impulse response to room in room impulse response is given. Thereafter, a review of the current insights on analytical impulse response models in the RinR research is given.

3.1 Impulse response

To quantify the acoustics of a room, it is common practice to measure the impulse response. Figure 3.1 abstractly shows the process of an impulse response measurement as a linear system of generation, transmission, and reception. Where s(t) is the input signal, h(t) is the time finite impulse response (FIR) filter, and s'(t) is the output signal. Note that for room acoustics the FIR filter is the combination of the characteristics of, the source, the room and the receiver.
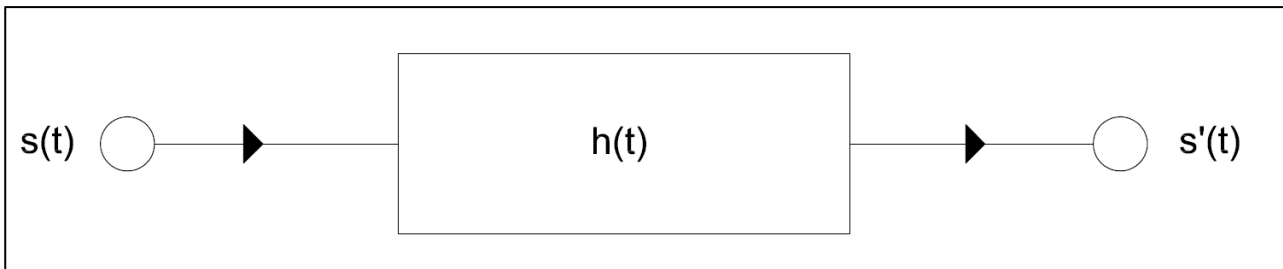
Figure 3.1 transmission system for the IR

Linearity in the system means that for every factor of change in signal s(t) the same change will be observed in signal s'(t). The filter is finite because it has a start and an end in the time domain. As the word impulse response suggest, the input signal is an impulse, mathematically presented by the Dirac delta function [21] defined in equation (3.1).

$$\delta(t) = \lim_{\delta \to \infty} \delta e^{-\delta t} \tag{3.1}$$

Where δ is a decay constant that turns the exponential into an impulse as it approaches infinity. The spectrum expressed by the spectral function is then [21]:

$$C(\omega) = \frac{\delta}{2\pi} \cdot \frac{1}{\delta + j\omega} = \frac{1}{2\pi} \; if \; \delta \to \infty \tag{3.2}$$

Where δ is again a decay constant, j is the imaginary unit, and ω is the angular frequency. In words, the spectrum of the Dirac delta function is flat, equal power in every frequency. Subsequent impulses of different amplitude can approximate any signal; the filter can be applied as an integral to all these impulses by the following equation [21]:

Theory

$$s'(t) = \int_0^t s(\tau) \cdot h(t - \tau) = \int_0^t h(\tau) \cdot s(t - \tau) \tag{3.3}$$

This is the convolution integral. Equation (3.4) shows the Dirac delta function inserted in equation (3.3). By definition, when the input of any FIR filter is δ(t), the output is its impulse response [23].

$$s'(t) = \int_0^t h(\tau) \cdot \delta(t - \tau) = h(t) \tag{3.4}$$

As well as a filter in the time domain, the FIR is also a filter in the frequency domain. Equation (3.3) expressed in this domain results in [21]:

$$S'(\omega) = H(\omega) \cdot S(\omega) \tag{3.5}$$

Where S'(ω), H(ω) and S(ω) are the spectral functions of s'(t), h(t) and s(t) respectively.

3.2 Room in room impulse response

The process of the room in room impulse response (IR_{RinR}) is visualised in figure 3.2. Where h_1 and h_2 are respectively the FIR filters representing the recording room and the listening room.
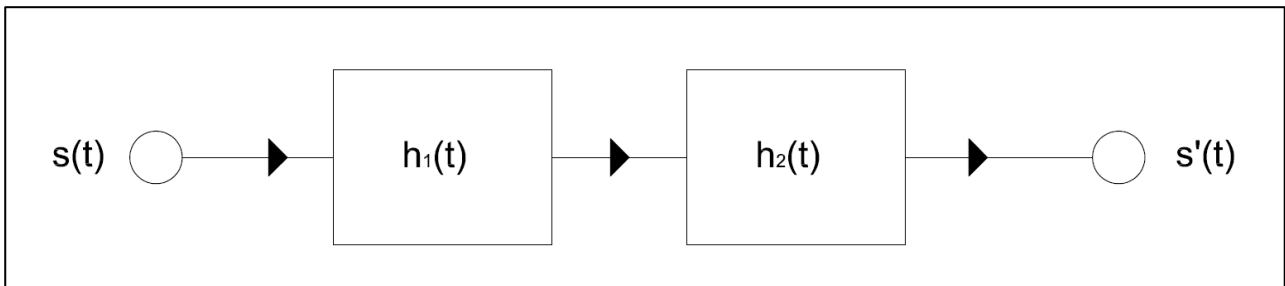
Figure 3.2 *transmission system for the IR$_{RinR}$*

The convolution integral for the IR_{RinR} system is derived from equation (3.3) assuming s(t) = δ(t) (Dirac delta function) and using the definition in equation (3.4):

$$s'(t) = \int_0^t h_1(\tau) \cdot h_2(t - \tau) = h_{12}(t) \;\; if \; s(t) = \delta(t) \tag{3.6}$$

Again, this is the convolution integral, where h_1 and h_2 are respectively the FIR filters for the recording and listening room, and h_{12} is the room in room FIR filter. Convolution is indicated with a star.

$$h_{12}(t) = h_1(t) * h_2(t) \tag{3.7}$$

3.3 Analytical impulse response models

At RinR research, analytical IR models are applied to calculate room acoustical parameters. These models are set-up as energy density distributions since sound energy is proportional to the squared sound pressure, $w \propto p^2$. The energy density balance in a room is a first order system defined by the differential equation (3.8) [21]:

$$V\frac{dw}{dt} = P_x(t) - \frac{c}{4}Aw \tag{3.8}$$

Where V is the volume of the room, w(t) is the energy density t is time, c is the speed of sound, $P_x(t)$ is time-dependent source power, and A is the total absorption area. Since we are interested in the IR, the solution for this model is for P = 0 as it was stationary until t = 0. The differential equation is then homogeneous and its solution yields [21]:

$$w(t) = w_0 e^{-cAt/4V} \tag{3.9}$$

Where the parameters are the same as in equation (3.8). The equation can be extended by accounting for, energy absorption at reflections (instead of continuous), arrhythmicity of the absorbing area, and absorption of the air. All these factors are relevant, especially for large rooms.

Equation (3.9) defines the energy density by an absorption process in the room. When a source emits sound waves part of the arriving waves are uninfluenced by the room, as the direct path between source and receiver is shorter than that of reflections. If the source radiates spherically, the energy density of the uninfluenced part can be modelled as decreasing with distance, as it would in the free field (i.e. $1/r^2$).

In his research on the effects of convoluted IRs Svensson adapted Barron's model [17], so it would allow the generation of IRs with software (e.g. with Matlab) [6], [24]. Equation (3.10) shows his discrete time model:

$$h(n) = D \cdot \Delta\left(n - \left\lfloor\frac{f_s r}{c}\right\rfloor\right) + R \cdot e^{-\frac{\delta n}{f_s}} \cdot wgn(n) \cdot H\left(n - \left\lfloor\frac{f_s r}{c}\right\rfloor\right) \tag{3.10}$$

Where $\Delta(n)$ is a unit pulse sequence, f_s is the sampling frequency, δ is the decay constant, n is a string of samples , wgn(n) is a white Gaussian noise sequence and H(n) is a Heaviside step sequence. D and R are respectively amplitudes for the direct and reverberant field according to equation (3.11).

$$D = \frac{r_{ref}}{r}; \quad R = r_{ref}\sqrt{\frac{4\pi c}{Vf_s Q_s Q_R}} \tag{3.11}$$

Where r_{ref} is a reference distance necessary for the calculation of absolute levels, r is the source-receiver distance, c is the speed of sound, V is the volume of the room, Q_s and Q_R are the directivity factors of the source and receiver respectively.

The direct part is modelled as a unit pulse or Dirac delta function, and the reverberant part is modelled in agreement with equation (3.9), i.e. as exponentially decaying function. This function is

then multiplied with a noise sequence to have a temporal distribution to represent reflections and spectral distribution.

Contrary to Barrons' revised model, this model has no part of early arriving reflections. This is a logical choice given that the function should be coherent after convolution, following equation (3.7). The convolution is given by equation (3.12).

$$\langle h_{12}^2(n) \rangle = h_{dd}^2(n) + \langle h_{dr}^2(n) \rangle + \langle h_{rd}^2(n) \rangle + \langle h_{rr}^2(n) \rangle \tag{3.12}$$

Where h is the pressure amplitude of the impulse response, subscripts denote direct or reverberant field and <> indicates the expected value of a random variable. For the precise elaboration with parameters see [6], [8]. A model with fewer parameters is proposed in [2] (subscript envelope added to the equation):

$$h_{1;env}(t) = e^{x_1 t} \; for \; t \geq 0 \tag{3.13}$$

Where h_1 is the (positive) envelope of the impulse response, x is -a/T, a is the decay constant valued 3ln(10), T is the reverberation time, and t is time. This model is used to represent a perfect diffuse sound field decay over time. One of the advantages of this model is that the convolution of the function is an equation with few parameters. However, it is missing a direct part. The IR$_{RinR}$ model as presented in [11] (subscript envelope added to the equation):

$$h_{12;env}(t) = e^{x_1 t} * e^{x_2 t} = \begin{cases} \dfrac{e^{x_1 t} - e^{x_2 t}}{x_1 - x_2} & if \; x_1 \neq x_2 \\ te^{xt} & if \; x_1 = x_2 \end{cases} \; for \; t \geq 0 \tag{3.14}$$

Parameters are the same as in equation (3.13). The primary application of this model is research into general trends since it lacks accuracy. The equations are representing the convolution of two correlated signals. In reality, the signals are uncorrelated due to the stochastic nature of reflections.

Adding noise sequences to the single room IRs solves this overestimation. It should be noted that this is a relatively uncomplicated process as long as the temporal distributions of reflections are not necessary. In [24], Appendix A, Svensson argues that the convoluted noise sequence is in itself a noise sequence with the same statistical properties (given a sufficient number of samples) so that it can be multiplied with the envelope function of the IR$_{RinR}$ which he described as:

$$h_{12;env}(t) = \sqrt{t}e^{xt} \cdot RV(t) \; if \; x_1 = x_2 \tag{3.15}$$

Where RV is a random variable with properties: mean = 0 and standard deviation = 1. This equation is very similar to the equation (3.14) with the difference that the first term t is rooted here; this root is a result of the convolution with statistical noise. This difference solves for the overestimation caused by the continuous functions.

4 Method

This chapter contains an overview of, the impulse response, directivity measurements, and numerical approach to obtain results concerning parameter deviations in the room in room scenario.

4.1 Acoustic measurements

Measurements conducted for this research are performed with the same material. The equipment is given in table 4.1.

Table 4.1 *measurement equipment*

Description	Type	Serial NO./ID
Laptop	Toshiba Satellite M50D-A-10D	LvA _tosh1 and LvA_tosh2
Software	Dirac B&K/Acoustics Engineering Type 7841 V6.0	-
USB Audio Interface	Acoustics Engineering – ICP Triton	03300353
Power amplifier	Acoustics Engineering – Amphion	0101
Microphone calibrator	B&K Type 4231	2652094
Microphone	B&K Type 4189	2471031
Microphone preamplifier	B&K Type 2671	2652959

The measurements are conducted with an exponential sweep as an excitation signal, created with Dirac 6.0 following the procedure as given in [25].

4.1.1 Impulse response quality

The parameter impulse response to noise ratio (INR) is used to assess the quality of the IR measurements, the INR is closely related to the decay range, and the calculation methods are based on the Schroeder and RMS curves. Detailed information for this parameter can be found in [26]. Figure 4.1 gives a schematic representation of the INR.

In [27] an extensive set of minimum values for the INR are defined, when this minimum is met, the parameter calculated from the IR is reliable. In this research, all used IR measurements have an INR of at least 60 dB which is well above the required value for calculating the most demanding parameter (i.e. T_{30} requiring an INR >43 dB), see Appendix C.
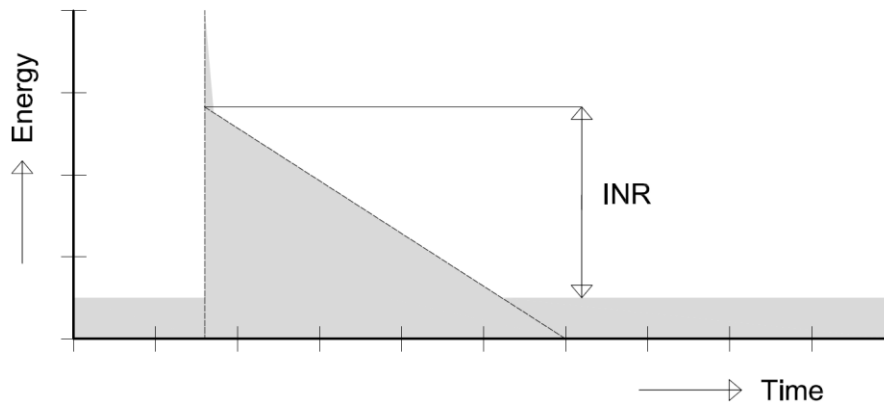
Figure 4.1 *Schematic overview of the impulse response to noise ratio (INR) or decay range inspired by [11].*

4.1.2 Reverberation chamber

To create a high-quality impulse response database focussed on parameter sensitivity for absorption, source directivity, and source-receiver distance a series of measurements were conducted in the reverberation room of the Echo building at the Eindhoven University of Technology. The goal of the measurement is to validate an analytical model used to predict deviations in parameters as a result of RinR; the model is given in chapter 5.

Two single driver sources were chosen to have different directivity characteristics. Absorbers in the form of polyester wool baffles were placed in the reverberation room to create five different reverberant scenarios. Multiple microphone positions were measured in every scenario and with every source.

Figure 4.2 shows the floor plan and side views of the reverberation chamber at the Echo building at Eindhoven University of Technology. The rectangle in the middle is the source; the bullets coming out of the centre are the measurement positions. The rectangles indicated A to D are placements of the absorbers.

4.1.3 Absorption

There were five different absorption scenarios created by adding polyester absorbers to the wall at the locations as shown in figure 4.2 by the hatched rectangles and letters A to D. The absorbers are 1.22 m x 0.60 m x 0.12m. In this study the parameter total absorption area (A) is relevant. The parameter follows after [20]:

$$A = \frac{55.3 \cdot V}{c \cdot T} \ [m^2] \qquad (4.1)$$

Where A is the total absorption area, V volume of the room, T the reverberation time and c is the speed of sound in air.
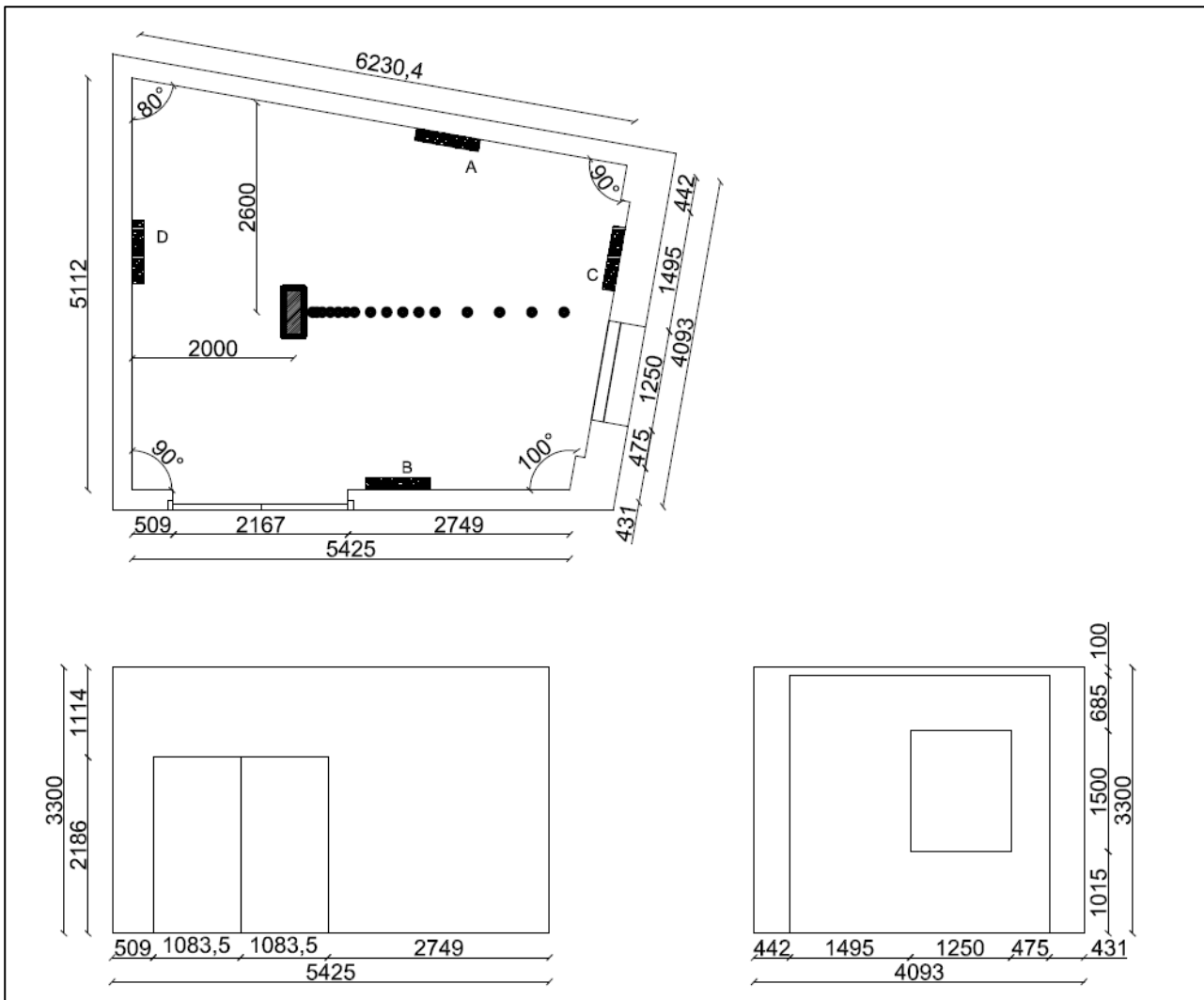
Figure 4.2 *floor plan and side views of the reverberation chamber at the Echo (laboratory for acoustics at TU/e), taken from* [28] *(modified)*

Table 4.2 presents the total absorption area for the five scenarios in octave bands 500 to 4000 Hz. Lower octave bands are disregarded because the measuring of reverberation time below 500 Hz octave band is capricious due to being below the Schroeder frequency, (see section 4.2).

Table 4.2 *values for the total absorption area in the different scenarios.*

	Absorption area [m^2]			
Octaveband	500 Hz	1000 Hz	2000 Hz	4000 Hz
no baffle	3,4	3,5	4,1	5,7
1 baffle	4,5	4,7	5,3	7,0
2 baffle	6,1	5,7	6,3	8,1
3 baffle	7,6	7,1	7,7	9,4
4 baffle	8,5	8,1	8,4	10,0

Method

4.1.4 Source-receiver distance

As indicated in figure 4.2 for each scenario 15 or 16 impulse responses were measured at various distances out from the centre of the source. The pressure amplitude of the direct proportion should decrease by halve with doubling of distance. Therefore, the measurement positions close to the source are closer to each other. Figure 4.3 gives the distances in millimetre. As for the distances, measurements are made from the front of the box.
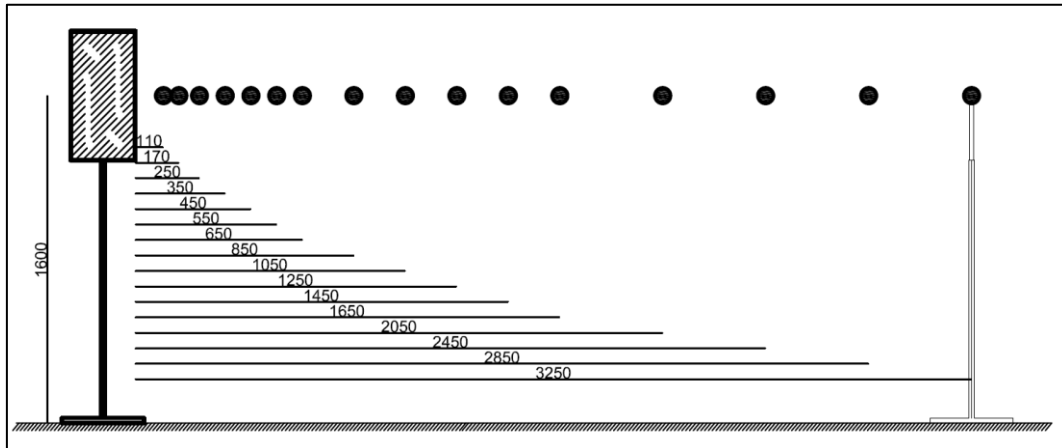
Figure 4.3 *Measurement distances for measurements in the reverberation chamber, positions close to the source are closer to each other; measures are in mm.*
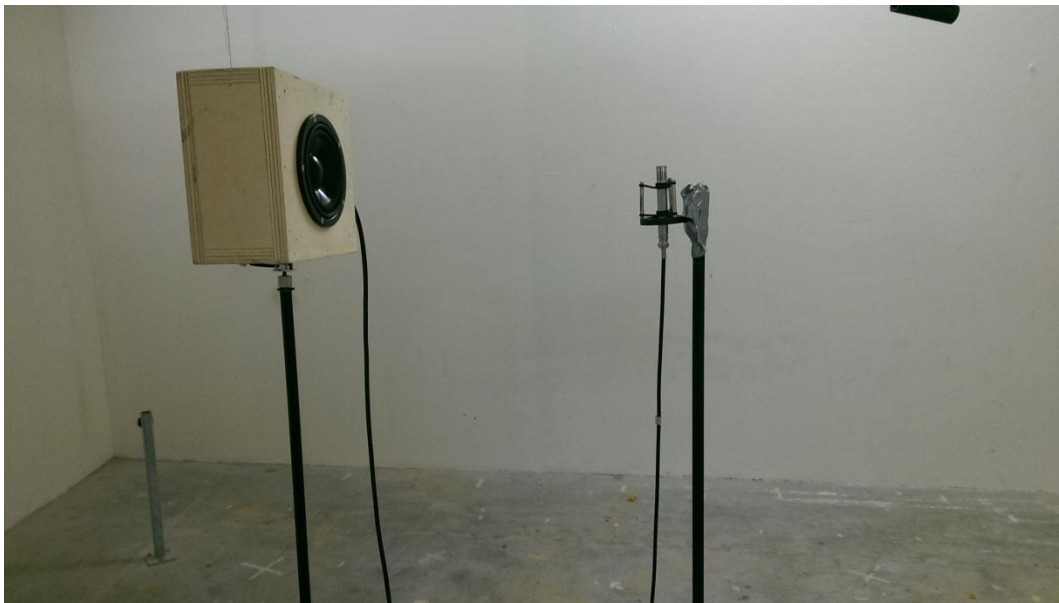
Figure 4.4 *Photo of the measurement set-up in the reverberation chamber*

4.1.5 Directivity

Source directivity is taken into account by using two single speaker sources of different dimensions. At the results they are named, they are called 'big box' and 'small box'. Dimensions of the big box are 22.5 cm x 22.5 cm x 12 cm, and the driver has a diameter of 12 cm, whereas small box is cube-shaped with ribs of12.4 cm the driver has a diameter of 9 cm.
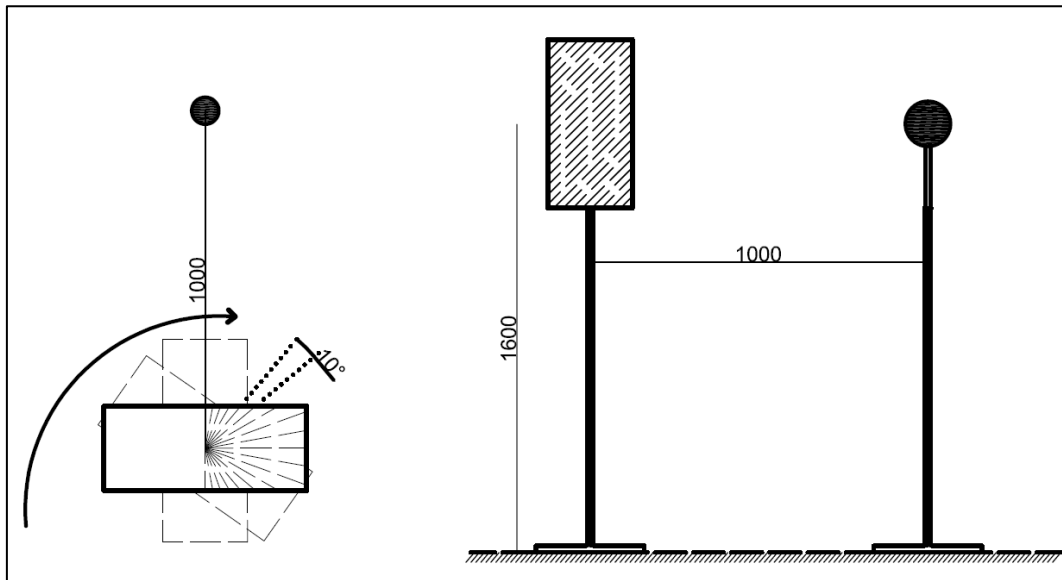
Figure 4.5 *Schematic representation of the directivity measurement, measures are in mm*

Figure 4.6 *Photo of the set-up directivity measurement*

Method

A measurement is designed to find the different directivity indices of the sources, see figure 4.6. The microphone and source are placed at the same height 1 m apart; the sources were rotated 10 degrees to form half a circle after 19 measurements, horizontal deviations were kept to a minimum by using a spirit level. The experiment was conducted outside to reduce the influence of unwanted reflections. The ground reflection is not significant due to only taking octave bands higher than 500 Hz into account, moreover because the ground was grass. The same equipment was used as in the reverberation chamber measurement; the only difference was an increased source power to compensate for the higher background noise.

Figure 4.7 *Photo of the wind rose on top of the big box used to aim the speaker*

Directivity factor Q(f) follows after equation (4.2) [29]:

$$Q(f) = \frac{\left(4\pi \, p_{rms}^2(\theta_0)\right)(180°/\pi)}{2\pi \sum_{n=1}^{180°/\Delta\theta} p_{rms}^2(\theta_n) \, sin(\theta_n) \, \Delta \theta} \tag{4.2}$$

Where 2π is a result of the assumption that there is an axis of symmetry, $\Delta\theta$ is the angle between two adjacent points measured. $180/\Delta\theta$ is then the number of measurements, $p_{rms}^2(\theta_0)$ is the squared pressure as measured directly in front of the source (or direction in which Q(f) is to be determined), $p_{rms}^2(\theta)$ is the squared pressure at angle θ in the horizontal plane. The equation to determine p_{rms} from a stationary signal, according to [20]:

$$p_{rms} = \left(\frac{1}{t_a} \int_0^{t_a} p^2 \, dt\right)^{0.5} \tag{4.3}$$

Where t_a is an indication for a time point chosen such that the background noise does not have significant influence and p is the pressure in the IR. The signal used here is an exponential sweep, the equation is still valid because the signal was the same for every measurement. Besides, after obtaining the IR from the measurement, the signal has a white spectrum. The directivity index (DI) is calculated with equation (4.4) [29]:

$$DI = 10 \cdot \log_{10}\big(Q(f)\big) \; [dB] \tag{4.4}$$

Figure 4.8 shows the directivity factor resulting after equation (4.2). The big box has a higher directivity in all frequency bands except for the 2000 Hz band. This is likely due to the dimensions of the driver and box.
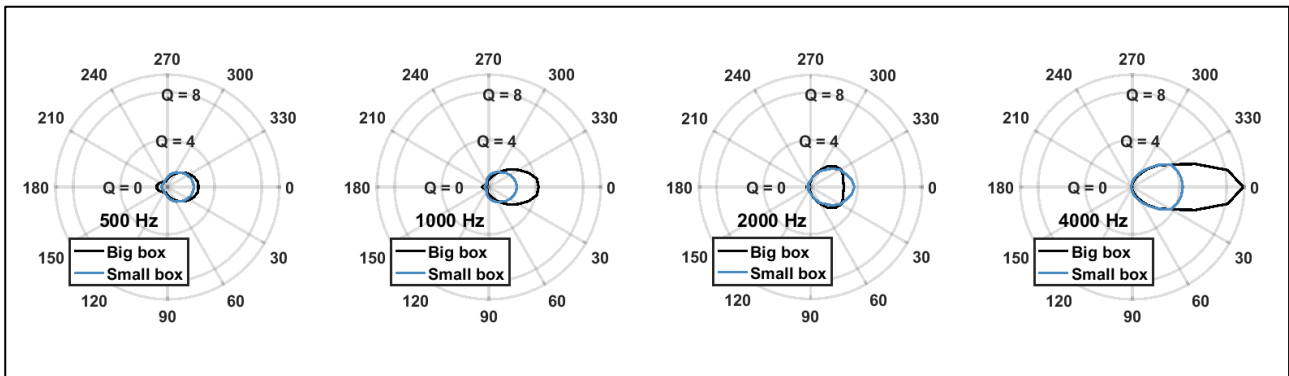
Figure 4.8 *polar plot for the directivity factor (Q) for the sources, following after applying equation (4.2) in all designated directions.*

In table 4.3 the directivity index is given for the 0° measurement angle. This angle is the measurement direction unless specified differently.

Table 4.3 *directivity index for both sources following after equation 4.4*

	Centre frequency octave bands			
	500 Hz	1000 Hz	2000 Hz	4000 Hz
Big box	4.2 dB	6.3 dB	4.5 dB	9.7 dB
Small box	3.5 dB	3.8 dB	5.7 dB	6.3 dB

The scripts used to reach the results as presented in this section can be found in Appendix B.5.

4.1.6   Volume

In earlier research, similar measurements have been performed in a gymnasium for a master project by the author in [12]. The focus of this study was primarily on the influence of the direct sound for RinR acoustics and a new parameter to express this proportion. Namely, the Initial Drop, as introduced in the introduction.

During measurements in this gymnasium, the big box source was used (among others). The design is slightly different from the measurement in the reverberation room; similarities are the source in the middle of the room and a line out of the centre from the source. Different was the use of three other source types that were applied to investigate the influence of source directivity. Considering this research, two different sized single driver sources were used for this thesis. In table 4.4 the room characteristics of the rooms are given.

Table 4.4 *room characteristics for the different halls used in this research*

Room	Volume [m³]	Length [m]	Width [m]	Height [m]	Absorption* [m²]	Reverberation time* [s]
Reverberation room	88	6	5	3	(see section 4.1.3)	Variable
Gymnasium	8400	42	29	7	467.3	2.93

* *RT is the average of the 500 and 1000 Hz octave bands. Subsequently, absorption is calculated from this RT*

4.1.7 Measurement conditions

During the measurements in the reverberation room the temperature was +/- 22°C and the relative humidity was +/- 53%. For the directivity measurements outside the temperature was 9 to 11 °C, the relative humidity was 44% to 50% and the wind speed between 4 and 5 m/s (3 Bft).

4.1.8 Measurement uncertainty

The source-receiver distance was measured with a tape line taped to the ground. The measurement uncertainty is +/- 1 cm. No tools were used to assure that the microphone was precisely aligned with the middle of the speaker. The height was equal within 0.5 cm accurate.

The angles for the directivity measurement were determined using a protractor, and the levelling with a spirit level, the measurement uncertainty is +/- 1°. Distance to the source was determined from the middle of said source, not from the driver. Results of the directivity measurement will be significantly different when the rotation point would be on the driver instead.

Usually, for the determination of the reverberation time an omnidirectional source is used according to the ISO-3382 standard. The reported reverberation times in this report were measured with single driver sources. For every scenario, an average is taken over the RTs measured after the critical distance.

4.2 Frequency range

The validity of the results will only be studied for frequency bands above the Schroeder frequency in the reverberation room. Below the Schroeder frequency, a room will have modal behaviour, and the reverberation time cannot be calculated accurately. The Schroeder frequency can be calculated using equation (4.5) [20]:

$$f_S = 2000 \sqrt{\frac{T}{V}} \ [Hz] \tag{4.5}$$

For the 500 Hz octave band, in the no baffle configuration, the reverberation time is 4.4 s, f_S is then 447 Hz. Therefore the frequency range starts at the 500 Hz octave band. The upper limit is set at 4000 Hz octave band because the analytical model does not keep air absorption into account.

4.3 Room acoustical parameters

The deviations caused by Room in Room acoustics are expressed with room acoustical parameters. The calculation methods for these parameters are presented in this section. All parameters in this section can be derived from the impulse response.

4.3.1 Reverberation time

Reverberation time was initially defined as the time sound took to reduce to 1 millionth of its original intensity. This was the definition used by Sabine over a hundred years ago and still stands today. By the works of Schroeder, the determination of the parameter has become a more straightforward task. To obtain the reverberation time an ensemble average had to be determined over a series of impulse responses, Schroeder discovered that backwards integration could obtain the average by a single measurement [30]. Equations (4.6) to (4.7) give the process to determine the reverberation time.

$$S(t) = 10 \cdot \log_{10}\left(\frac{\int_{t}^{\infty} h^2(t)\,dt}{\int_{0}^{\infty} h^2(t)\,dt}\right) [dB] \tag{4.6}$$

Where S(t) is the Schroeder curve, time infinity (∞) is the cross point in the IR, h(t) is the pressure amplitude of the impulse response., this equation will be necessary for the determination of other parameters as well, the script used to determine it is presented in Appendix B.6. On the resulting curve an evaluation range can be defined and extrapolated, for example in the case of T_{20}:

$$T_{20} = 3 * \left(t_{S_{\max-25}} - t_{S_{\max-5}}\right) [s] \tag{4.7}$$

Where T_{20} is reverberation time with an evaluation range between -5 dB and -25 dB on the decay curve. $t_{Lmax\,-\,5}$ = position in time where the sound level has decreased 5 dB since maximum level in [s] and $t_{Lmax\,-\,25}$ = position in time where the sound level dropped 25 dB since maximum level in [s].

4.3.2 Energy parameters

In room acoustics energy ratios are used to indicate the balance between useful and detrimental reflections. The energy parameters are linked to speech intelligibility and music intelligibility. One of the first such parameters was Definition from the German Deutlichkeit [31][6].

$$D_{50} = \frac{\int_{0}^{50} h^2(t)dt}{\int_{0}^{\infty} h^2(t)dt} [-] \tag{4.8}$$

Where h(t) is the pressure in the impulse response and time infinity the cross point. Later Clarity was introduced, meant initially to be a parameter for the transparency of music concert halls [20], [32]. Clarity as music parameter has 80 ms early arriving energy in the equation as opposed to the 50 ms in the Definition which is focussed on speech intelligibility.

---

[6] Text in German, the author of this work did not actually read it, however, from other articles it can be reasoned to be the right reference

$$C_{80} = 10 \log_{10}\left(\frac{\int_0^{80} h^2(t)dt}{\int_{80}^{\infty} h^2(t)dt}\right) \ [dB] \tag{4.9}$$

Where h is the pressure in the impulse response and time infinity the cross point. However, the parameters D_{50} and C_{80} are sensitive to the chosen start point for the calculations (i.e. t=0). As hinted to before in [18] Defrance et al. found significant differences in different techniques to determine the start point. Another issue with both these parameters is the abruptness of the time window, especially relevant for large rooms. If a significant reflection were to occur directly after the indicated time window, it will be counted equally heavy as when it would occur much later in the IR.

Any IR parameter presented here will be calculated with a start point determined as: directly in front of the peak where the normalised energy-time curve (ETC) is -20 dB unless specified differently, the ETC is calculated as in equation (4.10):

$$ETC(t) = 20 * \log_{10}\left(\frac{h}{h_{max}}\right) \ [dB] \tag{4.10}$$

A last energy-related parameter for consideration is the Centre Time that follows after [33][7]:

$$T_s = \frac{\int_0^{\infty} t \cdot h^2(t)dt}{\int_0^{\infty} h^2(t)dt} \cdot 1000 \ [ms] \tag{4.11}$$

Centre Time is especially useful since it has no issues with IR onset as it is the centre of gravity in the impulse response [20].

4.3.3 Initial drop

The initial drop (ID) is an indication of the strength of the direct sound and can be obtained directly from the IR decay curve, first defined in [12] later published in [7]. In this section, a more refined determination procedure is described. The decay curve can be calculated with equation (4.6).

In previous works, the ID was calculated as the level difference between t = 0s and t = 0.05s in the decay curve [7], [12]. Wittebol & Van der Putten performed additional research into the workings of the parameter [13]. This suggested having the start point for calculations set at the arriving time with source-receiver distance. The problem is that this distance is not always precisely known. A solution to this might be to choose the start point for calculation using ISO-3382, by reviewing steepness of the decay curve, or as $S(\vartheta)$ = -0.05 dB. The latter is chosen in this thesis because it proved most efficiently applicable.

$$ID_0 = S(0) - S(\vartheta + \tau)[dB] \tag{4.12}$$

Where ϑ is start point [s], τ is time window [s] and S(0) = 0 as a result of the normalization. So equation (4.12) becomes:

---

[7] Text in German, the author of this work did not actually read it, however, from other articles it can be reasoned to be the right reference

$$ID_0 \; = \; -S(\vartheta + \tau) \; = \; -10 \cdot \log_{10}\left(\frac{p_b(\vartheta + \tau)}{p_b(0)}\right)[dB] \tag{4.12a}$$

Where $p_b(0)$ is $p_b(t)_{max}$ as result of the backwards integration, ID is the initial drop in [dB] and $S(\vartheta)$ is -0.05 [dB] (start point). In measurements, the time window will overlap with the diffuse field. So a compensation for the diffuse field based on the decay rate is:

$$ID_{c;d} \; = \; \tau \cdot \frac{60}{T_{60}} \; [dB] \tag{4.13}$$

With $ID_{c;d}$ the Initial Drop compensation for the decay rate, т is the time window, 60 is the decay range of reverberation time, and T is the reverberation time of the room. With T_{60} approaching infinity $ID_{c;d}$ will approach zero. The other limit is ID = 60 dB since $ID_{c;d}$ will approach infinity because the T_{60} will approach zero. Finally, the compensation term is subtracted from the value obtained by equation (4.12a):

$$ID \; = \; ID_0 \; - \; ID_{c;d} \; [dB] \tag{4.14}$$

The compensation as proposed in this section has the benefit that the ID now indicates the strength of the direct proportion and early reflections. Based on the width of the time window early reflections can be taken into account or be omitted from the indicator. A script to determine the initial drop from a measurement is given in Appendix B.7. Figure 4.9 illustrates the compensation term.
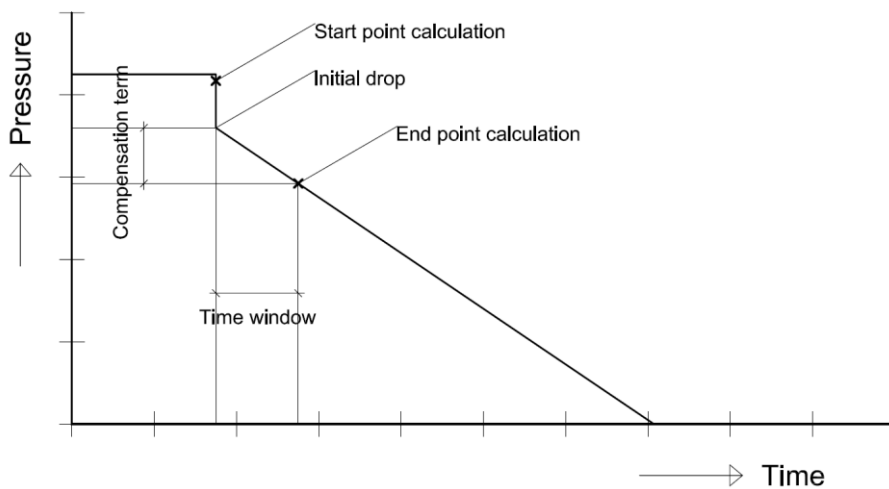
Figure 4.9 *Schematic representation of the initial drop and diffuse field compensation*

4.3.4 Curvature parameter

One of the first findings in the RinR acoustic research was that decay curves are not linear in the IR_{RinR} [1]. In the ISO 3382-2:2008(E) Annex B.3 a notion is added for the degree of curvature. In the text is referred to a situation where the decay curve has a slightly convex shape. The degree of curvature is then calculated using equation (4.15). The values of C should be between 0 and 5%. If

the value is higher than 10%, it is an indication that the calculated reverberation times are "suspicious".

$$C = 100 \cdot \left(\frac{T_{30}}{T_{20}} - 1 \right) \ [\%] \tag{4.15}$$

Where C is the curvature parameter, T_{20} and T_{30} are reverberation times over different evaluation ranges on the decay curve. In the RinR scenario, it is reported to be the case that the decay curve is nonlinear and concave.

To illustrate this nonlinearity figure 4.10 presents the different reverberation times for various evaluation ranges, resulting after convolution of two perfectly diffuse functions, i.e. equation (3.15).
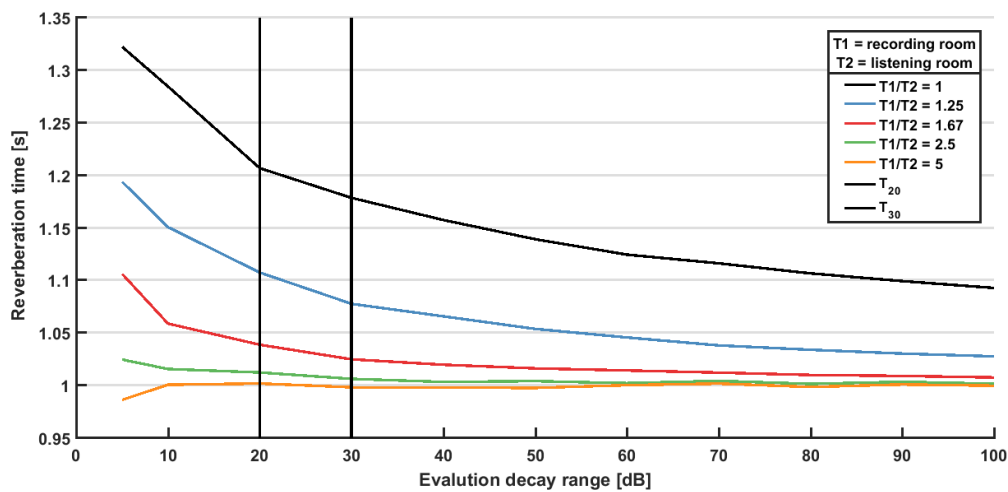
Figure 4.10 *reverberation time calculated from the IR$_{RinR}$ by using linear regression between -5dB and -5 (minus) "value indicated as evaluation decay range", the black vertical lines are indicating where T$_{20}$ and T$_{30}$ are calculated.*

Equation (4.15) will be used to keep the same idea to the indication of the linearity as in the standard. However, C will be negative for concave curves. Worst case scenario will be a self-convoluted function, i.e. when a reproduction happens in the same reverberant field. Moreover, the curvature parameter will assume a value between -3% and -0% in the case of perfectly diffuse functions.

In section 7.2 it is discussed that not all IR$_{RinR}$ have concave shapes. To keep unity in the approach to the curvature parameter, it should be between -5% and 5%.

4.4 Parameter deviations

This section presents the method for comparing room acoustical parameters and the scales on which the deviations are presented.

4.4.1 Absolute and percentage deviations

The calculations of the parameter deviations are relatively simple processes. Equation (4.16) shows how the difference between the IR_{rec} parameter and the IR_{RinR} parameter is calculated

$$\Delta P = P_{rec} - P_{RinR} \qquad (4.16)$$

Where P is any parameter derived from the IR, in this thesis Clarity, Centre Time and the Initial Drop. Exceptions to this formula are parameters for which the difference is indicated by a percentage, e.g. Reverberation Time T_{20} and T_{30}. For these parameters equation (4.17) determines their deviation.

$$\Delta P = \frac{|P_{RinR} - P_{rec}|}{P_{rec}} \cdot 100 \ [\%] \qquad (4.17)$$

Where the parameters are the same as in equation (4.16).

4.4.2 Reverberation ratio

Following the methods in [2], [3] the ratio of reverberation times between the recording and listening rooms will be used as a scale to express the deviation of room acoustical parameters in the RinR scenario. The RT ratio is calculated with equation (4.18):

$$T_{ratio} = \frac{T_{rec}}{T_{list}} \qquad (4.18)$$

Where T_{rec} and T_{list} are the reverberation times in the recording and listening rooms, respectively. In the results of chapter 7, this parameter is indicated as T_1/T_2.

4.4.3 Initial drop ratio

The reverberation ratio is the scale for deviation in the diffuse field; similarly, the Initial Drop ratio is the scale for deviation in the direct field. The Initial Drop is a decibel value. Therefore the ratio between ID_{rec} and ID_{list} is given by equation (4.19):

$$ID_{ratio} = ID_{rec} - ID_{list} \qquad (4.19)$$

Where ID_{rec} and ID_{list} are the Initial Drops in the recording and listening rooms, respectively. In the results of chapter 7 this parameter is indicated as $ID_1 - ID_2$.

4.5 Creating room in room impulse responses

The IR_{RinR} for the research are created with the (bulk) auralisation function in Dirac. This is a convolution with the option for noise suppression and the filtering of the source. However, noise suppression is not used, and for this research, the source characteristics have to stay intact therefore the operation used is a convolution.

Method

The approach is to choose one recording room IR and convolve this with IRs measured in the research. There are four IRs used as recording positions, two close to the source and two far from the source. These four IRs are from the measurement in the reverberation room without baffles. Thus the reverberation time is always longer or equal to the listening room reverberation time.

The IRs with direct sound are the first two positions in front of the big box so that (in most cases) the peak in the IR_{rec} is higher than the peak in the IR_{list}. The two IRs further from the source are measured at 3.25 m with the difference that for one the source is rotated with 160°, so (almost) no direct sound would reach the microphone. In table 4.5 the different source-receiver distances are listed. In figure 4.11 the parameter values for the used recording room IRs are given in the form of graphs.

Table 4.5 *source-receiver distance for the IRs used as recording room*

Scenario	Rec room 1	Rec room 2	Rec room 3	Rec room 4
Source-receiver distance [m]	0.17	0.25	3.25	3.25 (source rotation 160°)
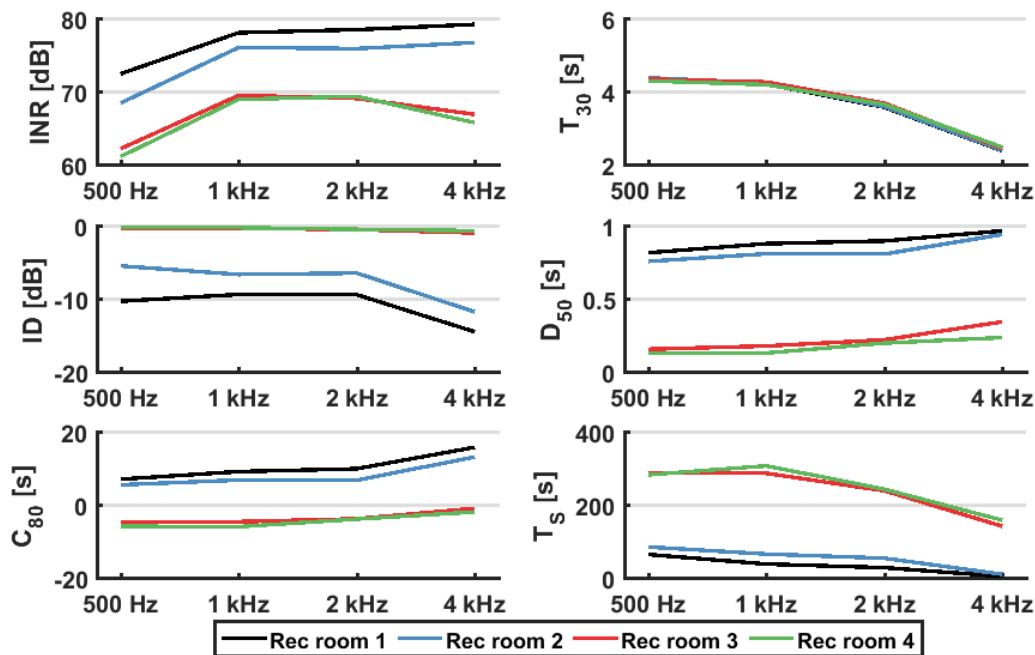
Figure 4.11 *Parameter values for the impulse responses used to create the $IR_{RinR}s$. T_{30} = reverberation time; C_{80} = Clarity; D_{50} = definition; T_S = centre time. Division of frequencies is in octave bands.*

4.6 Just noticeable difference

The just noticeable difference (JND) is used to quantify the deviations as caused by RinR acoustics. The JND is defined as a threshold; deviation when (trained) listeners could not distinguish the difference anymore, it is a limen.

The just noticeable difference is defined for a large number of room acoustical parameters. In a paper by Hak [27] an overview is given linked to the impulse response quality expressed by INR. In

table 4.6 the JND and minimum INR for parameters relevant for this research are given. These are values, where the accuracy of the calculated parameters are within the JND.

Table 4.6 *Just noticeable differences for acoustic parameters used in this research: T_{20} & T_{30} = reverberation time; C_{80} = Clarity; D_{50} = definition; T_S = centre time.*

	T_{20}	T_{30}	C_{80}	D_{50}	T_S
Just noticeable difference	5% [30], [34]	5% [30], [34]	1 dB [32]	0.05 [31]	10 ms [33]
Minimum INR for accuracy within 1 JND in [dB]	37	43	24	21	24
Minimum INR for accuracy within 0.5 JND in [dB]	41	48	25	24	27

In [35] Bradley et al. argue that the JND for Definition changes with its magnitude, this makes sense because the relationship between clarity (C) and definition (D) is not linear but can be expressed by equation (4.20):

$$C = 10 * \log_{10}\left(\frac{D}{1-D}\right) [dB] \tag{4.20}$$

Multiple studies agree that the JND for clarity measures is in the order of 0.9 to 1.1 dB over the whole range, e.g. [35], [36]. Therefore, the JND for definition cannot be linear.

As indicated in section 4.1.1 the INR for all IRs in this research is above 50 dB, so all parameters derived from them are within 0.5 JND accuracy. The only exceptions to this quality are the impulse responses used to obtain the directivity factor. This is due to the higher background noise outside. However, sound level parameters need a lower INR than energy ratios [27] (e.g. sound strength needs INR = 22 dB) it is, therefore, safe to assume that the impulses used are of high enough quality.

Method

5 Analytical model

In this chapter, an analytical equation is proposed adding a direct component and a ratio between the diffuse and direct components to the methodology in [11]. All equations in this chapter use t = 0s as impulse response onset and are only valid for positive values of t.

5.1 Direct component and direct/diffuse ratio

An IR usually has a peak at the start. Theoretically, this would be the Dirac delta function unaltered by the reverberant field of the room. Expanding equation (3.13) to have a peak as a result of direct sound would result in equation (5.1):

$$h_{env}(t) \approx D\delta(t) + Re^{xt} \tag{5.1}$$

Where: δ(t) is the ideal impulse represented by the Dirac delta function (equations (3.1) and (3.2)) D and R are the amplitudes for the direct and diffuse field, inspired by equation (3.10) [6]. This would agree with the method in equation (3.10) in that the peak is an ideal impulse. In practice, however, the peak will be the IR of the loudspeaker (IR_{lsp}), scaled by the source-receiver distance and directivity of the source and receiver.

If the goal is an analytical model for the IR_{RinR}, it is important that any function chosen to represent this peak is relatively easy to convolve. For this reason, all discontinuous functions are not considered[8]. Thus it makes sense to assume an exponential decay so that the chosen peak is an alteration of the ideal impulse (equation 3.1). Even though, discussions can arise over the validity of presenting the direct part in an IR as exponential decay. In fact, measurements performed for this study show that this can be a good approximation. Figure 5.1 shows three peaks in the IR, in the form of energy time curves (ETC). Note that these are all-pass representations. On the left side is the unfiltered impulse response, in the middle is the ETC filtered with the Hilbert Transform and on the right side, the peak is filtered by a root-mean-square (RMS) moving average filter of 0.4 ms.
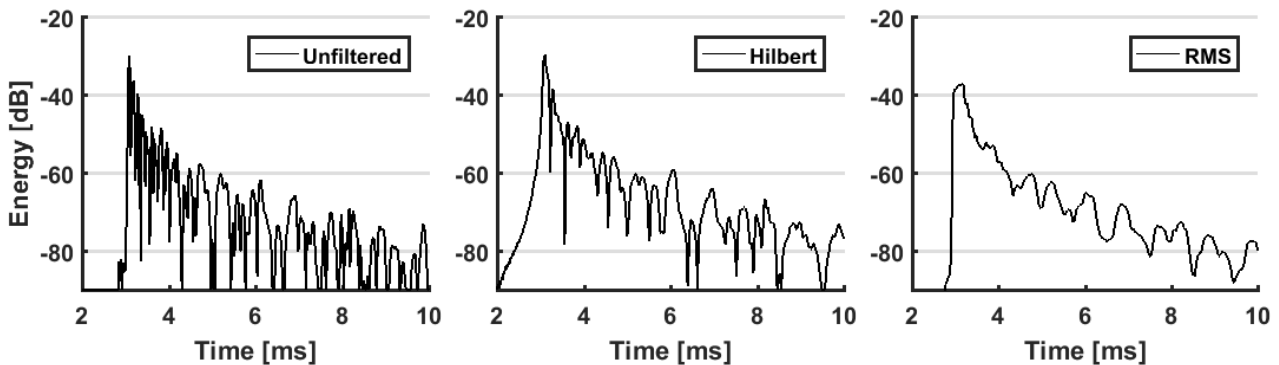
Figure 5.1 *Energy time curves of the first 10 ms of an IR measured at 1 m in front of a single loudspeaker, left side is unfiltered all-pass, the middle is Hilbert transform, right side is RMS filtered, data for the graphs exported from Dirac.*

---

[8] Discontinuous functions in this case would be peak representation by means of a block or a triangle in front of the decay curve.

A decaying linear line would indicate an exponential decay. However, in the figures, it is seen that the beginning of the decay is steeper than the remainder. Both parts can be represented by an exponential function. This results in a double-sloped decay curve where the first decay is steep.

Before calculating acoustic parameters, digital processing will influence the peak by the Butterworth filters applied to divide the signal in octave bands, see Appendix B.4 for the Matlab script. The used software, Dirac 6.0, has a minimum measurable T_{30} given in figure 5.2. The values presented are a result of a short-circuit measurement, which was performed, so the resulting reverberation time is the minimum of the filters.
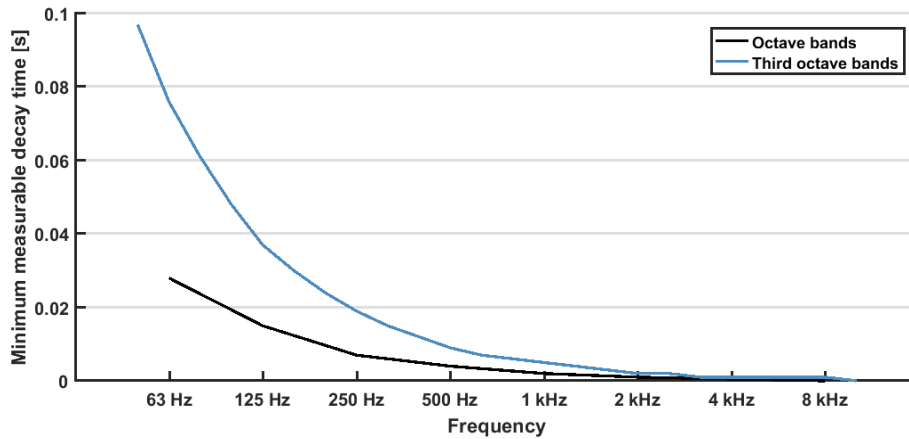
Figure 5.2 *decay time of the (third) octave band filters in Dirac*

The minimum measurable decay time is short enough to be disregarded. This assumption stems from the same argument as made in [2]: The reverberation time should be at max half that of the recording room to reproduce a decay characteristic in a listening room. In this research, the focus is on the frequency bands 500 Hz to 4 kHz, and the peak decay (if one would calculate the decay rate over the first 50 ms of an IR) is in the order of 0.06 s making it six times longer than the minimum measurable decay time. Therefore, it is possible to determine the decay in this early peak.

Next to being the peak itself, the IR_{lsp} is the excitation for the IR as a whole. In order to account for the IR_{lsp}, an exponential function with a steep decline is added to the diffuse field resulting in equation (5.2), where the IR_{lsp} and the room response are considered subsequent filters in a linear time-invariant system. This can be expressed as one filter by convolution of the two filters [23]:

$$h_{env;diffuse}(t) \approx \alpha e^{pt} * e^{xt} \tag{5.2}$$

Where α is the amplitude of the loudspeaker response (i.e. source power and the impedance of the loudspeaker), p is the decay term for the loudspeaker and x is the decay term of the diffuse field based on reverberation time. The direct sound in an IR, however, is dominated by the loudspeaker response and should therefore not be convolved with the room. This line of reasoning leads to an equation for the total IR envelope as follows.

$$h_{env;total}(\text{t}) \approx \alpha \left(D\, e^{pt} \;+\; R\, \frac{e^{pt} - e^{xt}}{p - x} \right) \tag{5.3}$$

Where the direct sound is added as the IR_{lsp} with a factor D to account for source-receiver distance and source directivity, factor R is representing the strength of the diffuse field. For the readability of the resulting equation (i.e. after convolution), the diffuse field will be modelled as exponentially decaying function. α is omitted as well because the goal of the model is to see how convolution affects energy ratios and the decay time of the IR_{RinR} since a multiplication of both sides would not affect any of these parameters. This arguing results in equation (5.4):

$$h_{env}(\text{t}) \approx D\, e^{pt} \;+\; R e^{xt} \tag{5.4}$$

Where D and R are amplitudes for the direct and diffuse proportions in the IR. The factors D and R have to incorporate all room acoustical parameters (i.e. volume, absorption, source-receiver distance and directivity). In [21] a division for the energy density, based on source-receiver distance and the critical distance is proposed, see equation (5.5). This equation is for a steady state scenario

$$w_{tot} = \frac{P}{4\pi c} \left(\frac{Q}{r^2} + \frac{1}{r_c^2} \right) \tag{5.5}$$

Where P is source power, r_c is the critical distance, following after equation (5.7) [20], Q is the directivity factor, and r is the source-receiver distance. Because we are only interested in the ratio between the diffuse and direct proportions the first term is left out. An adaptation is made for the relationship between energy and pressure. Where sound energy decays with distance according to $1/r^2$, sound pressure decays $1/r$. This results in equation (5.6) for factors R and D.

$$R = \frac{1}{r_c} \;\&\; D = \frac{\sqrt{Q}}{r} \tag{5.6}$$

Where the parameters are the same as in equation (5.5). As said before this division is in a steady state scenario, i.e. constant source power. Due to a lack of accuracy in the directivity measurements and a limited amount of sources it was not possible to validate the directivity factor. For the conclusions of this study, this bears no consequences, however, if a parameter sensitivity study is conducted this division needs to be revised.

$$r_c = \sqrt{\frac{Q \cdot A}{16 \cdot \pi}} \;\; [m] \tag{5.7}$$

Where Q is the directivity factor and A is the total absorption area following after Sabine equation for reverberation time [21] given by equation (5.8):

$$A = \frac{55.3 \cdot V}{c \cdot T} \;\; [m^2] \tag{5.8}$$

Analytical model

Where A is the total absorption area], V volume of the room, T the reverberation time and c is the speed of sound in air.

Summarizing the content in this section leads to an analytical IR model as is presented in equation (5.9) the generation for the production of numerical results are made in Matlab, the script is given in Appendix B.1. In Equation (5.9) equation (5.6) is inserted in equation (5.4) and the decay terms are written out.

$$h_{env}(t) \approx \frac{\sqrt{Q}}{r} e^{at/T_{peak}} + \frac{1}{r_c} e^{at/T_{room}} \tag{5.9}$$

Where parameters are the same as above, and a is the decay constant valued 3ln(10).

5.2 Analytical room in room impulse response model

To complete the model as proposed in [11] (i.e. equation (3.14)) a peak is added to the basic IRs according to the ideas in the previous section. This results in equation (5.10):

$$h_{env;conv}(t) \approx h_1(t) * h_2(t) = (D_1 e^{p_1 \cdot t} + R_1 e^{x_1 \cdot t}) * (D_2 e^{p_2 \cdot t} + R_2 e^{x_2 \cdot t}) \tag{5.10}$$

Where $h_{12}(t)$ is the IR_{RinR} and * is the sign for convolution, the solution for this convolution is:

$$h_{env;conv}(t) \approx D_1 D_2 \frac{e^{p_1 t} - e^{p_2 t}}{p_1 - p_2} + D_1 R_2 \frac{e^{p_1 t} - e^{x_2 t}}{p_1 - x_2} + R_1 D_2 \frac{e^{p_2 t} - e^{x_1 t}}{p_2 - x_1} + R_1 R_2 \frac{e^{x_1 t} - e^{x_2 t}}{x_1 - x_2}$$
$$\tag{5.11}$$

Where the parameters are the same as in previous equations, the derivation of this equation is given in Appendix A; the Matlab script is given in Appendix B.2. With this equation, trends can be investigated, similarly to equation (3.14). Similar is the way in which it overestimates the effects of RinR acoustics as it is made up of continuous functions. Again, the solution could be the modulation with a noise sequence in both signals (see section 5.3).

The different RinR scenarios are present in the equation. There are four terms, looking at the factors preceding them (i.e. the distribution of direct and diffuse terms) it can be seen how the process works. The peak is represented by an ideal impulse to show this process, so the equation becomes:

$$h_{env;conv}(t) \approx \lim_{\delta \to \infty}{}^{**} D_1 D_2 \delta(t) + D_1 R_2 e^{x_2 t} + R_1 D_2 e^{x_1 t} + R_1 R_2 \frac{e^{x_1 t} - e^{x_2 t}}{x_1 - x_2} \tag{5.12}$$

**Limit is when the decay term in the peak approaches infinity, the decay term of the reverberant field is unaltered

It can be seen that the two terms in the middle are the exponential decays amplified by the peak of the other room It is known that reproducing reverberant fields is without significant differences if $T_1 \geq 2T_2$ [2]. It is assumed that $T_{room} >> T_{peak}$, therefore, the two terms in the middle resemble the decay characteristic of the respective IRs closely, i.e. in equation (5.11). The first term is, in equation (5.12), the ideal impulse, in section 5.1 it is discussed that this is not realistic.

Every room IR will have either a dominant direct or diffuse proportion, except when an IR is measured close to the critical distance. This would give rise to 9 scenarios, however, then the RT ratio is ignored. Equation (5.11) is graphed for the 9 scenarios when $T_1 = T_2$ in table 5.1 and for T_1

= 2.7 T_2 in table 5.2. The graphs show that to obtain a peak in the listening room, both IR_{rec} and IR_{list} must have a peak on their own, in other words, the direct proportions need to be dominant. In the introduction, a table is shown where these nine scenarios are given with examples.

The ratio chosen to represent the respective amplitudes for the direct and diffuse fields is 1 to 20. So if the direct field is presented dominant, parameter D in equation (5.11) is 20 times bigger than parameter R and vice versa.

Table 5.1 *the nine RinR scenarios, this is the same table as in the introduction $T_1 = T_2$ 1 corresponds to the recording room and 2 with the listening room.*
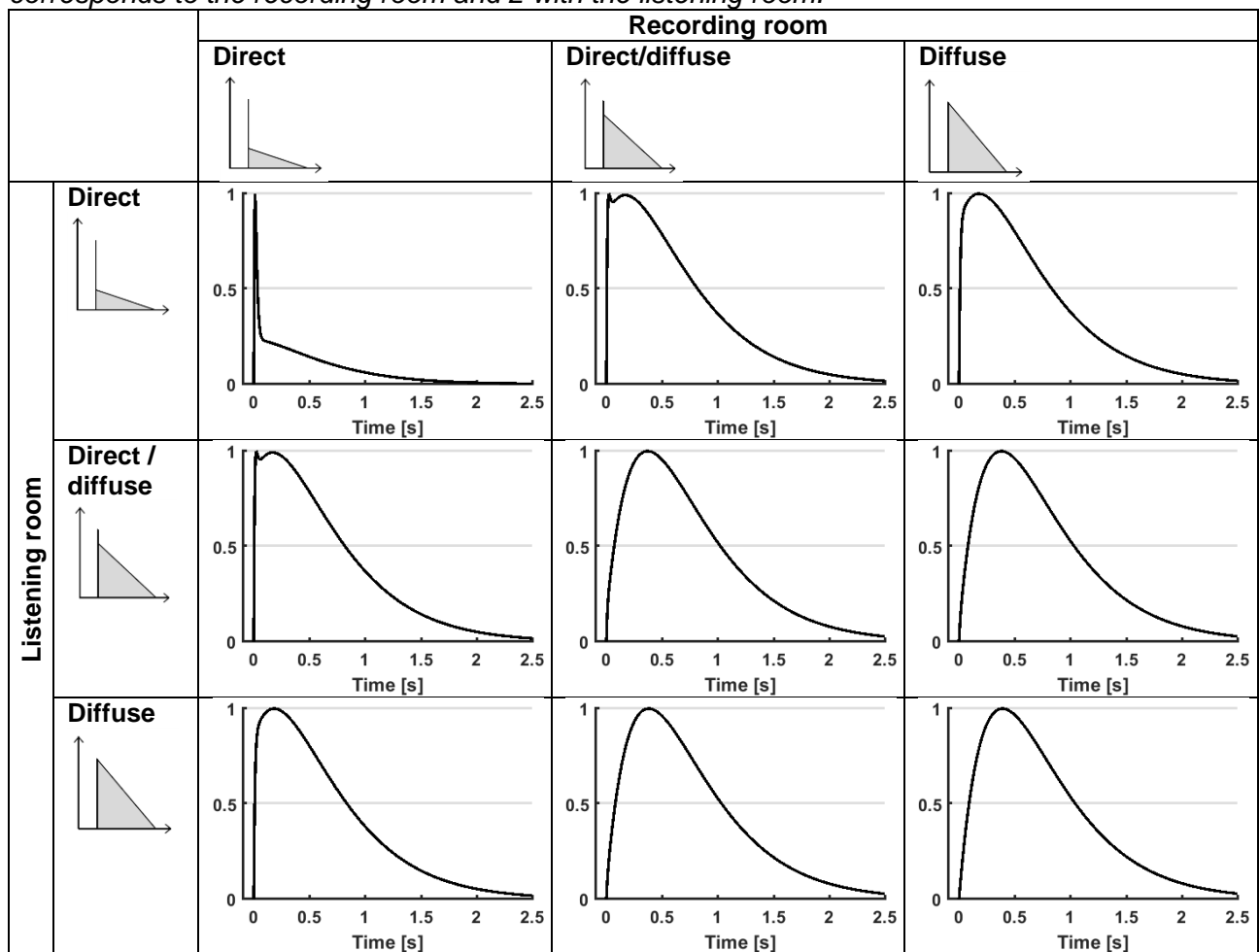
A small peak can be observed in the second graph as well (Direct - Direct/diffuse). This is a special case because this is not a peak but rather the decay from one of the two exponential decay terms in the middle of equation (5.11), see equation (5.12) and the explanation below. This scenario results in a double-sloped decay curve similar to what can be found in coupled rooms (shown in section 7.1).

Table 5.2 *the nine RinR scenarios, this is the same table as in the introduction $T_1 = 2.7 \, T_2$*
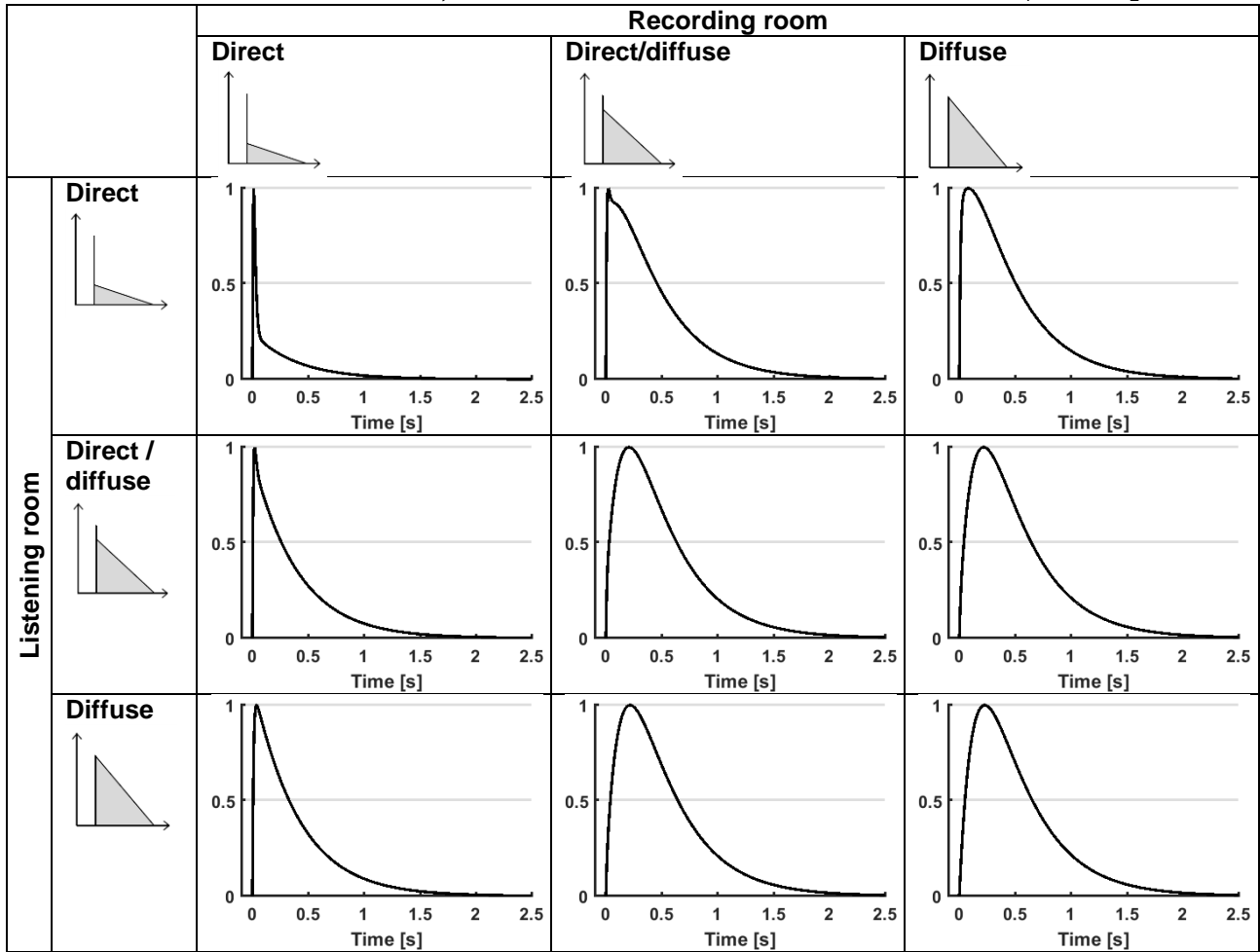
5.3 Modulation with noise

Similarly, as the equations for the IR$_{RinR}$ without direct sound, the RinR acoustics effects are overestimated due to the convolution of continuous functions. This overestimation can be solved by applying a modulation with white Gaussian noise of the single room IRs. If this modulation is applied to equation (5.4), the resulting equation is:

$$h(t) = (D \cdot e^{p_1 t} + R \cdot e^{x_1 t}) \cdot wgn(t) \tag{5.13}$$

Where h(t) is the IR for either the listening or the recording room, x is -a/T, a is the decay constant valued 3ln(10), T is the reverberation time, t is time, wgn(t) is a Gaussian white noise sequence, D is the amplitude of the peak and p is the decay term for the peak. It should be noted that modulating both the IR$_{lsp}$ and room IR with the same noise sequence is probably incorrect. However, the period where the influence of both parts is significant is concise and is therefore assumed to be of no significant influence on the results.

Working with Matlab, a string of Gaussian white noise was multiplied with the signal in the time domain. However, even with the addition of white noise strange values for the peaks and decay curves were noticed (i.e. when compared to measurements). Therefore when convoluting two IRs, both are multiplied with a different noise signal.

The first noise signal is the Matlab function add white Gaussian noise (awgn), the other is based on the (uncorrelated) pseudo-random number generator (rand):

$$wgn(t) = (rand(t) - 0.5) \cdot (\sqrt{3} \cdot 2) \tag{5.14}$$

Where rand(t) is the random number function in Matlab, -0.5 is so that the mean is 0, √3*2 is so that the standard deviation is 1. These values correspond to the 'awgn' function of Matlab.

Figure 5.3 shows T_{30} for the model with and without noise sequences to demonstrate that this overestimation is indeed solved, with the addition of noise to IR_{rec} and IR_{list}. These reverberation times are compared to values measured in the reverberation room. For this comparison, only scenario 3 and 4 are used because the calculation of reverberation time parameters should ideally be done outside of the critical distance. The figure demonstrates the overestimation for the model without noise and shows good agreement with the model with noise.
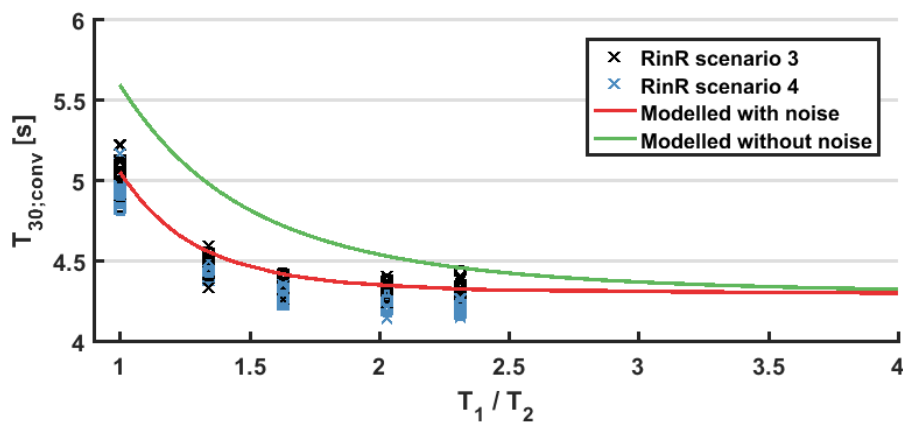
Figure 5.3 *reverberation times for the convoluted impulse responses, modelled and measured, results are from the 1 kHz octave band, all measurement positions further than 1.45m are included, both big box and small box are included.*

5.4 Numerical results from the model

The deviations caused by RinR acoustics are expressed in room acoustical parameters as presented in section 4.3. These equations are applied to the model in a Matlab script as presented in Appendix B.3.

The model is used to study the combined effect of the RT ratio and the difference in direct sound level as expressed by the initial drop. To create a complete set of parameters the input values of the IR_{list} are manipulated to have a broad range of reverberation times and a broad range of direct sound levels. The process is indicated by means of a flowchart in figure 5.4.
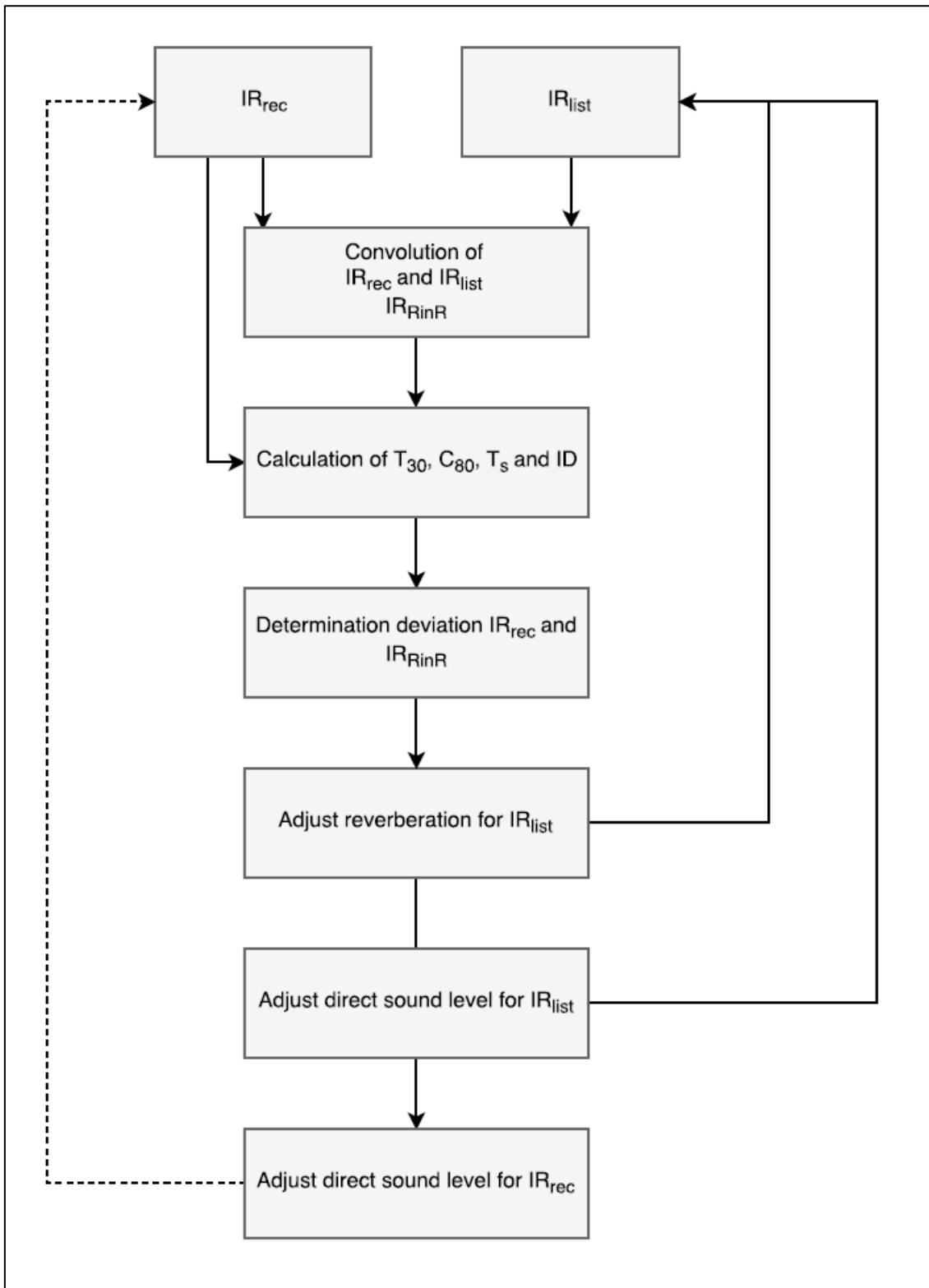
Figure 5.4 *Flowchart for the numerical study IR_{rec} and IR_{list} are created with equation (5.13), the dashed line indicates that the step is optional.*

6 Model validation

The model in this study is made using Matlab 2016a. The goal of the model is to produce results for a trend analysis and to give an insight in the deduction of the mechanism how RinR acoustics influences acoustical parameters. The model predicts the behaviour of room acoustical parameters when the ratio of RT is changed and when the difference of direct sound level is changed. The model with noise modulation is used in a numerical study, the script for the model can be found in Appendix B.3.

6.1 Single room impulse response

The analytical single room impulse response is made according to equation (5.9), in figure 6.1 this equation is plotted against time. Values for the parameters are as given in section 4.1. As said before, to obtain realistic results from the model after convolution, it is necessary to have the equation modulated with a noise sequence as is done in figure 6.1.
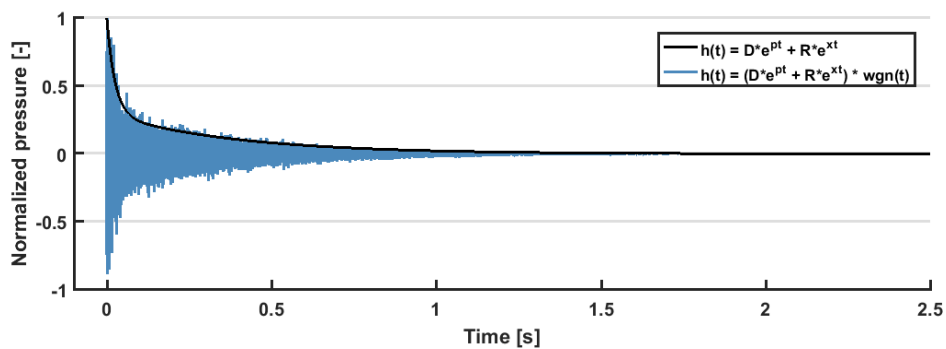
Figure 6.1 plot of equation (5.9) normalized and of equation (5.13) normalized

Figure 6.2 shows two decay curves for the measured and modelled IR. Although the peaks do not resemble each other, their order of magnitude is equal. Therefore when energy ratios are calculated all the energy in the peak is taken into account and makes this model valid for these determinations (e.g. Clarity).
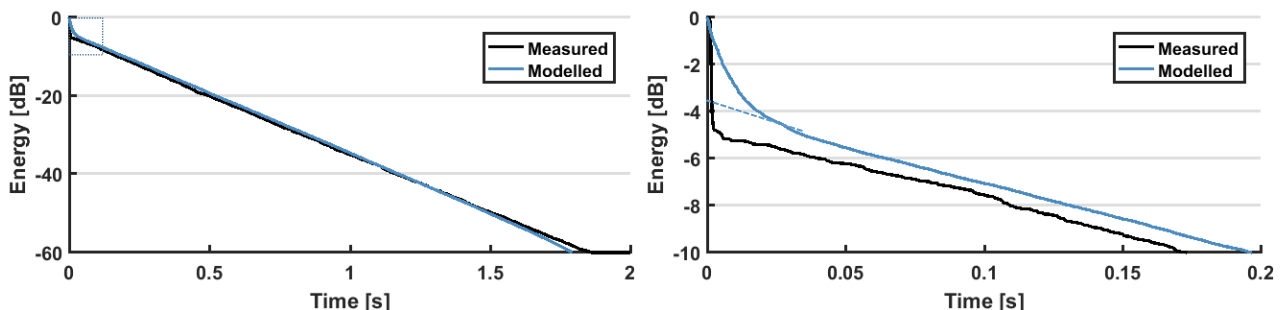
Figure 6.2 Measured and modelled decay curves for 2 kHz octave band at 35 cm from the source in the 3 baffle scenario. The dashed part indicates the diffuse field compensation for the ID determination.

Model validation

The difference in shape at the peak showed in figure 6.2 stems from the choice to present the peak as an exponential function. It is possible to make the peak resemble the measured peak, this would, however, cost in accuracy for all other parameters, i.e. the ratio between direct and diffuse in equation (5.9) would be incorrect.

Figure 6.3 shows the ID against the source-receiver distance for 1 kHz big box and 4 kHz small box, a slight overestimation of the effects of the absorption can be seen. It can also be concluded that the decrease of the direct sound level with distance is modelled in accordance with reality.
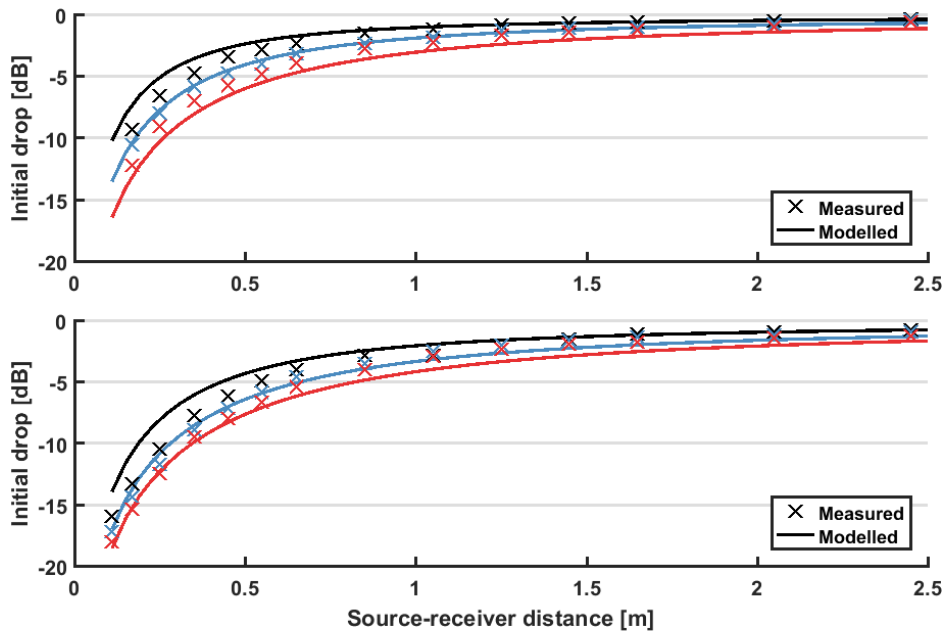
Figure 6.3 *initial drop against the source-receiver distance. Top: 1 kHz octave band, bottom: 4 kHz octave band. The different colours are the baffle scenarios; black is 0 baffles, blue is 2 baffles, and red is 4 baffles. The solid lines are from the model; the crosses are measurement positions.*

To prove that the model yields realistic results the clarity is plotted against the initial drop, calculated from both the measurements and from the model, see figure 6.4. The figure indicates that the trend for C_{80} is equal for the modelled and the measured results. It also shows that the model indicates the minimum for C_{80} given an Initial Drop value.
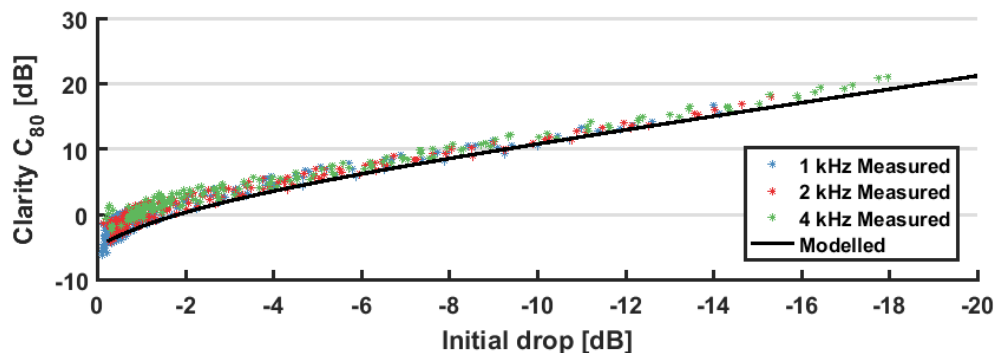
Figure 6.4 *Clarity against initial drop for the model and the measurements. All measurement position in the laboratory are included, i.e. 170 measurement positions times in 3 octave bands.*

The model is also predicting the influence of different absorptive scenarios for centre time correctly. In figure 6.5 the different colours indicate the different baffle scenarios. Moreover, centre time is chosen as a parameter, which is to show the model not only works for SR distance but also for various absorptive scenarios. In the figure, the directivity is fitted to the measurement.

It should be noted that not for all octave bands the same accuracy is attained, on some occasions the direct sound level seems to be systematically overestimated. This raises questions to the accuracy of the directivity measurements, see section 4.1.8. In all cases, the values reach a close agreement after the critical distance. This is a strong indication that the decay is modelled in accordance with reality.
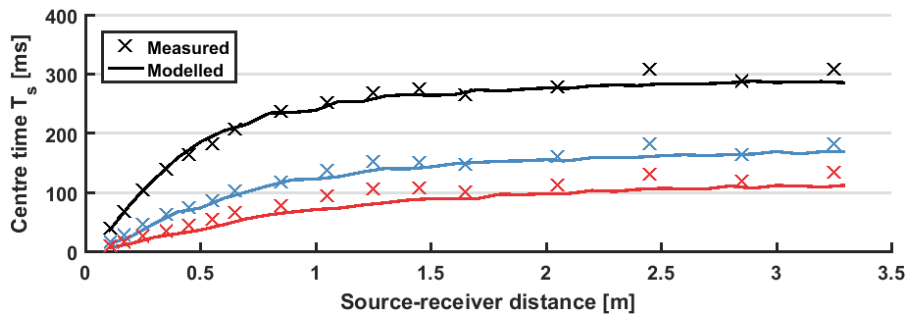
Figure 6.5 *Centre Time against source-receiver distance for the model and the measurements. 1 kHz octave band configuration with small box loudspeaker. The different colours are the baffle scenarios; black is 0 baffles, blue is 2 baffles, and red is 4 baffles. The solid lines are from the model; the crosses are measurement positions.*

6.2 Decay curves of a room in room impulse response

The reverberation time is calculated using the decay rate in the decay curve; this decay rate matches the measurements closely. This means that the reverberation time in the IR_{RinR} is predicted well within the bounds of the JND by the model, see figure 5.3 for a comparison with measurements. In figure 6.6, 2 decay curves are plotted for the 2 kHz octave band.
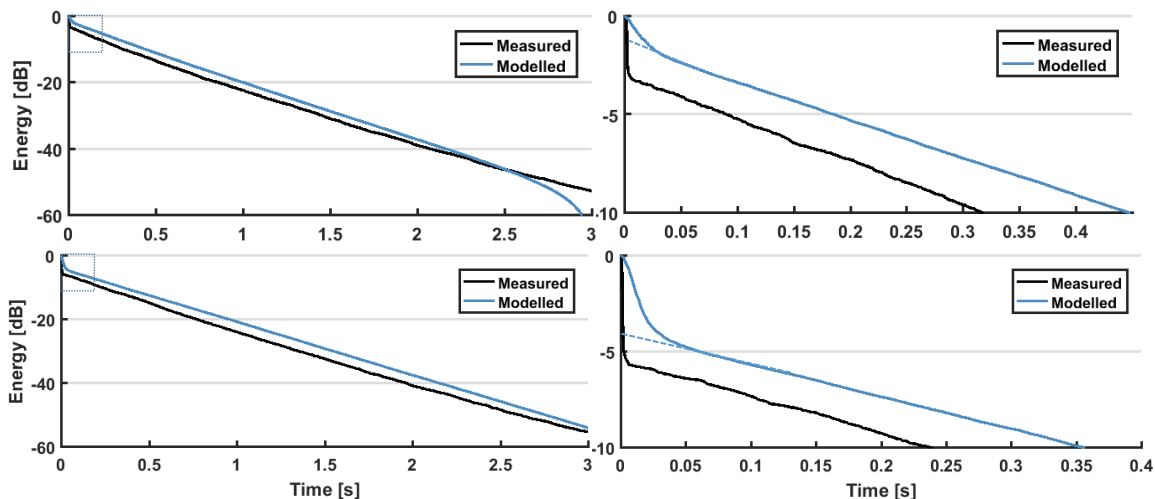
Figure 6.6 *2 kHz octave band decay curves for modelled and measured IR_{RinR}; Top: 2 baffle scenario at 0.55 m from the source. Bottom: RinR scenario 1, listening room 1 baffle, SR = 0.17 m at. The dashed parts indicate the diffuse field compensation for the ID determination.*

Figure 6.6 shows that the peak is underestimated. Some of this deviation can be assigned to the measurement uncertainty as discussed in section 4.1.8. Furthermore, the model uses a single value as decay rate for the peak; it may very well be that this rate is frequency dependent.

6.3 Reverberation time of a room in room impulse response

Figure 6.7 shows the reverberation time of the convoluted impulse response as a function of the reverberation time in the recording and listening room. The parameter for determination of the reverberation time is T_{30}; the impulse responses are modelled to have a dominant diffuse field.
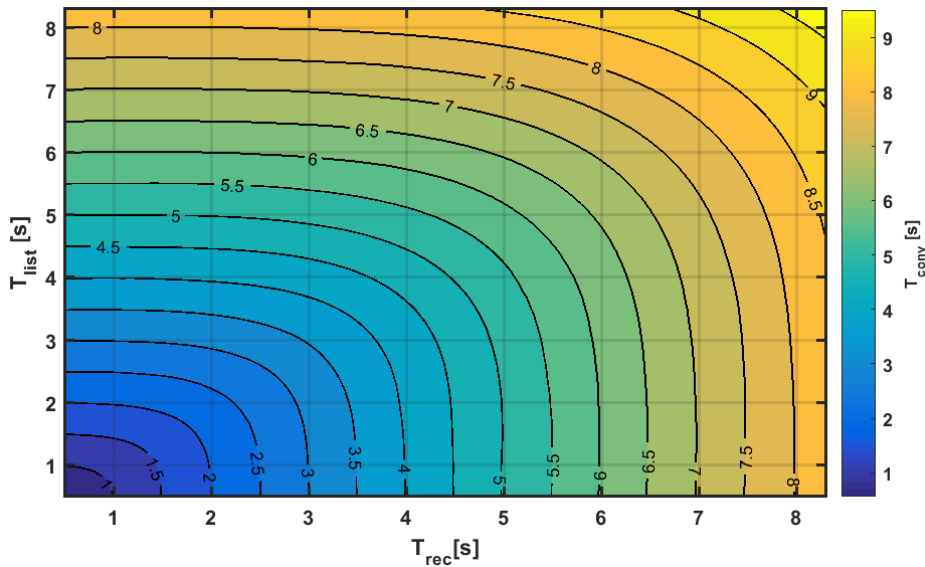
Figure 6.7 Contour plot for the reverberation time as a result of RinR acoustics

The comparison with the measurements is presented in figure 5.3.

6.4 Initial drop of a room in room impulse response

Figure 6.8 shows the initial drop of the convoluted impulse response as a function of the initial drop in the recording and listening room, ID_1 and ID_2 respectively. The effect of the direct sound fields of the recording and listening room on the convoluted ID can be seen. There is no difference when the ratio of the RTs is changed or when the width of the peaks is changed. For the model, the ID is calculated as the value of the Schroeder decay curve at 0.05s compensated for the decay rate.
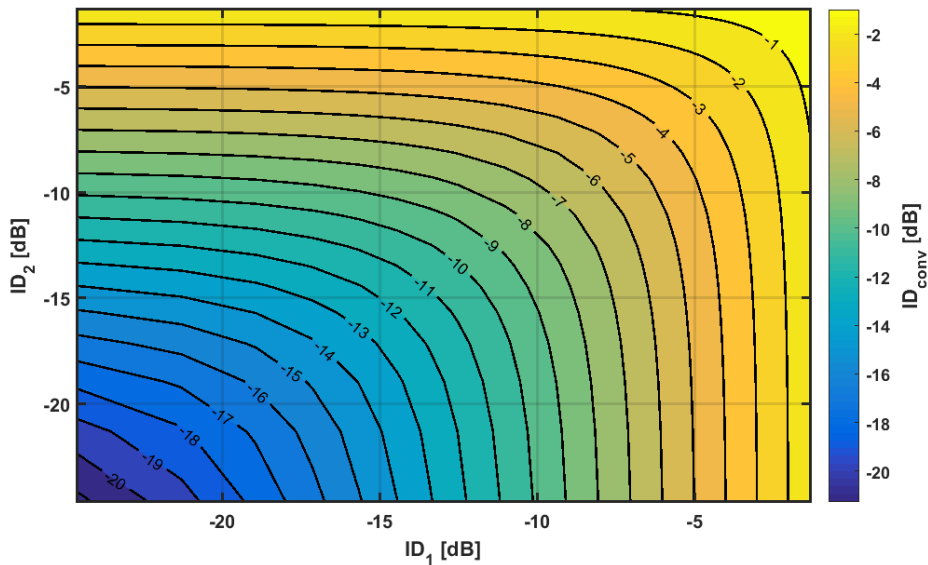
Figure 6.8 *Contour plot for initial drop as a result of RinR acoustics*

In the figure, it is seen that the ID of an IR_{RinR} is never higher than the ID in the IR_{rec} or IR_{list}. Figure 6.9 shows that the model is in close agreement with the measurements in the laboratory, measurements from all absorption scenarios for the 4 kHz octave band are presented. The close fit indicates that the ratio of RTs is not influencing the peak of the IR_{RinR}.
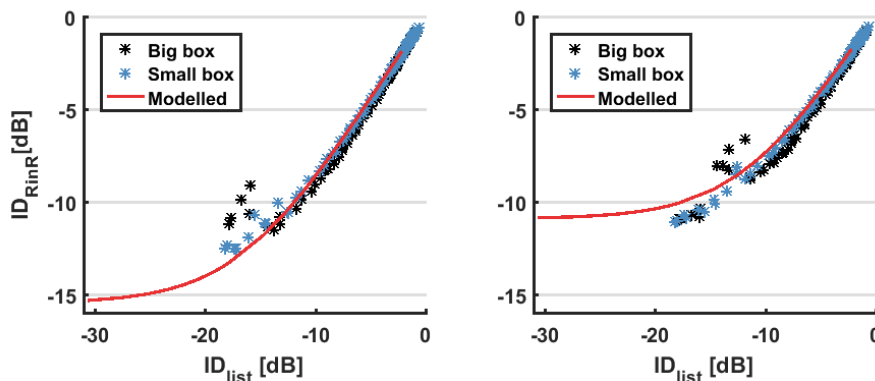
Figure 6.9 *Numerically modelled, and measured initial drops for the IR_{RinR}, left is RinR scenario 1 where the ID in the recording room is 15.8 dB, on the right the ID in the recording room is 11.7 dB. Measurement points are from all absorption scenarios.*

6.5 Energy-related parameters of a room in room impulse response

The start point for calculations of C_{80} if t = 0s this can be done because there is no delay or noise floor added to the model. Figure 6.9 shows a self-convoluted peak; this is done to show the decay the peak has in the IR_{RinR} of the model. Points are indicated for 0.05s and 0.08s.
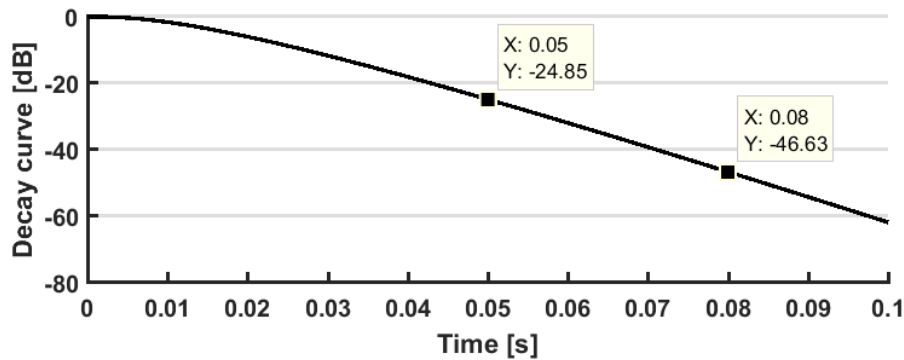
Figure 6.9 *Decay curve resulting after self-convolution for the peak, the data points indicate the maximum ID for which respectively the ID and C_{80} can be calculated for the model.*

0.05s corresponds to the point where ID is calculated in the previous section. With that methodology values approaching 24.5 dB are not accurate because the peak is wider than the time window. Using the diffuse field compensation as proposed in equation (4.16) an evaluation point much later can be chosen, as long as it is in the diffuse part of the decay curve. Note that calculating the decay rate for this compensation must also be done after the peak.

The value at 0.08s corresponds with the maximum value for ID where C_{80} can safely be calculated. This is sufficient for any value presented in this thesis.

6.6 Strengths and limitations of the model

The model shows promising results, some strengths of the model are:
- The model is an elegant analytical equation, the convolution of the equation is done numerically;
- To use the results only the ID and RT of the recording and listening positions have to be known, these can be obtained directly from the IR as defined by the model.

Some oversimplifying assumptions are made. For example:
- The reverberation tail is assumed to be perfectly diffuse; this is a non-existing condition;
- The model does not take any modal behaviour into account, and will therefore only produce valid predictions for frequencies above the Schroeder frequency;
- The width of the peak is an average decay rate over the first 0.05s over many impulse responses used in this research. The peak width is different for different sources and different frequencies;
- The model is independent of frequency;
- It is a biased model; the model is fit to the measurements used to validate;
- There were not enough different sources to validate the directivity factor, combined with an inaccurate measurement;
- White noise is used instead of reflections.

7 Results & discussion

In this chapter, the results are presented together with the discussions that arise from them. Then the model is used to show the effects of RinR acoustics on the shape of the IRs. The second section is about the calculation of T_{20} and T_{30} from the IR_{RinR}. The last sections are the parameter deviations resulting from the laboratory measurements and the deviations observed in the model.

7.1 Principle methods for reducing room in room effects

Figures 7.1 to 7.4 present the two principle methods that can be used to reduce the influence of RinR acoustics. The first method is decreasing the reverberation time in the listening room and thus increasing the ratio T_1/T_2 (figures 7.1 and 7.3), the second method is increasing the direct sound level in the listening room (figure 7.2 and 7.4). In the figures, three rows of graphs are shown. The top row shows the relative pressure amplitude; the middle row shows the energy time curve (ETC) that follows after equation (4.13) and the bottom row shows the decay curve as defined by equation (4.9).
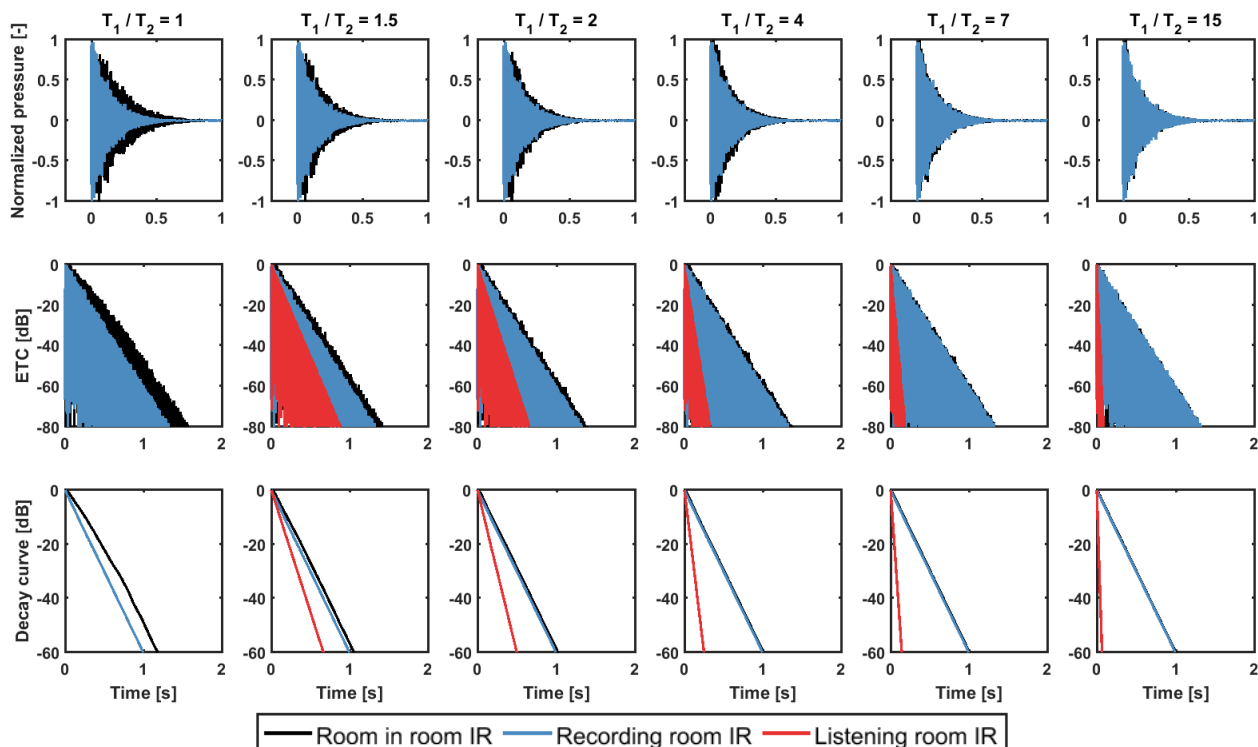
Figure 7.1 *Results for the convolution of two exponential functions that represent IRs in the diffuse field of a room, no direct sound is included. Top row relative pressure amplitude, middle row energy time curves and bottom row decay curves. Black represents the IR_{RinR}, blue the recording room IR and red the listening room IR. Red line is not shown in the first row for readability of the graph. The red curve is not showing in the first figure of the ETC and the decay curve since it would be overlapping exactly with the blue curve.*

Results & discussion

Figure 7.1 shows the effect of decreasing the reverberation time in the listening room. The decrease is indicated using T_1/T_2, where T_1 is the reverberation time in the recording room. Subsequently, T_2 is the reverberation time in the listening room. With decreasing reverberation time in the listening room, the IR_{RinR} becomes progressively similar to the IR_{rec}. The concave shape of the decay curve for the IR_{RinR} is visible; it can be seen that the concavity decreases with decreasing reverberation time in the listening room. To hear (judge) a recording in a listening room the listening room should have a lower reverberation time [2], [5] thus a listening room with longer reverberation time is not included in the graph.

Similarly, figure 7.2 shows a sequence of increasing direct sound levels in the listening room. The direct sound is indicated by the initial drop (ID). Again with increasing direct sound, the IR_{RinR} shows more significant similarity to the IR_{rec}. The difference with the other method is that the concavity is unaltered, apart from the whole IR_{RinR} being shifted towards the origin. Note that the most apparent concavity is at the beginning of the curve.
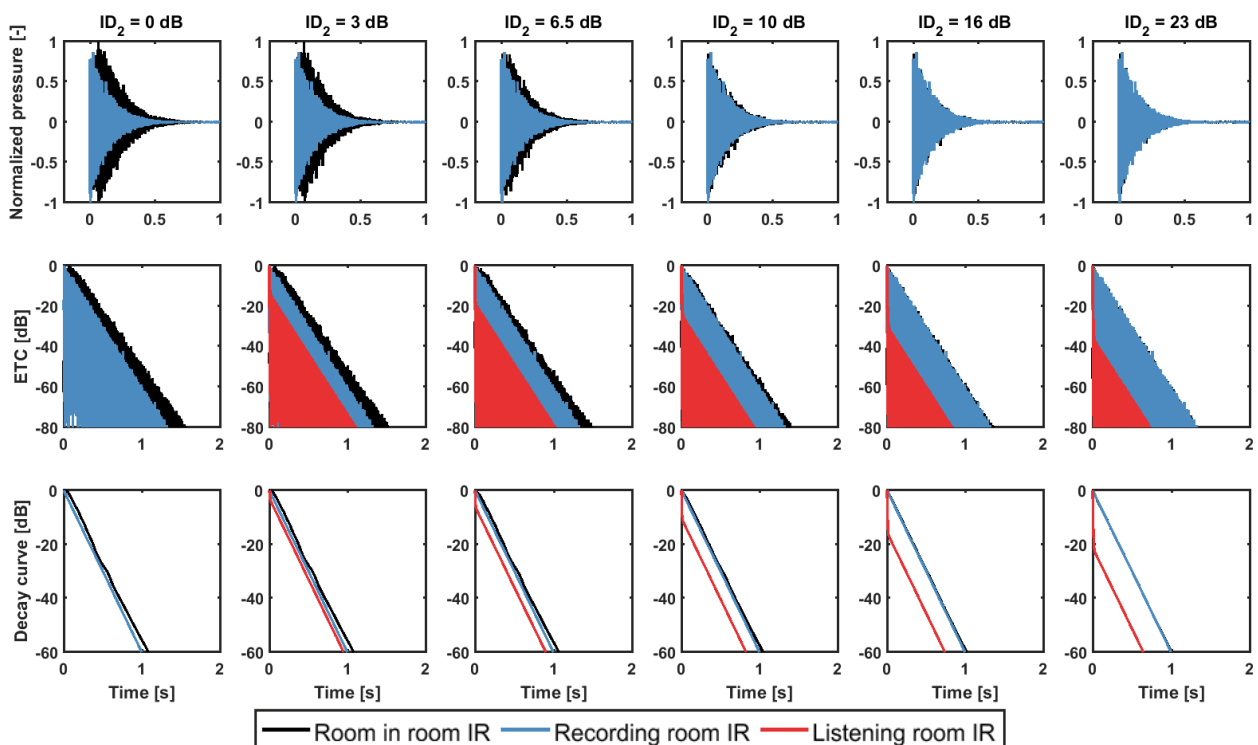
Figure 7.2 Results for the convolution of two exponential functions that represent an IR in the diffuse field (IR_{rec}) and an IR in the direct field of a room (IR_{list}). Top row relative pressure amplitude, middle row energy time curves and bottom row decay curves. Black represents the IR_{RinR}, blue the recording room IR and red the listening room IR. Red line is not shown in the first row for readability of the graph. The red curve is not showing in the first figure of the ETC and the decay curve since it would be overlapping exactly with the blue curve.

The same process is repeated for an IR_{rec} with direct sound, (ID = 16 dB). Striking is how the direct sound in the IR_{RinR} is always less pronounced than in IR_{rec} and IR_{list}. Figure 7.3 shows what happens when the reverberation time in the listening room is decreased. This image shows a double slope decay curve as found in coupled spaces [20].

Figure 7.4 shows what happens when the direct sound is increased in the listening room when listening to an IR_{rec} with direct sound, (ID = 16 dB). The peak in the IR_{RinR} will never be bigger than the lower of the two involved peaks.
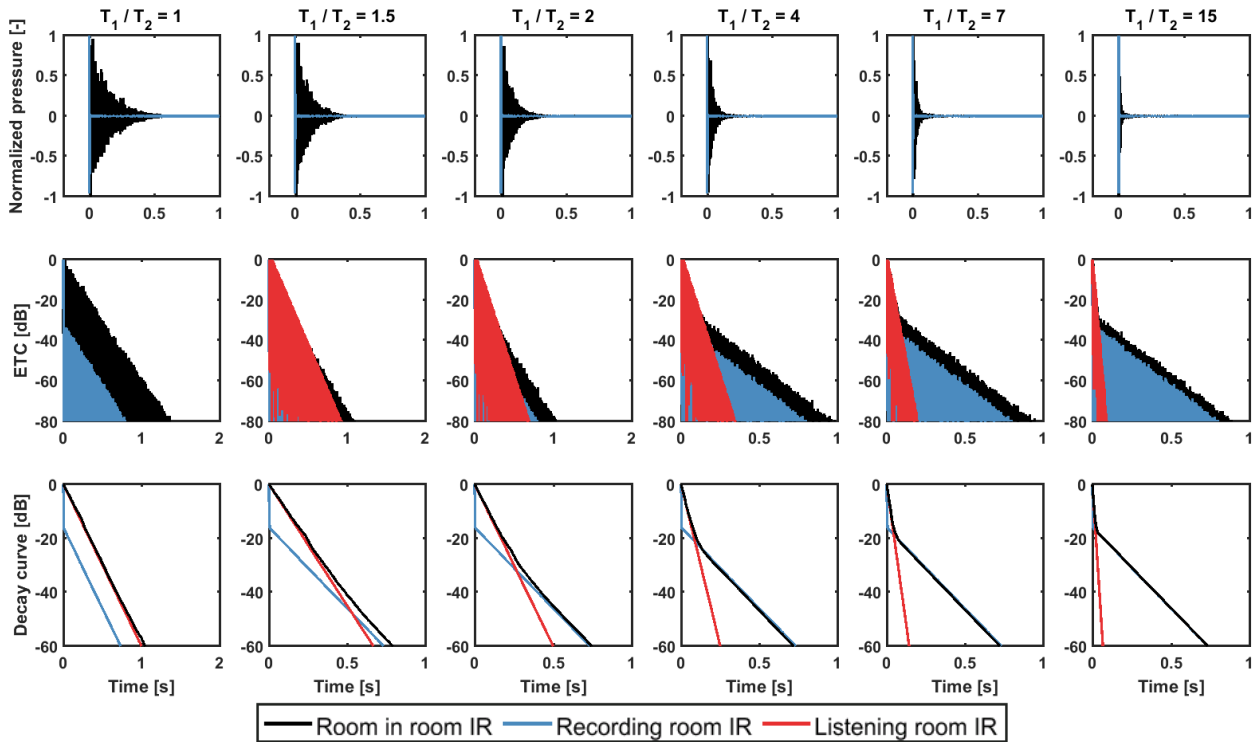
Figure 7.3 *Convolution of two exponential functions that represent IRs in the direct field and an IR in the diffuse field of a room. Top row relative pressure amplitude, middle row energy time curves and bottom row decay curves. Black represents the IR_{RinR}, blue the recording room IR and red the listening room IR. Red line is not shown in the first row for readability of the graph. The red curve is not showing in the first figure of the ETC and the decay curve since it would be overlapping exactly with the blue curve.*
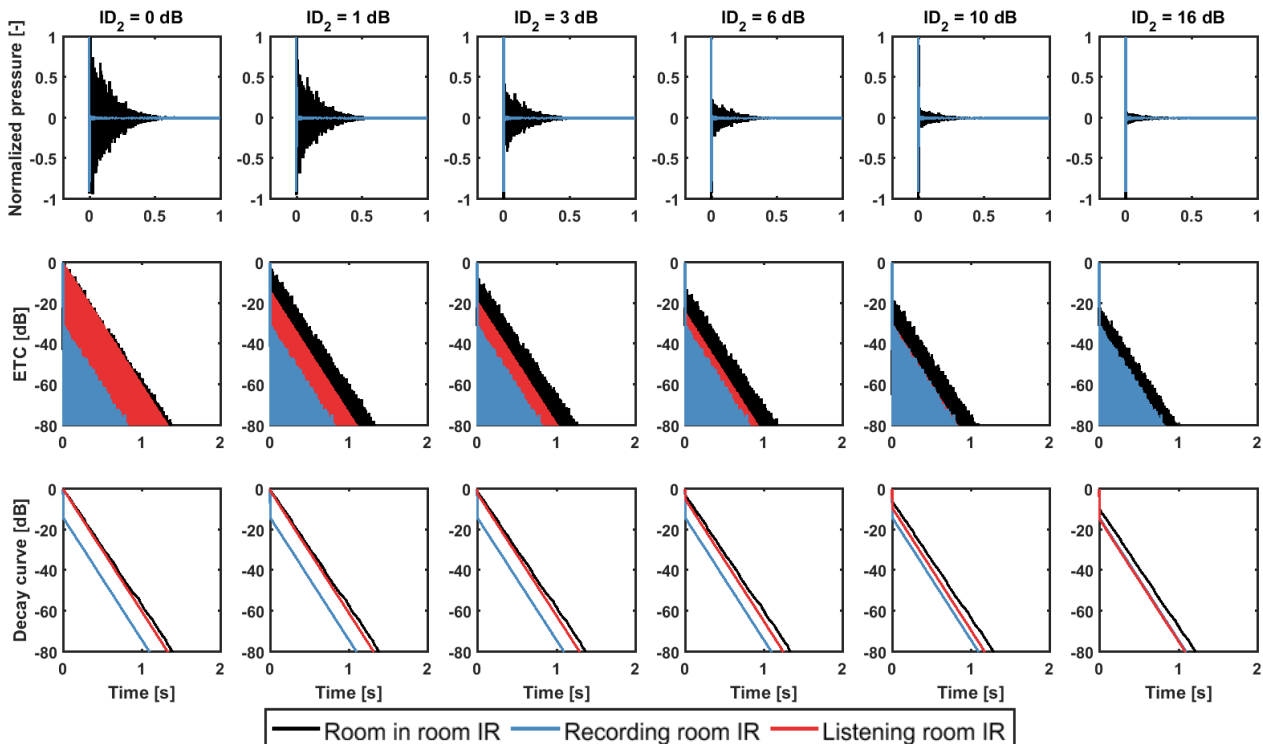
Figure 7.4 *Convolution of two exponential functions that represent IR's in the direct field. Top row relative pressure amplitude, middle row energy time curves and bottom row decay curves. Black represents the IR_{RinR}, blue the recording room IR and red the listening room IR. Red line is not shown in the first row for readability of the graph. The red curve is not showing in the last two figures of the ETC since the blue curve would overlap it.*

The figures in this section confirm that with decreasing the reverberation time or increasing the direct sound in the listening room, the deviation between the IR_{RinR} and the IR_{rec} decreases. In the case of decreasing the RT, the concavity of the decay curve is affected as well, while this does not occur when increasing the direct sound. The IR_{RinR} does not have a peak unless both IR_{rec} and IR_{list} have a peak. Similar to reverberation time, the direct sound level in the listening room must be higher than the peak in the recording room to reproduce it.

7.2 Calculating reverberation time from the room in room impulse response

When the curvature parameter (equation 4.16) is calculated for the IR_{RinR} used in this research, it becomes clear that not all decay curves have a concave shape. Figure 7.6 shows a boxplot of the curvature parameter for the measurements done in the Echo laboratory and the Gymnasium (see: [7], [12] for details on the Gymnasium measurements). All values for T_{20} and T_{30} are calculated in Dirac 6.0.
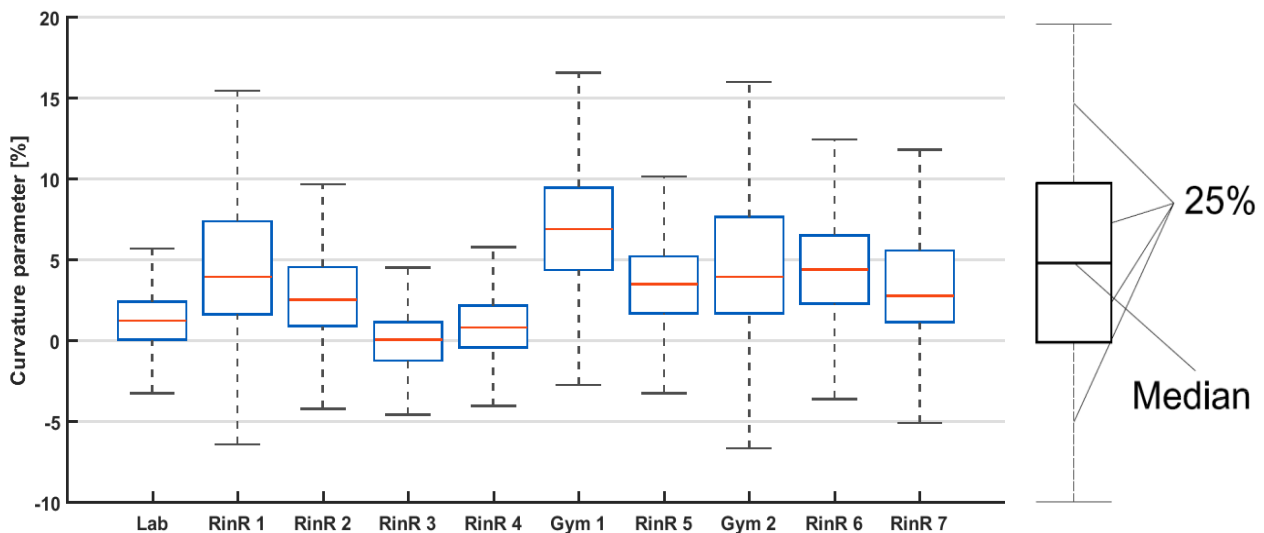
Figure 7.6 *Boxplot of the curvature parameter for the IR measurements performed in the Echo laboratory and the IR_{RinR} that are created with these measurements. N >400 comprised of all measurement positions available and octave bands above the Schroeder frequency. See table 7.1 for the explanation of the x-axis.*

When reviewing RinR scenarios at a diffuse position in the reverberation chamber (RinR 3 and 4 in the boxplot). The curvature parameter ranges between -6% and 6%, for octave bands above the Schroeder frequency. This is not very unlike values for the single room IR which range between -4% and 8% (Lab in the boxplot). Although literature strongly suggests that the reverberation time is not defined for an IR_{RinR} as the decay is not exponential, the numbers here show that the deviation from exponential is not more significant in IR_{RinR} than in regular single room IRs.

The figure confirms that based on the curvature parameter, it is safe to calculate a reverberation time for an IR_{RinR}. Another interesting conclusion that can be drawn from the boxplot in figure 7.6 is that the IR_{RinR} decay curves are not by definition concave, in fact, the majority shows to be convex.

Table 7.1 *Explanation of the x-axis for figure 7.6: Lab is the measurement as described in section 4.1 and consists of 170 measurement positions, RinR 1 to 4 are the scenarios described in section 4.5 and each consist of 170 positions as well, Gym 1 is the measurement in the gymnasium with a dodecahedron source, RinR 5 is a RinR scenario in the gymnasium, Gym 2 and RinR 6 to 7 are the same but measured with the bigbox and the RinR scenarios are convolutions with a dodecahedron and the bigbox respectively. RC is the reverberation chamber at the Eindhoven University of Technology*

Axis label	Recording position	Listening room	N
Lab	-	RC (5 absorptive scenarios, 2 boxes, 17 positions)	680
RinR 1	0.15m from the source in the RC	RC	680
RinR 2	0.25m from the source in the RC	RC	680
RinR 3	3.25m from the source in the RC	RC	680
RinR 4	3.25m from the source in the RC, source rotated 160°	RC	680
Gym 1	-	Gym 1 (dodecahedron speaker)	480
RinR 5	10m from the source in the Gym 1	Gym 1	480
Gym 2	-	Gym 2 (big box speaker)	480
RinR 6	10m from the source in Gym 1	Gym 2	480
RinR 7	10m from the source in Gym 2	Gym 2	480

7.3 Reverberation time deviation

In figure 7.7 the deviation in percentage in T_{30} is shown as a function of the ratio between RTs in the recording and listening room and the difference in ID. Upper left shows a 3D view of the combined effects of direct and reverberant fields. Upper right shows the influence of RT ratio on the ID. At the same measurement position, the direct sound level is higher for lower reverberation times. The bottom row indicated the deviation of T_{30} under the influence of RT ratio and direct sound level difference. The figures are created using the model.

Figure 7.7 shows that the deviation in T_{30} is primarily dependent on the ratio between the RTs of recording and listening room. The decreasing deviation with increasing difference in ID is a result of the calculation process. If the peak is higher than 5 dB, the first point for linear extrapolation is located on the peak leading to a steeper decay rate, causing an underestimated value for T_{30}. This underestimation is visualized in figure 7.8.
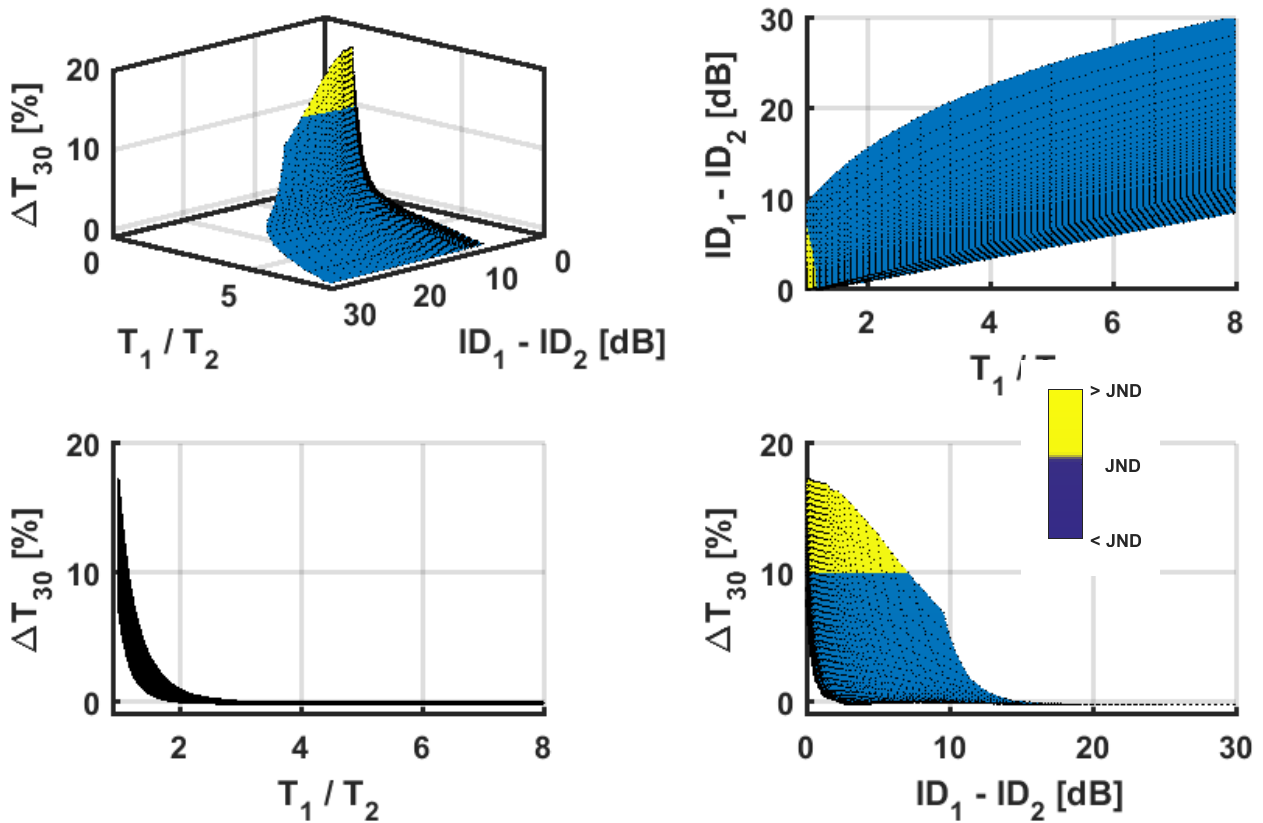
Figure 7.7 *Surace plot of deviation in reverberation time as a result of RinR, yellow indicates that the deviation is above the JND. T_1/T_2 is the ratio of reverberation times and $ID_1 - ID_2$ is the difference in initial drop between the recording and listening room*
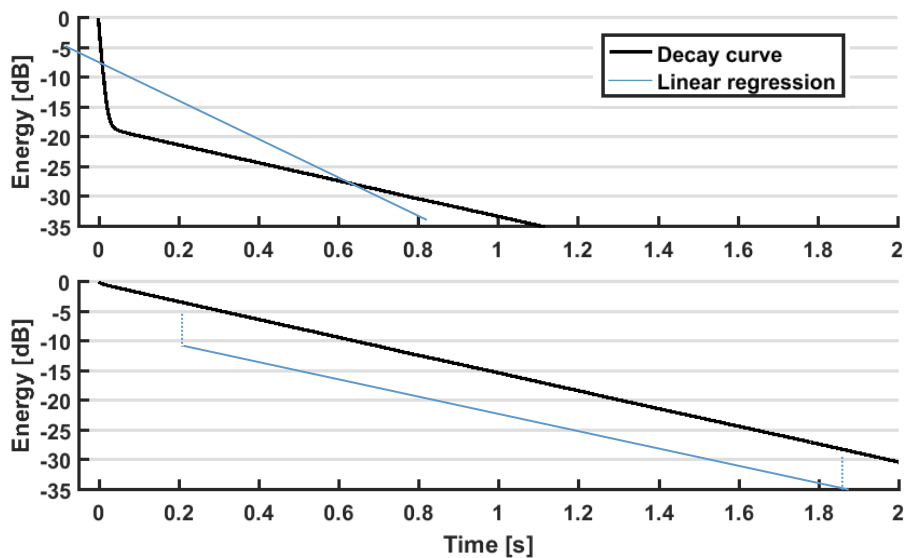
Figure 7.8 *two decay curves, the blue line indicates the linear extrapolation used to determine T_{30}. Both decay curves have a reverberation time of 4s.*

To reproduce reverberation time within 1 JND (i.e. 10%) the ratio T_{rec}/T_{list} should be 1.2. In figure 7.9 a comparison is made with the measurements performed in the laboratory. The model shows good agreement with the measurements. It also shows that the deviation in T_{30} spreads out for the measurements.
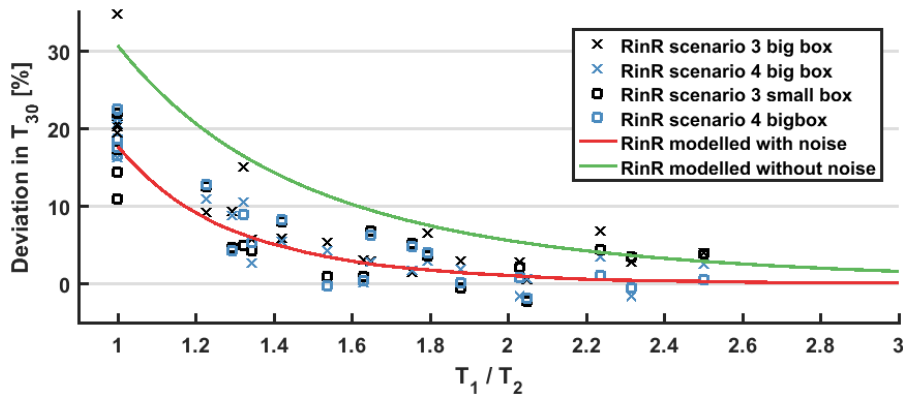
Figure 7.9 *Deviation in reverberation time for measurements and the model with and without noise modulation of the single room IRs. Measurements for the octave bands 500 Hz, 1 kHz, 2 kHz and 4 kHz are included.*

Curve fitting to the red line in figure 7.9 lead to equation (7.1). With this equation, the absolute reverberation time (decay rate) for the IR$_{RinR}$ can be estimated, equation (7.2).This equation corresponds to the curve shown in figure 5.3.

$$\Delta T_{30} = 0.18 \cdot \left(\frac{T_{30;rec}}{T_{30;list}}\right)^{-3.73} \cdot 100 \ [\%] \ for \ T_{30;rec} \geq T_{30;list} \tag{7.1}$$

Where ΔT_{30} is the percentage deviation of T_{30}, $T_{30;rec}$ and $T_{30;list}$ are the reverberation times in the recording and listening rooms respectively. To find the reverberation time in the RinR scenario

$$T_{30;RinR} = T_{30;rec} \cdot \left(1 + 0.18 \cdot \left(\frac{T_{30;rec}}{T_{30;list}}\right)^{-3.73}\right) \ [s] \ for \ T_{30;rec} \geq T_{30;list} \tag{7.2}$$

7.4 Initial drop deviation

From the graph in figure 6.8 and the curve in figure 6.9, a relation between ID$_{rec}$, ID$_{list}$ and ID$_{RinR}$ can be observed[9].

$$ID_{RinR} = 10 \cdot \log_{10}\left(10^{ID_{rec}/10} + 10^{ID_{list}/10}\right) \ [dB] \tag{7.3}$$

Figure 7.10 is the same figure as figure 6.9 with the addition of the curve coming from equation (7.3).

---

[9] The shape of the curves consistently showed similarity to the addition of decibels
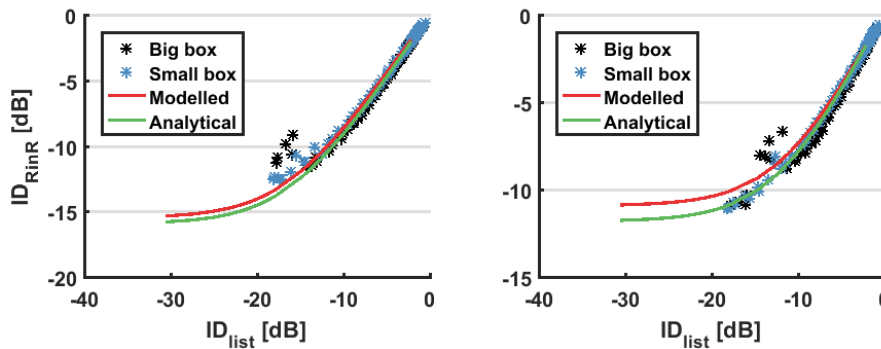
Figure 7.10 *Same figure as 6.9 with the addition of equation (7.3). Numerically modelled, analytically modelled, and measured initial drops for the IR_{RinR}, left is RinR scenario 1 where the ID in the recording room is 15.8 dB, on the right the ID in the recording room is 11.7 dB. Measurement points are from all absorption scenarios.*

Figure 7.11 shows the decrease of the direct sound in the IR_{RinR}, note that it is assumed that $ID_{rec} > ID_{list}$ (higher peak in the listening room, ID_{list}). The reduction in ID should then be subtracted from ID_1 (towards zero). Note that a higher direct sound level would translate to a lower ID.
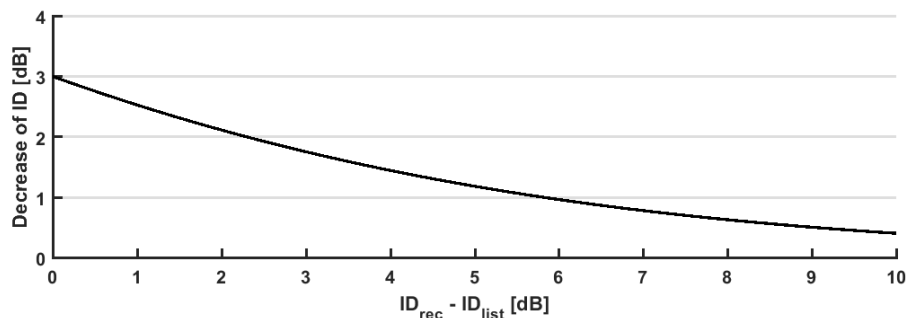
Figure 7.11 *The decrease in ID for the difference between direct sound levels according to equation (7.3),*

Most parameters that are expressed in decibel have a JND of 1 dB, e.g. Clarity, sound strength, sound levels. The threshold for ID is therefore set to 1 dB as well; additional research should identify the JND for the ID. So to reproduce the ID within 1 dB, the difference between the ID in the recording and listening room should be at least 6 dB.

7.5 Clarity deviation

Surface plots are made incorporating both the ratio between RTs and the difference in ID to visualise the deviation of energy ratios. Figure 7.11 shows the deviation of C_{80} as a result of RinR acoustics; the yellow part shows the deviation above the JND. Upper left shows a 3D view of the combined effects of direct and reverberant fields. Upper right shows the influence of RT ratio on the ID. The bottom row indicated the deviation of T_{30} under the influence of RT ratio and direct sound level difference. In the figure, it can be seen that the deviation of C_{80} is primarily dependent on the direct sound.

The difference in magnitude of clarity between the recording and listening room is dependent on the measurement position. The deviations in figure 7.12 are all calculated with the same IR in the

recording room. If a different recording is used, a similarly shaped surface appears, but this surface will then have another position.
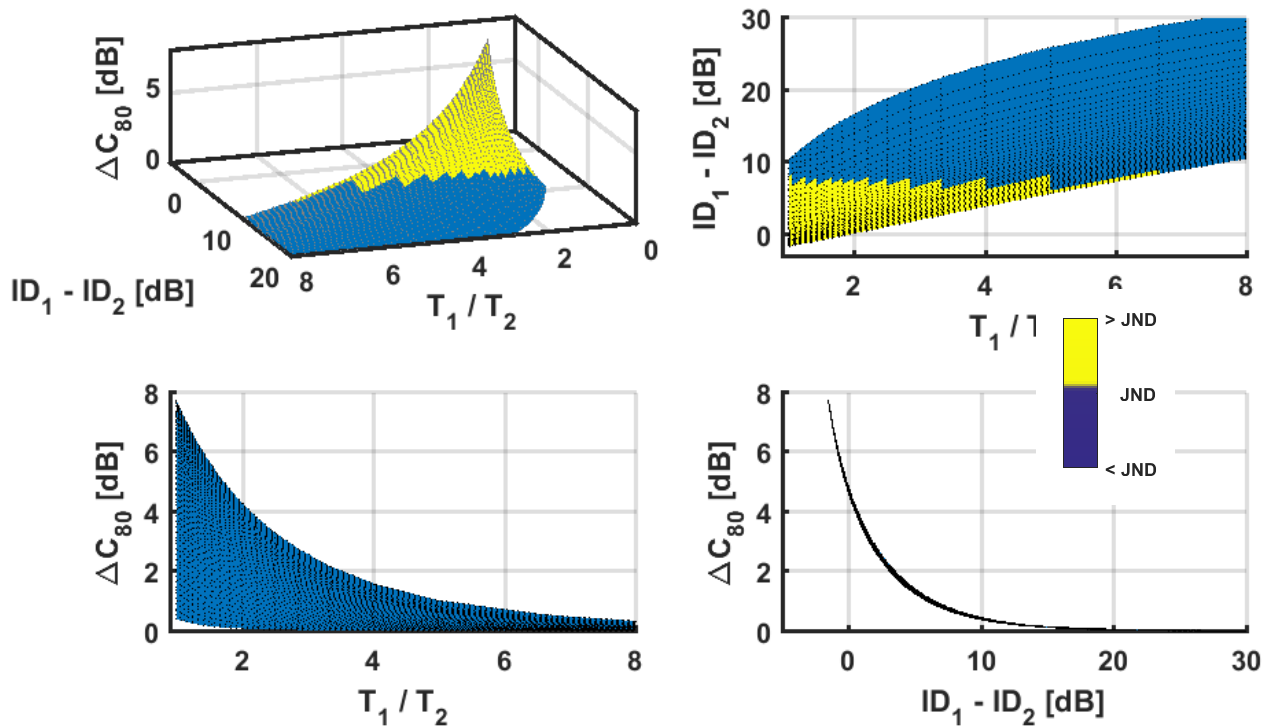
Figure 7.12 *Surface plot of deviation in clarity as a result of RinR, yellow indicates that the deviation is above the JND. T_1/T_2 is the ratio of reverberation times and $ID_1 - ID_2$ is the difference in initial drop between the recording and listening room*

The reason for this changed position of the surface is visualized in figure 7.13, where the deviation is calculated similarly as in figure 7.12. However, instead of varying T_1/T_2, the direct proportion in the IR of the recording room is varied, i.e. ID_1. T_1 / T_2 is set on 1. If the reverberation time in the listening room were to decrease, the deviation in C_{80} will also decrease (slightly).

Figure 7.13 shows that for increasing direct sound in the recording room the maximum deviation increases, this is a logical consequence of the calculation method. The C_{80} of the recording IR is increasing with increasing direct sound, allowing more substantial deviations.

From the figures, it can be concluded that the deviation in C_{80} can be expressed as the difference in ID between the listening and recording room. Figure 7.12 shows agreement with conclusions from the research in [3], to reproduce C_{80} in diffuse field conditions within 1 JND, the decay rate should be 10 times shorter in the listening room (bottom left figure).

If the direct sound level in the recording room is low, the ratio between reverberation times wins in influence over the deviation in Clarity. However, the RT ratio has to be impractically large for most situations.
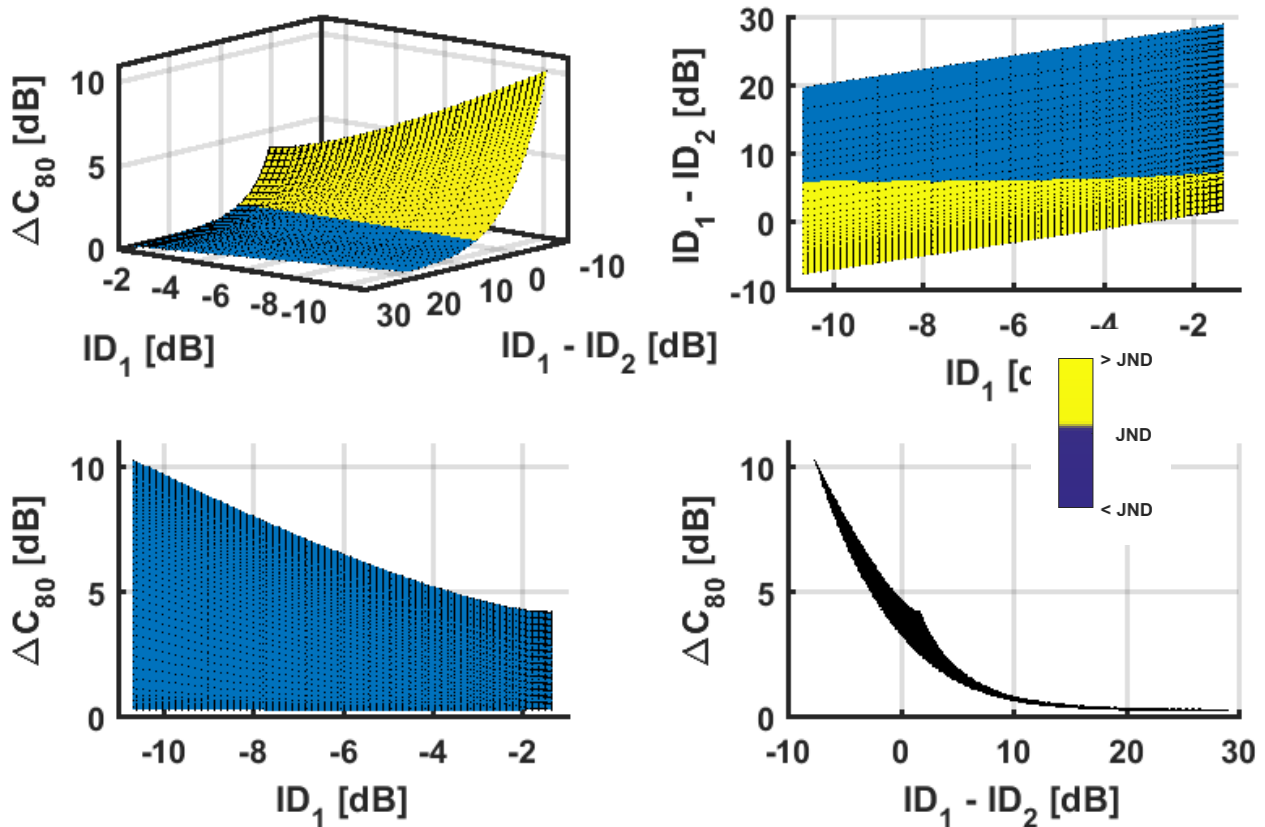
Figure 7.13 *Deviation in clarity as consequence of RinR, yellow indicates that the deviation is above the JND, T_1/T_2 is 1. $ID_1 - ID_2$ is the difference in initial drop between the recording and listening room*

7.6 Centre time deviations

Figure 7.14 shows the deviation of centre time in surface plots. Upper left surface is in 3D and shows the combined effects of the reverberation ratio and the ID. The other three graphs are the side and top views. The just noticeable difference (JND) for Centre time is 10 ms.

From the graphs on the bottom row, it can be seen that both the RT ratio and the direct sound are of significant influence. So to predict the deviation of the centre time both must be known. Similarly as with C_{80}, the higher the centre time in the recording room IR, the higher the deviations.
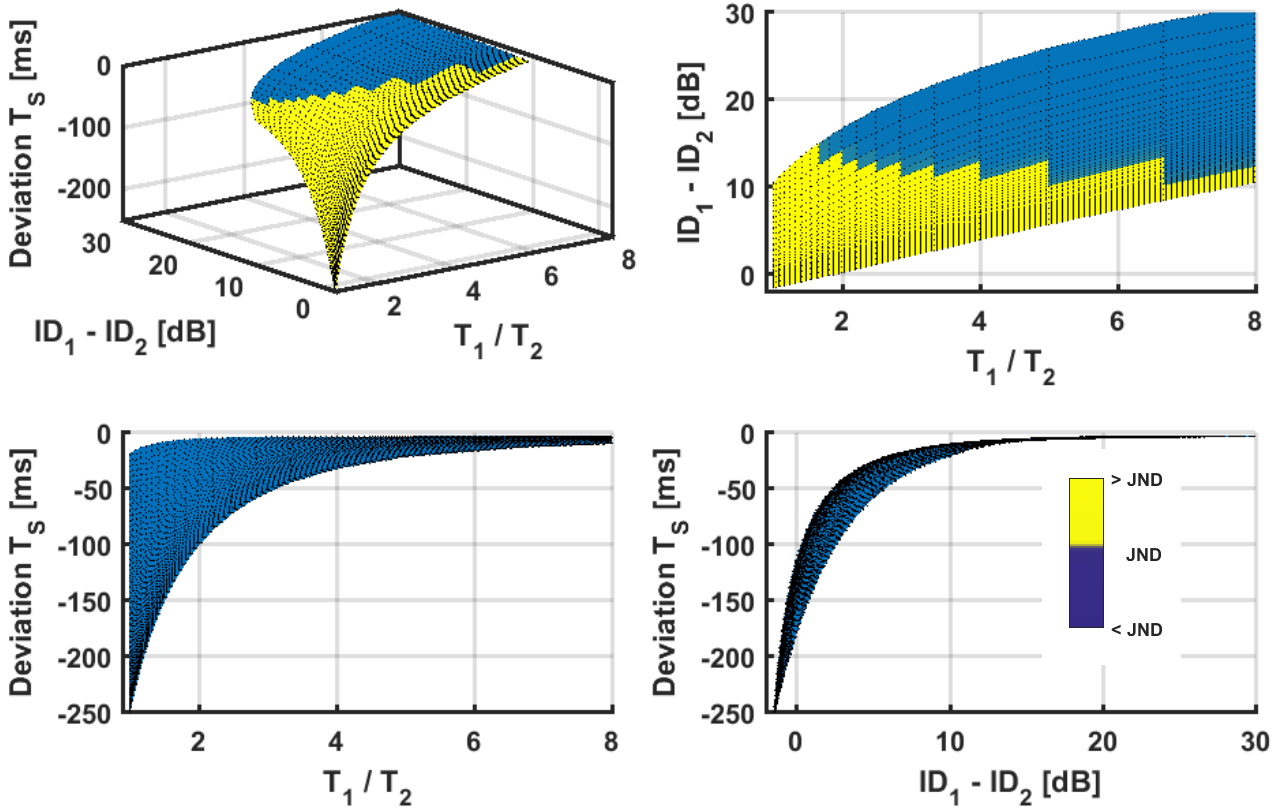
Figure 7.14 *Surface plot of deviation in centre time as a result of RinR,T_1/T_2 is the ratio of reverberation times and $ID_1 - ID_2$ is the difference in initial drop between the recording and listening room yellow indicates that the deviation is above the JND*

Results & discussion

8 Conclusions and recommendations

When a recorded sound is reproduced in a reverberant environment, the recording is influenced by this environment this influence is referred to as deviation. To reduce RinR caused deviations, either the ratio of reverberation time in the recording and listening rooms need to increase, or the direct sound level in the listening room need to be increased. The observation is made that the closer the IR in the listening room resembles the ideal impulse the smaller the deviations between the IR_{RinR} and the IR_{rec}. This chapter answers the research question and lists recommendations for future studies.

8.1 Research question

The research question for this thesis is:

"What is the influence of direct and diffuse sound fields in recording rooms on the perceived acoustics in listening rooms?"

The properties in which the influence can be shown are the ratio between reverberation times and the difference in direct sound levels indicated by the Initial Drop.

8.2 Conclusions

8.2.1 Measurements

The most important conclusion that can be drawn from the measurements is:
- Contrary to what is reported in some of the literature, calculating T_{20} and T_{30} for IR_{RinR} is no problem, even when convolutions are done with IRs that have the same reverberation time. This statement is based on the Curvature Parameter (see section 7.2). This curvature is indicated by the ratio of T_{20} and T_{30}.

8.2.2 Model

The conclusions that can be drawn from the numerical model:
- The deviation between T_{RinR} and T_{rec} primarily depends on the ratio of reverberation times in the recording and listening room.
- The initial drop in an IR_{RinR} is the energetic subtraction of the two initial drops in the recording and listening room.
- The deviation between $C_{80;RinR}$ and $C_{80;rec}$ is primarily dependent on the difference of the direct sound expressed by the Initial Drop. Deviations reported about C_{80} are higher when the C_{80} is higher for the IR in the recording room.
- The deviation between $T_{s;RinR}$ and $T_{s;rec}$ is dependent on a combination of the ratio of RT and the difference of the direct sound expressed by the Initial Drop.

8.2.3 Parameter deviations

The values for the RT ratio and ID difference to reach a reproduced accuracy within 1 JND:

Conclusions and recommendations

- According to the model, the ratio $T_{30;rec}/T_{30;list}$ must be 1.2 to reproduce $T_{30;rec}$. According to the measurements, the ratio must be 1.5 this is because the results are a bit spread out, (see figure 7.9).
- Reproducing direct sound levels within 1 dB accurate asks for initial drop levels of 6 dB higher in the listening room.
- Needed Initial Drop values for reproducing C_{80} within 1 dB accurate, depends on the direct sound in the recording IR. It can be stated that a 6 dB difference in ID is sufficient in most cases.
- For the reproduction of centre time, the RT ratio should be the same as for the reverberation time determination. The direct sound level can be assumed to ask for the same accuracy as C_{80} so a difference of 6 dB should be reached.

8.3 Further research

An analytical solution for the convolution of equation (5.13) should be easy to figure out for a mathematician if a solution exists. Then all parameter deviations can be expressed using an analytical equation.

For the work in this thesis, ID shows promising results. The Initial Drop can be investigated thoroughly as a parameter to describe the direct sound level. To this end equation (5.9) can be used to investigate the parameter sensitivity.

A just noticeable difference for the initial drop and direct sound levels can be determined.

A single indication can be sought to quantify how far an impulse response differs from the ideal impulse. If the difference between two IRs, in this respect, is known a suitable indicator can be deduced.

A study should be conducted into the perceptual properties of parameters calculated from the IR_{RinR}. Do they describe the same perceptual attributes?

9 References

[1]   A. P. Hill, "COMBINED REVERBERATION TIME OF ELECTRICALLY COUPLED ROOMS," *J. Acoust. Soc. Am.*, vol. 4, no. 1A, p. 63, 1932.

[2]   C. C. J. M. Hak and R. H. C. Wenmaekers, "The Effect of Room Acoustics on the Perceived Acoustics of Reproduced Sound," *Proceedings of the Internoise*, 2008. .

[3]   C. C. J. M. Hak and R. H. C. Wenmaekers, "The impact of sound control room acoustics on the perceived acoustics of a diffuse field recording," *WSEAS Trans. Signal Process.*, vol. 6, no. 4, pp. 175–185, 2010.

[4]   A. Haeussler and S. van de Par, "Spectral and perceptual properties of a transfer chain of two rooms," *Euronoise 2015, 10th Eur. Congr. Noise Control Eng.*, pp. 2077--2082, 2015.

[5]   J. Grosse and S. Van De Par, "Perceptually optimized room-in-room sound reproduction with spatially distributed loudspeakers," in *European Signal Processing Conference*, 2014, pp. 1362–1366.

[6]   U. P. Svensson, H. El-Banna Zidan, and J. L. Nielsen, "Properties of convolved room impulse responses," *IEEE Work. Appl. Signal Process. to Audio Acoust.*, vol. 2, pp. 205–208, 2011.

[7]   C. C. J. M. Hak and R. H. C. Wenmaekers, "Room in Room Acoustics: the influence of the direct/diffuse sound field ratio in a listening room on played back recorded acoustics," *Euronoise 2015, 10th Eur. Congr. Noise Control Eng.*, 2015.

[8]   H. E.-B. Zidan, U. P. Svensson, and J. L. Nielsen, "Room acoustical parameters of two electronically connected rooms.," *J. Acoust. Soc. Am.*, vol. 138, no. 4, pp. 2235–45, Oct. 2015.

[9]   International Organisation for Standardization, "ISO 3382-1 Acoustics - Measurement of room acoustic parameters - Part 1: Performance spaces," *ISO*, 2009.

[10]   C. C. J. M. Hak and R. H. C. Wenmaekers, "The Impact of Sound Control Room Acoustics on the Perceived Acoustics of a Diffuse Field Recording," *WSEAS Trans. SIGNAL Process.*, vol. 6, no. 4, pp. 175–185, 2010.

[11]   C. C. J. M. Hak and R. H. C. Wenmaekers, "Room in Room Acoustics : Using Convolutions to find the Impact of a Listening Room on Recording Acoustics," *ISRA 2013*, pp. 1–9, 2013.

[12]   W. Reijnders, "Room in Room Acoustics: The distance in parameter deviations," 2015.

[13]   W. Wittebol and P. Putten, "Room in room acoustics: Initial drop as a parameter for direct diffuse sound ratio," Eindhoven, 2016.

[14]   J. Grosse and S. van de Par, "Evaluation of a perceptually optimized room-in-room reproduction method for playback room compensation," *Euronoise 2015, 10th Eur. Congr. Noise Control Eng.*, pp. 2071–2076, 2015.

[15]   J. Grosse and S. Van De Par, "Perceptually Accurate Reproduction of Recorded Sound Fields in a Reverberant Room Using Spatially Distributed Loudspeakers," *IEEE J. Sel. Top. Signal Process.*, vol. 9, no. 5, pp. 867–880, 2015.

[16]   H. el-Banna Zidan and U. P. Svensson, "Early Energy Conditions in Small Rooms and in Convolutions of Small-Room Impulse Responses," in *Audio Engineering Society Convention 129*, 2010.

[17]   M. Barron, "Energy relations in concert auditoriums. I," *J. Acoust. Soc. Am.*, vol. 84, no. 2, p. 618, 1988.

[18]   G. Defrance, L. Daudet, and J.-D. Polack, "Finding the onset of a room impulse response: Straightforward?," *J. Acoust. Soc. Am.*, vol. 124, no. 4, p. EL248, 2008.

[19]   M. R. Schroeder, "Modulation Transfer Functions: Definition and Measurement."

[20]   H. Kuttruff, *Room acoustics.* Spon Press/Taylor & Francis, 2009.

[21]   H. Kuttruff, *Acoustics: An Introduction.* 2007.

[22]   M. Vorländer, "Revised relation between the sound power and the average sound pressure

level in rooms and consequences for acoustic measurements," *Acta Acust. united with Acust.*, vol. 81, no. 4, pp. 332–343, 1995.

[23] J. H. McClellan, R. W. Schafer, and M. A. (Mark A. . Yoder, *Signal processing first*. Pearson/Prentice Hall, 2003.

[24] U. P. Svensson, "Energy-time relations in a room with an electroacoustic system," *J. Acoust. Soc. Am.*, vol. 104, no. 3, p. 1483, 1998.

[25] A. Farina, "Advancements in impulse response measurements by sine sweeps," *Proc. 122nd AES Conv.*, pp. 1–21, 2007.

[26] C. C. J. M. Hak, J. Hak, and R. H. C. Wenmaekers, "INR as an Estimator for the Decay Range of Room Acoustic Impulse Responses," *Proc. 124th AES Conf.*, pp. 2–5, 2008.

[27] C. C. J. M. Hak, R. H. C. Wenmaekers, and L. C. J. van Luxemburg, "Measuring Room Impulse Responses: Impact of the Decay Range on Derived Room Acoustic Parameters," *Acta Acust. united with Acust.*, vol. 98, no. 6, pp. 907–915, Nov. 2012.

[28] N. Hoekstra, "Sound absorption of periodically spaced baffles," p. 2014, 2014.

[29] L. L. (Leo L. Beranek and T. J. Mellow, *Acoustics: Sound Fields and Transducers*. Academic Press, 2012.

[30] M. R. Schroeder, "New Method of Measuring Reverberation Time," *J. Acoust. Soc. Am.*, vol. 37, no. 3, p. 409, Jul. 1965.

[31] R. Thiele, "Richtungsverteilung und Zeitfolge der Schallrückwürfe in Räumen," *Acta Acust. united with Acust.*, vol. 3, no. 4, pp. 291–302, 1953.

[32] W. Reichardt, O. Alim, and W. Schmidt, "Definition and basis of making an objective evaluation to distinguish between useful and useless clarity defining musical performances," *Acta Acust. united with …*, 1975.

[33] R. Kürer, "Zur gewinnung von einzahlkriterien bei impulsmessung in der raumakustik," *Acustica*, 1969.

[34] M. R. Schroeder, "Integrated-impulse method measuring sound decay without using impulses," *J. Acoust. Soc. Am.*, vol. 66, no. 2, p. 497, Aug. 1979.

[35] J. S. Bradley, R. Reich, and S. G. Norcross, "A just noticeable difference in C50 for speech," *Appl. Acoust.*, vol. 58, no. 2, pp. 99–108, Oct. 1999.

[36] T. J. Cox, W. J. Davies, and Y. W. Lam, "The Sensitivity of Listeners to Early Sound Field Changes in Auditoria."

Appendix A Derivation of equation (5.11)

Starting with the convolution, equation (5.10) in the report.

$$h_{12}(t) = h_1(t) * h_2(t) = (D_1 e^{p_1 \cdot t} + R_1 e^{x_1 \cdot t}) * (D_2 e^{p_2 \cdot t} + R_2 e^{x_2 \cdot t}) \ (A.1)$$

Convolution integral

$$h_{12}(t) = \int (R_1 e^{x_1 \tau} + D_1 e^{x_1 \tau}) \cdot (R_2 e^{x_2(t-\tau)} + D_2 e^{x_2(t-\tau)}) \, d\tau \ (A.2)$$

Expand the equation

$$h_{12}(t) = \int (R_1 R_2 e^{-x_2\tau + x_1\tau + x_2 t} + D_1 R_2 e^{-x_2\tau + p_1\tau + x_2 t} + R_1 D_2 e^{-x_1\tau + p_2\tau + p_2 t}$$
$$+ D_1 D_2 e^{-p_1\tau + p_2\tau + p_2 t}) \, d\tau \ (A.3)$$

Get constants out of the integral

$$h_{12}(t) = R_1 R_2 e^{x_2 t} \int e^{-x_2\tau + x_1\tau} \, d\tau + D_1 R_2 e^{x_2 t} \int e^{-x_2\tau + p_1\tau} \, d\tau + R_1 D_2 e^{p_2 t} \int e^{-x_1\tau + p_2\tau} \, d\tau$$
$$+ D_1 D_2 e^{p_2 t} \int e^{-p_1\tau + p_2\tau} \, d\tau \ (A.4)$$

Solving separate integrals

$$= \int e^{-x_2\tau + x_1\tau} \, d\tau \ (A.5)$$

Applying u substitution:

$$u = -x_2\tau + x_1\tau \ (A.6)$$

$$d\tau = \frac{1}{x_1 - x_2} \, du \ (A.7)$$

$$= \frac{1}{x_1 - x_2} \int e^u \, du = \frac{e^u}{x_1 - x_2} \ (A.8)$$

Repeat for all parts of equation (A.4) undo u substitution, plug in solved integrals and add the constant.

$$h_{12}(t) = D_1 D_2 \frac{e^{-p_1\tau + p_2\tau + p_2 t}}{p_1 - p_2} + D_1 R_2 \frac{e^{-x_2\tau + x_1\tau + x_2 t}}{p_1 - x_2} + \cdots$$
$$\cdots R_1 D_2 \frac{e^{-x_1\tau + p_2\tau + p_2 t}}{p_2 - x_1} + R_1 R_2 \frac{e^{-x_2\tau + x_1\tau + x_2 t}}{x_1 - x_2} + C \ (A.9)$$

Definite integral
The limits of the integral are 0 and t.

Appendix A Derivation of equation (5.11)

$$h_{12}(t) = \int_0^t (R_1 e^{x_1 \tau} + D_1 e^{x_1 \tau}) \cdot (R_2 e^{x_2(t-\tau)} + D_2 e^{x_2(t-\tau)}) \, d\tau \ (A.10)$$

Because there are four similar parts only one is shown, see equation (A.3).

$$= \int_0^t (R_1 R_2 e^{-x_2 \tau + x_1 \tau + x_2 t}) \, d\tau \ (A.11)$$

The solution for this integral is given by equations (A.4) to (A.9) Filling in the limits:

$$R_1 R_2 \frac{e^{-x_2 0 + x_1 0 + x_2 t}}{x_1 - x_2} = R_1 R_2 \frac{e^{x_2 t}}{x_1 - x_2} \ for \ \tau = 0 \ (A.12)$$

And:

$$R_1 R_2 \frac{e^{-x_2 t + x_1 t + x_2 t}}{x_1 - x_2} = R_1 R_2 \frac{e^{x_1 t}}{x_1 - x_2} \ for \ \tau = t \ (A.13)$$

Combined that makes:

$$R_1 R_2 \frac{e^{x_1 t} - e^{x_2 t}}{x_1 - x_2} \ (A.14)$$

Repeating the process for all parts results in equation (A.15), which is equation (5.11) in the report.

$$h_{12}(t) = D_1 D_2 \frac{e^{p_1 t} - e^{p_2 t}}{p_1 - p_2} + D_1 R_2 \frac{e^{p_1 t} - e^{x_2 t}}{p_1 - x_2} + R_1 D_2 \frac{e^{p_2 t} - e^{x_1 t}}{p_2 - x_1} + R_1 R_2 \frac{e^{x_1 t} - e^{x_2 t}}{x_1 - x_2}$$
$$(A.15)$$

Appendix B Matlab scripts

- B.1 Single room analytical impulse response
- B.2 Room in room analytical impulse response
- B.3 Numerical result model
- B.4 Split octave bands
- B.5 Directivity equation
- B.6 Schroeder curve from measurements
- B.7 Initial drop determination from measurements

B.1 Single room analytical impulse response

W. Reijnders

```
clearvars

close all

IR_a = 3*log(10);          %Decay constant
IR_s = 3.5;                %length of the IR [s]
IR_fs = 48000;             %sampling frequency [Hz]
IR_dt = 1/IR_fs;           %sample spacing [Hz]
t = 0:IR_dt:IR_s;          %time string [s]
T_1 = 1.7;                 %Reverberation time [s]
T_p = 0.069;               %RT based decay term loudspeaker [s]

x1 = exp(-IR_a.*t/T_1);    %exponential decay function reverberant field
p1 = exp(-IR_a.*t/T_p);    %exponential decay function speaker

V = 88;                    % room volume [m^3]
Q1 = 10^(6.2/10);          %directivity factor [-]
r1 = 0.55;                 %Source receiver distance [m]
rh1 = 0.057*(Q1*V/T_1)^0.5; %critical distance [m]
R1 = 1/rh1;                %diffuse portion
D1 = Q1^0.5/r1;            %direct portion

wd1 = awgn((zeros(1,length(t))),0.000001);%noise sequence

h1 = (D1.*p1 + R1.*x1).*wd1; % impulse response

S_ch(length(t):-1:1) = 10*log10(cumsum(h1(length(t):-1:1).^2)); %Schroeder curve
S_ch = S_ch - S_ch(1);     %normalization
ETC = 10*log10(h1.^2);     %energy time curve
ETC = ETC - max(ETC);      %normalization
```

B.2 Room in room analytical impulse response

W. Reijnders

```
clearvars
close all


IR_s = 3.5;          %length of the IR [s]
IR_fs = 48000;       %sampling frequency [Hz]
IR_dt = 1/IR_fs;     %sample spacing [Hz]
t = 0:IR_dt:IR_s;    %time string [s]
```

Parameters for the equation

```
T_rec = 2;           %Reverberation time recording room [s]
T_lis = 2.0001;      %Reverberation time listening room [s]
T_prec = 0.069;      %RT based decay term loudspeaker recording [s]
T_plis = 0.0691;     %RT based decay term loudspeaker listening [s]
IR_a = 3*log(10);    %Decay constant
```

Exponential parts for equation 5.11

```
x1e = -IR_a/T_rec;
p1e = -IR_a/T_prec;

x1 = exp(-IR_a.*t/T_rec);
p1 = exp(-IR_a.*t/T_prec);

x2e = -IR_a/T_lis;
p2e = -IR_a/T_plis;

x2 = exp(-IR_a.*t/T_lis);
p2 = exp(-IR_a.*t/T_plis);
```

Ratio direct diffuse for tables 5.1 and 5.2

```
R1 = [ 1  1  1 20 20 20 20 20 20];  %direct proportion recording room
D1 = [20 20 20 20 20 20  1  1  1];  %diffuse proportion recording room
R2 = [ 1 20 20  1 20 20  1 20 20];  %direct proportion listening room
D2 = [20 20  1 20 20  1 20 20  1];  %diffuse proportion listening room
```

equation 5.11 with normalization

```
for n = 1:9
h_12(n,:) = D1(n)*D2(n)*(p1-p2)/(p1e-p2e)+D1(n)*R2(n)*(p1-x2)/(p1e-
x2e)+R1(n)*D2(n)*(x1-p2)/(x1e-p2e)+R1(n)*R2(n)*(x1-x2)/(x1e-x2e);
h_12(n,:) = h_12(n,:) / max(h_12(n,:));
end
```

B.3 Numerical result Room in Room Impulse Response model

W. Reijnders

```
clearvars
close all

IR_s = 4.5;                              %length of the IR [s]
IR_fs = 48000;                           %sampling frequency [Hz]
IR_dt = 1/IR_fs;                         %sample spacing [Hz]
t = 0:IR_dt:IR_s;                        %time string [s]
IR_a = 3*log(10);                        %Decay constant
```

Input parameters

```
T_rec = 4;                               %RT recording
V_rec =88;                               %volume
Q_rec = 10.^([5.7]/10);                  %directivity (inverse of equation (4.6))
r_rec = 1.5;                             %source receiver distance
rh_rec = 0.057.*(Q_rec.*V_rec./T_rec).^0.5;    %critical distance equation (5.7)
R_rec = 1./rh_rec;                       %Diffuse portion equation (5.6)
D_rec = Q_rec^0.5./r_rec;                    %Direct portion equation (5.6)


T_list = 4;                              %RT listening
V_list = 88;                             %volume
Q_list = 10.^([6.3]/10);                 %directivity (inverse of equation (4.6))
r_list = 0.35;                           %source receiver distance
rh_list = 0.057.*(Q_list.*V_list./T_list).^0.5; %critical distance equation (5.7)
R_list = 1./rh_list;                     %Diffuse portion equation (5.6)
D_list = Q_list^0.5./r_list;                 %Direct portion equation (5.6)


T_peak = 0.069;                          %RT based decay term loudspeaker
```

Exponential parts equation 5.9

```
x_rec = exp(-IR_a.*t/T_rec);
p_rec = exp(-IR_a.*t/T_peak);
x_list = exp(-IR_a.*t/T_list);
p_list = exp(-IR_a.*t/T_peak);
```

Noise sequences (section 5.3)

```
wd1 = awgn((zeros(1,length(t))),0.000001);
wd2 = (rand(1,length(t))-0.5)*(1*sqrt(3)*2);    %equation (5.14)
```

Impulse responses, Equation (5.13)

```
h1 = (D_rec.*p_rec + R_rec.*x_rec).*wd1;     %IR for recording room
h2 = (D_list.*p_list + R_list.*x_list).*wd2; %IR for listening room
h_conv = IR_dt * cconv(h1,h2,length(h1));    % IR_RinR circular convolution of
equation 5.13
```

Schroeder curves

```
S_h1(:,length(t):-1:1) = 10*log10(cumsum(h1(:,length(t):-1:1).^2));
S_h1(:,:) = S_h1(:,:) - S_h1(:,1);
S_h2(:,length(t):-1:1) = 10*log10(cumsum(h2(:,length(t):-1:1).^2));
```

```
S_h2 = S_h2 - S_h2(1);
S_conv(:,length(t):-1:1) = 10*log10(cumsum(h_conv(:,length(t):-1:1).^2));
S_conv = S_conv - S_conv(1);
```

Room acoustical parameters

```
%Clarity
val80 = find(t > 0.08 ,1,'first'); %Evaluation point 80 ms
C80_h1 = 10 * log10(sum(h1(:,1:val80).^2)/sum(h1(:,val80:end).^2));
C80_h2 = 10 * log10(sum(h2(:,1:val80).^2)/sum(h2(:,val80:end).^2));
C80_conv = 10 * log10(sum(h_conv(:,1:val80).^2)/sum(h_conv(:,val80:end).^2));
C80dev = C80_h1-C80_conv;

%Centre time
TS_h1  = sum(t.*h1.^2)/sum(h1.^2)*1000;
TS_h2  = sum(t.*h2.^2)/sum(h2.^2)*1000;
TS_conv  = sum(t.*h_conv.^2)/sum(h_conv.^2)*1000;
TSdev = TS_h1-TS_conv;

%Reverberation time
T_h1 = round(t(find(S_h1> -35.1,1,'last'))-t(find(S_h1 > -5.1,1,'last')),4)*2;
T_h2 = round(t(find(S_h2> -35.1,1,'last'))-t(find(S_h2 > -5.1,1,'last')),4)*2;
T_conv = round(t(find(S_conv> -35.1,1,'last'))-t(find(S_conv > -
5.1,1,'last')),4)*2;
Tdev = (T_conv - T_rec)./ T_rec .*100;

%Initial drop
taw = .15; %time window
ID_h1 = S_h1(round(taw*IR_fs))+taw*60/T_rec;
ID_h2 = S_h2(:,round(taw*IR_fs))+taw*(60/T_list);
ID_conv = S_conv(:,round(taw*IR_fs))+taw*(60/T_conv);
IDdev =  ID_h1 - ID_conv;
```

B.4 Split octave bands

W. Reijnders and W. Wittebol, based on a script delivered for the course Architectural acoustics in 2014.

```
function[cmtrx]=FUNCTION_FILTER_OCTAVE_BANDS(FolderName,FileName,obcf,order,x)
%octave band filtering
D = dir([FolderName, '\*.wav']);
Num = length(D(not([D.isdir])));
for p=1:1:Num
q=num2str(p);
str = strcat(FolderName,FileName,'  (',q,').wav');
[p1,fs]=audioread(str);
fc=obcf; %octave band center frequencies
f_h = 2.^((1/2)*(1/x)).*fc; %upper limits vector
f_l = 2.^((-1/2)*(1/x)).*fc;%lower limits vector
% 6th order Butterworth filter
fnq=fs/2; % Nyquist frequency
for n=1:length(fc)
    Wn=[f_l(n)/fnq f_h(n)/fnq]; % Butterworth bandpass non-dimensional frequency
    [z,b,a]=butter(order,Wn,'bandpass'); % construct the filter
    [sos,g]=zp2sos(z,b,a);%to counteract the numerical instability that occurs at
orders higher than 3
    yfilt_p1(n,:)=filtfilt(sos,g,p1(:,1)); % time-signal filtered for the
respective octave bands
end
cmtrx{p,:,:}=yfilt_p1;
clear yfilt_p1
end
end
```

B.5 Directivity equation

W. Reijnders

```
function [ Q,DI,prms ] = FUNCTION_DIRECTIVITY( cmtrx,ta )
%Pressure prms and directivities according to equations
%Input:
% cmtrx is the matrix where the octave bands are separated see script ...
%ta is an indication for a time point chosen such that the
% background noise does not have significant influence
% Output
% Q is the directivity factor
% DI is the directivity index
% prms is the root mean square of the pressure

[m]=length(cmtrx);  %no of files
[n]=size(cmtrx{1,1}); %octave bands + all pass

fs = 48000; %sampling frequency
dt = 1/fs; %frequency spacing

t=0:dt:ta; %time string from t = 0 to t = a

for i=1:1:m
for j=1:1:n

cmtrx1{i,1}(j,:) = cmtrx{i,1}(j,1:length(t)); %cutting of p

prms(j,i) = (1/(ta*fs) * sum(cmtrx1{i,1}(j,:).^2))^0.5; %implementation of equation
4.5
end
end
for j=1:1:n


theta = deg2rad(0:10:180); %converting degrees to radials
prms0(j,:) = prms(j,:); %Prms in the designated direction
Q(j,:) = 4*pi*prms0(j,:).^2*(180/pi)./
((2*pi)*sum(abs(prms(j,:).^2).*sin(theta)*10)); %directivity factor according to
equation 4.4
DI(j,:) = 10*log10(abs(Q(j,:))); %directivity index according to equation 4.6
Q1(j,:) = [Q(j,:) Q(j,end-1:-1:1)]; %mirror along main axis
theta1 = deg2rad(0:10:360); %string for polar plot
end


end
```

B.6 Schroeder curve from measurements

W. Reijnders and W. Wittebol

```matlab
%filmat = matrix met gefilterde IR
%ilsf = crosspoint (optioneel)

function [schrmtrx]=FUNCTION_BACKWARDS_INTEGRATION(cmtrx,crosspoint)

[m]=length(cmtrx);  %no of files
[n]=size(cmtrx{1,1}); %octave bands + allpass
if crosspoint==0

for i=1:1:m
for j=1:1:n

pr=cmtrx{i,1}(j,:).^2; %IR squared i=meetnummer j=frequentieband
pt(length(pr):-1:1)=cumsum(pr(length(pr):-1:1)/sum(pr(1:length(pr)))); %schroeder
integratie
lsc{j,:}=10*log10(pt); %10log en daarmee de schroeder curve voor de frequentieband
j

end
schrmtrx{i,1}=lsc; %wegschrijven schroeder curve
end
else
for i=1:1:m
for j=1:1:n
pr=cmtrx{i,1}(j,:).^2;
ps(crosspoint(i,j):-1:1)=cumsum(pr(crosspoint(i,j):-
1:1)/sum(pr(1:crosspoint(i,j))));
lsc{j,:}=10*log10(ps);
end
schrmtrx{i,1}=lsc;
end
end
end
```

B.7 Initial drop determination from measurements

W. Reijnders and W. Wittebol

```
function[idropmatrix,idropmatrix_uncorrected]=FUNCTION_DETERMINE_INITIAL_DROP_RTCOR
RECTION(schrmtrx,ms,rt)
%Function to determine the initial drop with compensation for the diffuse field
% input: schrmtrx, matrix with octave band separated Schroeder decay curves
% ms: with of the time window
% rt: reverberation time

[o,p]=size(schrmtrx);
[q,r]=size(schrmtrx{1,1}); %


s=ms*10^-3; %from ms to s
us=floor(s*48000); %sample number

for i=1:1:o
for j=1:1:q
    pr= schrmtrx{i,1}{j,1}; %schroedercurve i=measurement number j=frequency band
 start=find(pr<-0.05,1); %start point 0.05 dB below start

ID_cd = s(j) * 60 / rt(i,j); %ID difusse field compensation
 id(j)=pr(start+us(j))+ID_cd; %initialdrop
 id2(j)=pr(start+us(j)); %initialdrop without compensation

end
idropmatrix(i,:)=id;
idropmatrix_uncorrected(i,:)=id2;

end


end
```

Appendix B Matlab scripts

Appendix C Measurement results

- C.1 Impulse response to noise ratio INR
- C.2 Reverberation time T_{20}
- C.3 Reverberation time T_{30}
- C.4 Initial drop ID
- C.5 Clarity C_{80}
- C.6 Centre time T_s

Since there are 170 measurement positions (total over all measured absorptions) and 6 parameters, results for every parameter the values are available in table form digitally.

C.1 Impulse response to noise ratio (INR)

Table C.1.1 INR for the big box measurement in the 0 Baffle configuration

Measurement position	500 Hz	1 kHz	2 kHz	4 kHz
1	72,6	78,2	78,6	79,3
2	68,6	76,2	76,0	76,8
3	68,5	75,4	74,3	75,0
4	69,0	73,3	72,9	73,1
5	68,9	71,6	71,7	71,8
6	70,4	71,8	70,9	71,1
7	68,5	70,4	71,3	69,6
8	64,0	70,6	70,2	68,4
9	65,5	70,9	70,2	67,9
10	66,3	69,7	69,8	67,4
11	65,0	69,2	68,4	65,8
12	63,1	68,9	69,9	67,4
13	62,0	69,7	69,8	66,6
14	65,6	69,3	69,5	66,8
15	62,3	69,6	69,2	67,0
16	61,2	69,1	69,5	65,9

Table C.1.2 INR for the big box measurement in the 1 Baffle configuration

Measurement position	500 Hz	1 kHz	2 kHz	4 kHz
1	74,6	79,6	79,4	80,0
2	71,6	77,5	77,2	77,7
3	68,5	75,7	74,6	75,7
4	70,2	74,1	73,6	73,8
5	71,3	73,1	73,0	72,6
6	69,5	73,3	72,1	72,0
7	68,7	71,5	71,7	70,1
8	66,2	71,7	70,9	68,8
9	65,0	71,3	70,8	68,5
10	66,4	69,8	70,3	67,7
11	67,2	69,9	70,3	67,5
12	65,8	70,9	70,2	67,5
13	65,9	70,2	70,4	66,8
14	68,1	69,9	70,0	67,2
15	63,0	70,1	69,9	66,7
16	62,6	68,6	68,9	64,9

Table C.1.3 INR for the big box measurement in the 2 Baffle configuration

Measurement position	500 Hz	1 kHz	2 kHz	4 kHz
1	75,9	80,3	80,6	81,0
2	72,3	78,6	77,8	78,3
3	70,1	77,1	75,5	76,0
4	70,9	75,8	74,4	74,3
5	71,6	74,7	73,5	73,1
6	72,1	73,7	72,7	72,3
7	69,6	72,7	72,4	70,8
8	66,8	72,0	71,3	69,4
9	64,0	71,7	71,0	68,8
10	67,6	69,9	70,6	68,1
11	67,8	70,7	70,5	67,8
12	68,8	71,5	70,6	67,6
13	65,0	70,3	70,5	67,0
14	67,8	70,6	70,3	67,2
15	64,8	70,8	70,0	67,3
16	64,6	69,8	69,9	66,2

Table C.1.4 INR for the big box measurement in the 3 Baffle configuration

Measurement position	500 Hz	1 kHz	2 kHz	4 kHz
1	76,6	80,8	81,0	81,3
2	73,3	79,4	78,4	78,7
3	71,4	77,9	76,1	76,8
4	70,8	76,1	74,7	75,2
5	71,2	74,3	73,5	73,2
6	71,4	74,1	73,1	72,5
7	68,3	72,9	72,2	70,9
8	67,0	72,4	71,2	69,8
9	64,5	71,8	70,6	68,9
10	67,0	70,9	70,5	68,2
11	67,4	67,9	70,5	67,9
12	68,2	71,2	70,5	67,8
13	65,8	70,7	70,7	67,0
14	67,5	70,1	70,2	67,7
15	64,7	70,7	69,8	67,1
16	65,2	70,4	70,0	66,3

Table C.1.5 INR for the big box measurement in the 4 Baffle configuration

Measurement position	500 Hz	1 kHz	2 kHz	4 kHz
1	79,2	82,1	81,4	81,6
2	74,7	80,0	78,5	79,0
3	71,8	78,7	76,6	77,2
4	69,8	76,0	75,1	75,1
5	71,6	75,4	74,3	73,9
6	71,8	75,0	73,7	73,1
7	68,2	73,2	72,7	71,3
8	66,6	73,2	71,8	70,0
9	62,2	72,3	71,3	69,2
10	68,6	71,4	71,0	68,5
11	65,7	67,1	63,0	67,4
12	67,5	71,6	70,7	68,0
13	67,4	71,4	70,7	67,4
14	66,9	70,2	70,0	67,7
15	65,4	71,3	70,3	67,2
16	65,9	69,7	69,4	65,8

Table C.1.6 INR for the small box measurement in the 0 Baffle configuration

Measurement position	500 Hz	1 kHz	2 kHz	4 kHz
1	76,4	78,5	79,4	82,3
2	74,9	77,6	81,4	81,0
3	80,0	82,2	86,0	85,0
4	69,0	73,0	77,7	76,6
5	68,6	72,5	76,5	74,8
6	71,1	70,6	74,7	73,4
7	71,1	69,6	74,7	73,2
8	67,2	68,9	74,0	71,8
9	74,5	77,0	80,6	78,2
10	71,3	70,9	78,3	77,1
11	68,6	75,2	78,3	76,7
12	77,2	75,8	79,5	76,3
13	74,7	75,0	78,7	76,3
14	71,8	73,9	77,5	75,5
15	73,1	71,3	74,4	74,8
16	68,8	73,6	74,3	74,2
17	70,4	76,8	78,4	75,7

Table C.1.7 INR for the small box measurement in the 1 Baffle configuration

Measurement position	500 Hz	1 kHz	2 kHz	4 kHz
1	76,7	80,2	84,0	84,0
2	72,9	74,9	81,1	81,8
3	68,6	73,9	79,7	79,4
4	66,9	69,1	76,0	76,9
5	65,3	69,3	75,2	75,2
6	70,5	70,4	75,9	74,2
7	69,8	69,0	74,5	73,5
8	65,1	65,0	72,1	71,9
9	63,9	64,8	72,0	71,3
10	64,1	65,9	71,8	70,7
11	65,5	68,3	71,7	70,3
12	67,5	66,2	71,9	70,1
13	64,4	63,3	70,0	70,0
14	64,9	65,8	71,8	69,8
15	65,2	65,2	72,0	70,0
16	65,0	67,5	71,6	69,6
17	64,8	68,2	72,1	69,1

Table C.1.8 INR for the small box measurement in the 2 Baffle configuration

Measurement position	500 Hz	1 kHz	2 kHz	4 kHz
1	80,0	81,2	82,5	84,0
2	76,9	78,0	82,6	82,2
3	73,7	76,4	80,8	79,8
4	70,3	74,2	79,0	77,7
5	69,0	70,7	77,3	75,7
6	72,2	71,7	74,9	74,4
7	69,4	70,4	75,8	74,0
8	69,7	69,3	73,2	72,2
9	67,8	69,1	73,8	71,5
10	64,0	70,1	73,2	71,0
11	65,9	67,4	72,3	70,3
12	68,3	69,9	72,7	70,0
13	67,9	66,6	70,9	70,5
14	64,9	67,7	72,4	70,3
15	66,0	65,9	71,7	70,0
16	64,4	68,4	72,4	69,9
17	65,3	66,2	72,3	69,3

Table C.1.9 INR for the small box measurement in the 3 Baffle configuration

Measurement position	500 Hz	1 kHz	2 kHz	4 kHz
1	81,0	83,7	85,9	85,1
2	69,4	70,1	71,3	68,2
3	74,5	77,1	82,1	80,7
4	71,9	76,3	80,1	78,2
5	71,5	74,1	78,4	76,7
6	73,1	72,9	77,3	75,2
7	74,2	72,7	76,6	74,4
8	69,8	70,7	75,4	72,8
9	70,3	71,0	74,5	72,0
10	67,6	70,8	74,3	71,5
11	70,1	69,8	74,0	70,9
12	69,4	69,9	73,9	70,7
13	68,5	70,3	73,2	70,7
14	67,4	69,5	73,3	70,4
15	67,3	69,2	72,8	70,4
16	67,9	70,6	73,0	70,3
17	67,6	69,7	72,8	69,5

Table C.1.10 INR for the small box measurement in the 4 Baffle configuration

Measurement position	500 Hz	1 kHz	2 kHz	4 kHz
1	81,8	83,7	86,4	85,5
2	79,4	80,9	84,6	83,3
3	63,2	72,2	79,6	78,6
4	73,0	76,2	79,9	78,6
5	71,6	74,7	78,8	76,7
6	72,9	74,1	77,6	75,5
7	73,1	73,2	77,0	74,8
8	70,2	71,7	75,8	73,2
9	68,7	71,9	75,0	72,4
10	63,5	70,8	74,3	71,6
11	69,5	70,3	74,1	71,1
12	67,3	70,5	74,0	71,0
13	70,8	70,4	73,7	70,9
14	68,0	70,3	73,6	70,3
15	70,5	69,9	73,5	70,8
16	68,2	70,8	73,1	69,9
17	61,7	62,5	67,5	68,0

C.2 Reverberation time (T_{20})

Table C.2.1 T20 for the big box measurement in the 0 Baffle configuration

Measurement position	500 Hz	1 kHz	2 kHz	4 kHz
1	4,4	4,2	3,6	2,4
2	4,4	4,2	3,6	2,4
3	4,3	4,1	3,6	2,3
4	4,2	4,1	3,5	2,4
5	4,1	4,2	3,6	2,4
6	4,2	4,2	3,7	2,4
7	4,3	4,3	3,6	2,4
8	4,3	4,1	3,7	2,4
9	4,3	4,4	3,6	2,4
10	4,3	4,3	3,7	2,4
11	4,3	4,1	3,6	2,4
12	4,5	4,3	3,7	2,4
13	4,3	4,3	3,6	2,4
14	4,3	4,2	3,7	2,4
15	4,3	4,3	3,7	2,4
16	4,2	4,1	3,6	2,5

Table C.2.2 T20 for the big box measurement in the 1 Baffle configuration

Measurement position	500 Hz	1 kHz	2 kHz	4 kHz
1	3,1	3,2	2,7	1,9
2	3,0	3,0	2,7	2,0
3	3,0	3,0	2,8	2,0
4	3,0	3,0	2,7	2,0
5	3,0	3,1	2,7	1,9
6	2,9	3,2	2,9	1,9
7	3,2	3,1	2,6	2,0
8	3,1	3,1	2,8	2,0
9	3,0	3,1	2,7	2,0
10	3,0	3,2	2,8	2,0
11	2,9	3,1	2,7	2,0
12	3,1	3,1	2,8	1,9
13	3,1	3,0	2,7	2,0
14	3,0	3,2	2,8	2,0
15	3,0	3,1	2,7	2,0
16	3,2	3,1	2,7	2,0

Appendix C Measurement results

Table C.2.3 T20 for the big box measurement in the 2 Baffle configuration

Measurement position	500 Hz	1 kHz	2 kHz	4 kHz
1	3,2	3,1	2,7	2,0
2	3,2	3,1	2,7	2,0
3	2,3	2,4	2,2	1,7
4	2,2	2,4	2,2	1,7
5	2,3	2,3	2,2	1,7
6	2,3	2,4	2,2	1,8
7	2,3	2,5	2,3	1,7
8	2,3	2,4	2,3	1,7
9	2,3	2,5	2,2	1,7
10	2,5	2,5	2,2	1,7
11	2,4	2,4	2,3	1,7
12	2,3	2,6	2,3	1,8
13	2,3	2,6	2,3	1,7
14	2,2	2,5	2,3	1,7
15	2,4	2,4	2,3	1,7
16	2,3	2,6	2,3	1,7

Table C.2.4 T20 for the big box measurement in the 3 Baffle configuration

Measurement position	500 Hz	1 kHz	2 kHz	4 kHz
1	2,0	2,1	2,0	1,5
2	2,0	2,0	2,0	1,6
3	2,0	2,0	2,0	1,6
4	2,0	2,1	2,0	1,5
5	2,0	2,2	2,0	1,5
6	2,0	2,1	2,0	1,5
7	2,0	2,1	2,0	1,6
8	2,1	2,2	2,0	1,5
9	2,1	2,1	2,0	1,5
10	2,1	2,1	2,0	1,6
11	2,1	2,1	2,0	1,6
12	2,0	2,2	2,0	1,6
13	2,1	2,1	2,0	1,6
14	2,0	2,2	2,1	1,5
15	2,2	2,2	2,0	1,5
16	2,1	2,2	2,0	1,5

Table C.2.5 T20 for the big box measurement in the 4 Baffle configuration

Measurement position	500 Hz	1 kHz	2 kHz	4 kHz
1	1,7	1,7	1,7	1,3
2	1,7	1,8	1,7	1,4
3	1,7	1,8	1,7	1,3
4	1,7	1,8	1,7	1,3
5	1,6	1,8	1,7	1,3
6	1,6	1,8	1,7	1,4
7	1,6	1,8	1,7	1,4
8	1,7	1,8	1,7	1,3
9	1,7	1,8	1,7	1,4
10	1,8	1,8	1,7	1,4
11	1,7	1,8	1,7	1,4
12	1,7	1,8	1,7	1,4
13	1,8	1,8	1,7	1,3
14	1,7	1,9	1,8	1,4
15	1,8	1,8	1,7	1,3
16	1,7	1,8	1,8	1,4

Table C.2.6 T20 for the small box measurement in the 0 Baffle configuration

Measurement position	500 Hz	1 kHz	2 kHz	4 kHz
1	4,5	4,1	3,4	2,3
2	4,4	4,0	3,4	2,4
3	4,4	4,1	3,4	2,4
4	4,2	4,3	3,4	2,4
5	4,1	4,0	3,4	2,4
6	4,1	4,1	3,5	2,4
7	4,3	4,1	3,5	2,3
8	4,3	4,1	3,5	2,4
9	4,3	4,2	3,5	2,4
10	4,3	4,2	3,5	2,4
11	4,1	4,2	3,6	2,5
12	4,2	4,1	3,4	2,5
13	4,4	4,2	3,6	2,5
14	4,3	4,3	3,5	2,5
15	4,4	4,3	3,5	2,5
16	4,3	4,3	3,6	2,4
17	4,1	4,1	3,5	2,5

Appendix C Measurement results

Table C.2.7 T20 for the small box measurement in the 1 Baffle configuration

Measurement position	500 Hz	1 kHz	2 kHz	4 kHz
1	3,1	3,2	2,6	1,9
2	3,1	3,1	2,8	2,1
3	3,1	3,0	2,7	2,0
4	3,0	3,0	2,6	2,0
5	2,9	3,0	2,7	2,0
6	2,9	3,1	2,6	2,0
7	3,0	3,2	2,6	2,0
8	3,1	3,1	2,7	2,0
9	3,1	3,1	2,7	2,0
10	3,0	3,1	2,7	2,0
11	3,0	3,1	2,7	2,0
12	2,9	3,1	2,6	2,0
13	3,1	3,1	2,7	2,0
14	3,1	3,1	2,6	2,0
15	3,1	3,1	2,7	2,0
16	3,1	3,2	2,8	2,1
17	3,1	3,1	2,7	2,1

Table C.2.8 T20 for the small box measurement in the 2 Baffle configuration

Measurement position	500 Hz	1 kHz	2 kHz	4 kHz
1	2,3	2,6	2,2	1,6
2	2,3	2,4	2,2	1,7
3	2,3	2,4	2,1	1,7
4	2,3	2,4	2,2	1,7
5	2,3	2,4	2,2	1,7
6	2,3	2,5	2,2	1,8
7	2,4	2,5	2,2	1,7
8	2,4	2,5	2,3	1,7
9	2,4	2,5	2,3	1,8
10	2,4	2,5	2,3	1,7
11	2,3	2,5	2,2	1,7
12	2,2	2,5	2,2	1,8
13	2,3	2,5	2,3	1,7
14	2,4	2,4	2,2	1,7
15	2,3	2,5	2,3	1,7
16	2,5	2,5	2,2	1,7
17	2,2	2,5	2,2	1,7

Table C.2.9 T20 for the small box measurement in the 3 Baffle configuration

Measurement position	500 Hz	1 kHz	2 kHz	4 kHz
1	1,9	2,1	1,8	1,4
2	2,0	2,1	1,9	1,5
3	1,8	2,0	1,8	1,5
4	1,9	2,0	1,9	1,5
5	1,9	2,0	1,9	1,5
6	1,9	2,0	1,9	1,5
7	1,9	2,1	1,9	1,5
8	1,9	2,0	1,9	1,5
9	1,9	2,0	1,9	1,5
10	2,0	2,0	1,9	1,5
11	1,9	2,0	1,9	1,5
12	1,8	2,0	1,8	1,5
13	1,9	2,0	1,9	1,5
14	2,0	2,0	1,9	1,5
15	1,9	2,1	1,9	1,5
16	2,0	2,0	1,8	1,5
17	1,8	2,0	1,8	1,5

Table C.2.10 T20 for the small box measurement in the 4 Baffle configuration

Measurement position	500 Hz	1 kHz	2 kHz	4 kHz
1	1,7	1,9	1,6	1,3
2	1,7	1,8	1,7	1,3
3	1,7	1,7	1,6	1,4
4	1,7	1,7	1,7	1,4
5	1,6	1,8	1,6	1,4
6	1,6	1,8	1,6	1,4
7	1,6	1,8	1,6	1,4
8	1,7	1,8	1,6	1,4
9	1,7	1,8	1,6	1,3
10	1,7	1,8	1,6	1,4
11	1,8	1,8	1,6	1,4
12	1,6	1,8	1,7	1,4
13	1,7	1,9	1,6	1,4
14	1,8	1,8	1,6	1,4
15	1,7	1,9	1,7	1,4
16	1,7	1,8	1,7	1,4
17	1,6	1,8	1,7	1,4

C.3 Reverberation time (T_{30})

Table C.5.1 T30 for the big box measurement in the 0 Baffle configuration

Measurement position	500 Hz	1 kHz	2 kHz	4 kHz
1	4,4	4,2	3,6	2,4
2	4,4	4,3	3,6	2,4
3	4,4	4,2	3,6	2,3
4	4,4	4,2	3,7	2,4
5	4,3	4,2	3,6	2,4
6	4,4	4,3	3,7	2,4
7	4,4	4,2	3,7	2,5
8	4,4	4,3	3,7	2,5
9	4,4	4,3	3,7	2,5
10	4,4	4,3	3,7	2,4
11	4,3	4,2	3,7	2,5
12	4,5	4,2	3,7	2,5
13	4,3	4,2	3,7	2,5
14	4,4	4,3	3,7	2,5
15	4,4	4,3	3,7	2,5
16	4,3	4,2	3,7	2,5

Table C.5.2 T30 for the big box measurement in the 1 Baffle configuration

Measurement position	500 Hz	1 kHz	2 kHz	4 kHz
1	3,1	3,1	2,8	2,0
2	3,1	3,0	2,7	2,0
3	3,1	3,1	2,8	2,0
4	3,0	3,0	2,7	2,0
5	3,0	3,1	2,8	2,0
6	3,1	3,1	2,9	2,0
7	3,2	3,1	2,7	2,0
8	3,1	3,1	2,8	2,0
9	3,1	3,1	2,8	2,0
10	3,1	3,1	2,8	2,0
11	3,1	3,1	2,7	2,0
12	3,2	3,1	2,8	2,0
13	3,1	3,1	2,8	2,0
14	3,1	3,2	2,8	2,0
15	3,1	3,1	2,7	2,0
16	3,2	3,1	2,8	2,0

Table C.3.3 T30 for the big box measurement in the 2 Baffle configuration

Measurement position	500 Hz	1 kHz	2 kHz	4 kHz
1	3,2	3,1	2,8	2,0
2	3,2	3,1	2,8	2,0
3	2,4	2,5	2,3	1,7
4	2,4	2,5	2,3	1,7
5	2,4	2,5	2,3	1,7
6	2,3	2,5	2,3	1,8
7	2,3	2,5	2,3	1,7
8	2,4	2,5	2,3	1,7
9	2,4	2,5	2,2	1,7
10	2,5	2,5	2,3	1,8
11	2,4	2,5	2,3	1,8
12	2,4	2,5	2,3	1,8
13	2,4	2,6	2,3	1,8
14	2,4	2,5	2,3	1,7
15	2,4	2,5	2,3	1,8
16	2,4	2,5	2,3	1,8

Table C.3.4 T30 for the big box measurement in the 3 Baffle configuration

Measurement position	500 Hz	1 kHz	2 kHz	4 kHz
1	2,0	2,1	2,0	1,5
2	2,1	2,1	2,0	1,6
3	2,1	2,1	2,0	1,5
4	2,0	2,1	2,0	1,5
5	2,0	2,2	2,0	1,6
6	2,1	2,1	2,0	1,5
7	2,0	2,2	2,0	1,6
8	2,1	2,2	2,0	1,6
9	2,1	2,1	2,0	1,6
10	2,1	2,1	2,0	1,6
11	2,1	2,2	2,0	1,6
12	2,1	2,2	2,0	1,6
13	2,1	2,2	2,0	1,6
14	2,1	2,2	2,1	1,6
15	2,2	2,2	2,0	1,6
16	2,1	2,2	2,0	1,5

Appendix C Measurement results

Table C.3.5 T30 for the big box measurement in the 4 Baffle configuration

Measurement position	500 Hz	1 kHz	2 kHz	4 kHz
1	1,8	1,8	1,7	1,4
2	1,7	1,7	1,7	1,4
3	1,7	1,8	1,7	1,3
4	1,7	1,8	1,7	1,4
5	1,6	1,8	1,7	1,4
6	1,7	1,8	1,7	1,4
7	1,7	1,8	1,7	1,4
8	1,7	1,8	1,7	1,4
9	1,8	1,8	1,7	1,4
10	1,8	1,8	1,7	1,4
11	1,8	1,8	1,7	1,4
12	1,7	1,8	1,7	1,4
13	1,7	1,8	1,7	1,4
14	1,8	1,8	1,7	1,4
15	1,8	1,8	1,7	1,4
16	1,7	1,8	1,7	1,4

Table C.3.6 T30 for the small box measurement in the 0 Baffle configuration

Measurement position	500 Hz	1 kHz	2 kHz	4 kHz
1	4,4	4,2	3,5	2,4
2	4,4	4,1	3,5	2,4
3	4,4	4,2	3,5	2,4
4	4,3	4,2	3,5	2,4
5	4,3	4,1	3,5	2,4
6	4,3	4,2	3,5	2,5
7	4,3	4,2	3,5	2,4
8	4,3	4,2	3,5	2,4
9	4,3	4,2	3,5	2,5
10	4,3	4,3	3,6	2,5
11	4,3	4,2	3,6	2,5
12	4,3	4,2	3,5	2,5
13	4,4	4,2	3,6	2,5
14	4,3	4,2	3,6	2,5
15	4,4	4,2	3,5	2,5
16	4,3	4,3	3,6	2,5
17	4,3	4,2	3,5	2,5

Table C.3.7 T30 for the small box measurement in the 1 Baffle configuration

Measurement position	500 Hz	1 kHz	2 kHz	4 kHz
1	3,1	3,1	2,6	2,0
2	3,1	3,1	2,7	2,0
3	3,1	3,0	2,7	2,0
4	3,0	3,1	2,7	2,0
5	3,0	3,0	2,7	2,0
6	3,0	3,1	2,7	2,0
7	3,1	3,1	2,7	2,0
8	3,2	3,1	2,7	2,1
9	3,1	3,1	2,7	2,0
10	3,1	3,0	2,7	2,0
11	3,1	3,0	2,8	2,0
12	3,1	3,1	2,7	2,1
13	3,2	3,0	2,7	2,0
14	3,0	3,1	2,7	2,0
15	3,1	3,2	2,7	2,1
16	3,2	3,1	2,8	2,1
17	3,2	3,1	2,7	2,1

Table C.3.8 T30 for the small box measurement in the 2 Baffle configuration

Measurement position	500 Hz	1 kHz	2 kHz	4 kHz
1	2,4	2,5	2,2	1,7
2	2,4	2,4	2,2	1,7
3	2,4	2,4	2,2	1,7
4	2,4	2,5	2,2	1,7
5	2,4	2,4	2,2	1,7
6	2,4	2,5	2,2	1,7
7	2,5	2,5	2,2	1,7
8	2,4	2,5	2,3	1,8
9	2,5	2,5	2,3	1,8
10	2,5	2,5	2,3	1,8
11	2,4	2,5	2,3	1,8
12	2,3	2,5	2,3	1,8
13	2,4	2,5	2,3	1,8
14	2,4	2,5	2,3	1,7
15	2,4	2,5	2,3	1,8
16	2,4	2,5	2,3	1,7
17	2,4	2,5	2,3	1,8

Table C.3.9 T30 for the small box measurement in the 3 Baffle configuration

Measurement position	500 Hz	1 kHz	2 kHz	4 kHz
1	2,0	2,1	1,9	1,5
2	2,0	2,0	1,9	1,5
3	1,9	2,0	1,9	1,5
4	1,9	2,0	1,8	1,5
5	1,9	2,0	1,9	1,5
6	1,9	2,0	1,9	1,5
7	2,0	2,1	1,9	1,5
8	1,9	2,0	1,9	1,5
9	2,0	2,0	1,9	1,5
10	2,0	2,0	1,9	1,5
11	1,9	2,0	1,9	1,5
12	1,9	2,1	1,9	1,6
13	1,9	2,0	1,9	1,5
14	2,0	2,1	1,9	1,5
15	1,9	2,1	1,9	1,5
16	2,0	2,0	1,9	1,5
17	1,9	2,0	1,9	1,5

Table C.3.10 T30 for the small box measurement in the 4 Baffle configuration

Measurement position	500 Hz	1 kHz	2 kHz	4 kHz
1	1,7	1,9	1,7	1,4
2	1,7	1,9	1,7	1,4
3	1,7	1,8	1,6	1,4
4	1,7	1,7	1,7	1,4
5	1,6	1,8	1,7	1,4
6	1,6	1,8	1,7	1,4
7	1,7	1,8	1,7	1,4
8	1,7	1,8	1,7	1,4
9	1,7	1,8	1,7	1,4
10	1,7	1,8	1,7	1,4
11	1,8	1,8	1,6	1,4
12	1,7	1,8	1,7	1,4
13	1,7	1,8	1,7	1,4
14	1,7	1,8	1,7	1,4
15	1,7	1,8	1,7	1,4
16	1,7	1,8	1,7	1,4
17	1,7	1,8	1,7	1,4

C.4 Initial drop (ID)

Table C.4.1 ID for the big box measurement in the 0 Baffle configuration

Measurement position	500 Hz	1 kHz	2 kHz	4 kHz
1	-10,2	-9,3	-9,3	-14,4
2	-5,4	-6,5	-6,3	-11,7
3	-4,1	-4,7	-4,4	-9,0
4	-3,0	-3,4	-3,2	-7,5
5	-2,2	-2,8	-2,3	-6,2
6	-1,7	-2,3	-2,0	-5,4
7	-1,2	-1,5	-1,2	-4,1
8	-0,7	-1,1	-0,9	-3,1
9	-0,6	-0,8	-0,7	-2,3
10	-0,4	-0,6	-0,6	-1,9
11	-0,3	-0,5	-0,5	-1,5
12	-0,3	-0,5	-0,5	-1,3
13	-0,3	-0,3	-0,5	-1,0
14	-0,3	-0,2	-0,4	-0,9
15	-0,2	-0,2	-0,4	-0,8
16	-0,1	-0,1	-0,4	-0,6

Table C.4.2 ID for the big box measurement in the 1 Baffle configuration

Measurement position	500 Hz	1 kHz	2 kHz	4 kHz
1	-11,0	-10,0	-10,2	-15,1
2	-8,9	-7,4	-7,3	-12,3
3	-5,1	-5,4	-5,2	-10,0
4	-3,7	-4,1	-3,8	-8,3
5	-2,6	-3,4	-2,8	-6,9
6	-2,2	-2,9	-2,6	-6,2
7	-1,7	-1,9	-1,4	-4,5
8	-1,0	-1,5	-1,2	-3,7
9	-0,8	-1,0	-0,9	-2,7
10	-0,6	-0,8	-0,7	-2,2
11	-0,4	-0,7	-0,6	-1,6
12	-0,4	-0,6	-0,6	-1,5
13	-0,4	-0,3	-0,6	-1,2
14	-0,4	-0,3	-0,5	-1,1
15	-0,2	-0,3	-0,5	-1,1
16	-0,2	-0,2	-0,4	-0,3

Table C.4.3 ID for the big box measurement in the 2 Baffle configuration

Measurement position	500 Hz	1 kHz	2 kHz	4 kHz
1	-8,8	-10,5	-11,1	-15,9
2	-9,8	-7,9	-7,9	-13,0
3	-5,3	-5,8	-5,5	-10,2
4	-4,4	-4,7	-4,2	-8,7
5	-3,2	-4,0	-3,2	-7,3
6	-2,7	-3,1	-2,7	-6,5
7	-2,2	-2,2	-1,7	-4,9
8	-1,2	-1,8	-1,3	-3,9
9	-1,0	-1,2	-1,0	-2,9
10	-0,7	-1,0	-0,8	-2,4
11	-0,6	-0,9	-0,8	-2,0
12	-0,5	-0,7	-0,7	-1,7
13	-0,5	-0,4	-0,7	-1,4
14	-0,5	-0,4	-0,6	-1,1
15	-0,3	-0,3	-0,5	-1,1
16	-0,1	-0,2	-0,3	-0,7

Table C.4.4 ID for the big box measurement in the 3 Baffle configuration

Measurement position	500 Hz	1 kHz	2 kHz	4 kHz
1	-11,8	-11,4	-11,5	-16,3
2	-10,0	-8,6	-8,5	-13,4
3	-6,4	-6,5	-6,5	-11,2
4	-5,0	-5,2	-4,9	-9,0
5	-3,6	-4,2	-3,4	-7,6
6	-3,1	-3,4	-3,0	-6,9
7	-2,4	-2,4	-2,0	-5,3
8	-1,4	-2,1	-1,5	-4,2
9	-1,1	-1,4	-1,2	-3,3
10	-0,9	-1,2	-1,0	-2,6
11	-0,7	-1,1	-0,8	-2,1
12	-0,6	-0,8	-0,8	-1,8
13	-0,6	-0,5	-0,8	-1,6
14	-0,6	-0,5	-0,6	-1,4
15	-0,4	-0,4	-0,7	-1,2
16	-0,1	-0,2	-0,2	-0,8

Table C.4.5 ID for the big box measurement in the 4 Baffle configuration

Measurement position	500 Hz	1 kHz	2 kHz	4 kHz
1	-12,1	-12,2	-12,0	-16,4
2	-10,3	-9,0	-9,0	-13,5
3	-6,6	-6,9	-6,7	-11,2
4	-5,2	-5,7	-5,2	-9,3
5	-4,0	-4,8	-3,8	-8,1
6	-3,5	-3,8	-3,4	-7,4
7	-2,6	-2,7	-2,2	-5,6
8	-1,6	-2,2	-1,7	-4,5
9	-1,3	-1,7	-1,4	-3,6
10	-1,0	-1,3	-1,1	-2,8
11	-0,9	-1,2	-1,0	-2,4
12	-0,7	-1,0	-0,9	-2,0
13	-0,7	-0,5	-0,8	-1,7
14	-0,8	-0,5	-0,7	-1,5
15	-0,4	-0,4	-0,8	-1,5
16	-0,1	-0,2	-0,4	-0,7

Table C.4.6 ID for the small box measurement in the 0 Baffle configuration

Measurement position	500 Hz	1 kHz	2 kHz	4 kHz
1	-8,2	-10,7	-12,5	-15,9
2	-7,0	-7,9	-10,8	-13,2
3	-6,3	-5,9	-8,5	-10,4
4	-3,6	-3,2	-6,0	-7,7
5	-2,4	-2,3	-4,3	-6,1
6	-1,9	-1,7	-3,2	-4,8
7	-1,4	-1,4	-2,7	-4,0
8	-1,0	-0,9	-1,8	-2,8
9	-1,0	-0,9	-1,8	-2,8
10	-0,6	-0,6	-1,3	-2,0
11	-0,4	-0,5	-1,0	-1,5
12	-0,3	-0,3	-0,7	-1,0
13	-0,3	-0,3	-0,6	-0,8
14	-0,3	-0,1	-0,5	-0,7
15	-0,3	-0,2	-0,4	-0,8
16	-0,2	-0,2	-0,4	-0,7
17	-0,1	-0,1	-0,3	-0,3

Appendix C Measurement results

Table C.4.7 ID for the small box measurement in the 1 Baffle configuration

Measurement position	500 Hz	1 kHz	2 kHz	4 kHz
1	-9,5	-11,9	-13,7	-17,0
2	-7,9	-9,1	-12,1	-14,3
3	-7,4	-6,6	-9,2	-11,2
4	-5,4	-3,9	-6,6	-8,3
5	-3,1	-2,8	-5,0	-6,7
6	-2,5	-2,3	-3,9	-5,4
7	-2,1	-1,8	-3,3	-4,4
8	-1,4	-1,1	-2,1	-3,2
9	-0,8	-0,9	-1,6	-2,2
10	-0,6	-0,6	-1,3	-1,7
11	-0,5	-0,5	-1,0	-1,4
12	-0,4	-0,4	-0,8	-1,2
13	-0,4	-0,4	-0,7	-1,0
14	-0,3	-0,2	-0,6	-0,9
15	-0,5	-0,2	-0,7	-0,8
16	-0,3	-0,2	-0,4	-0,7
17	-0,1	-0,2	-0,5	-0,2

Table C.4.8 ID for the small box measurement in the 2 Baffle configuration

Measurement position	500 Hz	1 kHz	2 kHz	4 kHz
1	-10,2	-12,6	-14,0	-17,2
2	-8,6	-9,4	-12,2	-14,3
3	-7,1	-6,7	-9,9	-11,6
4	-5,7	-4,5	-7,2	-8,8
5	-3,8	-3,1	-5,6	-7,1
6	-3,4	-2,6	-4,3	-5,7
7	-2,4	-2,0	-3,5	-4,5
8	-1,7	-1,3	-2,4	-3,4
9	-1,0	-1,0	-1,9	-2,4
10	-0,8	-0,7	-1,6	-1,9
11	-0,7	-0,6	-1,2	-1,6
12	-0,6	-0,5	-0,9	-1,3
13	-0,5	-0,4	-0,8	-1,1
14	-0,4	-0,3	-0,7	-0,9
15	-0,6	-0,2	-0,8	-0,8
16	-0,4	-0,2	-0,5	-1,0
17	-0,2	-0,2	-0,3	-0,3

Table C.4.9 ID for the small box measurement in the 3 Baffle configuration

Measurement position	500 Hz	1 kHz	2 kHz	4 kHz
1	-11,1	-14,1	-14,7	-17,7
2	-0,6	-0,8	-0,3	-0,4
3	-7,4	-7,7	-10,3	-12,3
4	-6,5	-4,7	-7,6	-9,0
5	-4,6	-3,8	-6,1	-7,3
6	-3,6	-3,2	-4,7	-6,2
7	-3,0	-2,5	-4,1	-5,1
8	-2,0	-1,5	-2,5	-3,7
9	-1,2	-1,2	-2,0	-2,7
10	-0,9	-0,9	-1,5	-2,1
11	-0,8	-0,7	-1,3	-1,7
12	-0,7	-0,6	-1,1	-1,5
13	-0,5	-0,6	-0,9	-1,3
14	-0,5	-0,3	-0,8	-1,1
15	-0,7	-0,3	-0,9	-0,9
16	-0,5	-0,3	-0,6	-1,0
17	-0,1	-0,2	-0,3	-0,3

Table C.4.10 ID for the small box measurement in the 4 Baffle configuration

Measurement position	500 Hz	1 kHz	2 kHz	4 kHz
1	-11,2	-14,0	-15,3	-18,0
2	-9,6	-11,0	-13,6	-15,3
3	-8,8	-8,4	-10,9	-12,4
4	-6,3	-5,1	-8,1	-9,4
5	-4,9	-4,0	-6,3	-7,9
6	-3,9	-3,3	-5,0	-6,6
7	-3,4	-2,5	-4,3	-5,4
8	-2,3	-1,7	-2,9	-4,0
9	-1,4	-1,3	-2,1	-2,8
10	-1,0	-1,0	-1,8	-2,3
11	-0,9	-0,8	-1,5	-1,9
12	-0,8	-0,8	-1,2	-1,7
13	-0,6	-0,6	-1,1	-1,4
14	-0,6	-0,3	-0,9	-1,2
15	-0,9	-0,4	-0,9	-1,1
16	-0,5	-0,3	-0,7	-1,1
17	-0,2	-0,2	-0,2	-0,3

C.5 Clarity (C$_{80}$)

Table C.5.1 C80 for the big box measurement in the 0 Baffle configuration

Measurement position	500 Hz	1 kHz	2 kHz	4 kHz
1	7,3	9,4	10,2	16,0
2	5,7	7,1	7,0	13,4
3	3,6	4,6	4,7	10,6
4	1,7	2,9	2,7	8,8
5	0,8	1,8	1,4	7,3
6	0,0	1,0	0,9	6,2
7	-1,9	-0,5	-0,9	4,4
8	-3,2	-1,3	-1,6	3,1
9	-3,7	-2,5	-2,4	2,0
10	-5,0	-3,3	-3,0	1,3
11	-5,2	-3,8	-2,7	1,3
12	-3,6	-2,7	-2,4	0,7
13	-3,7	-4,1	-2,8	-0,4
14	-5,2	-5,8	-2,7	-0,3
15	-4,6	-4,3	-3,5	-0,7
16	-5,6	-5,7	-3,6	-1,7

Table C.5.2 C80 for the big box measurement in the 1 Baffle configuration

Measurement position	500 Hz	1 kHz	2 kHz	4 kHz
1	8,9	10,7	11,5	17,1
2	7,4	8,6	8,5	14,4
3	5,3	6,1	6,2	12,0
4	3,2	4,5	4,1	10,0
5	2,2	3,3	2,8	8,7
6	1,7	2,8	2,4	7,8
7	0,1	1,1	0,5	5,5
8	-1,4	0,5	-0,2	4,2
9	-1,8	-0,7	-1,0	3,3
10	-3,2	-2,2	-1,3	2,4
11	-3,4	-2,3	-1,4	2,2
12	-2,1	-1,4	-1,4	1,7
13	-2,0	-2,4	-1,3	0,8
14	-3,3	-4,1	-1,4	0,8
15	-2,6	-2,7	-2,1	0,4
16	-3,0	-3,7	-3,4	-1,6

Table C.5.3 C80 for the big box measurement in the 2 Baffle configuration

Measurement position	500 Hz	1 kHz	2 kHz	4 kHz
1	10,5	12,2	12,8	18,3
2	8,8	9,6	9,5	15,5
3	6,5	7,2	7,0	12,6
4	4,6	5,8	5,2	11,0
5	3,8	4,6	3,9	9,5
6	3,4	3,6	3,0	8,2
7	1,8	2,4	1,6	6,3
8	0,2	1,8	1,0	4,8
9	-0,4	0,3	-0,1	3,9
10	-1,8	-1,1	-0,4	3,2
11	-2,0	-1,0	-0,2	2,9
12	-0,8	-0,4	-0,5	2,4
13	-0,6	-1,2	-0,6	1,3
14	-2,2	-3,1	-0,5	1,2
15	-1,4	-1,5	-1,4	1,2
16	-2,9	-3,2	-1,7	-0,3

Table C.5.4 C80 for the big box measurement in the 3 Baffle configuration

Measurement position	500 Hz	1 kHz	2 kHz	4 kHz
1	11,1	12,9	13,4	18,8
2	9,5	10,7	10,4	16,3
3	7,9	8,5	8,2	13,7
4	5,9	7,2	6,1	11,5
5	4,9	5,5	4,5	10,1
6	4,3	4,5	4,0	8,9
7	2,5	3,2	2,9	7,4
8	1,0	2,8	1,8	5,7
9	0,5	1,2	0,9	5,1
10	-0,9	-0,3	0,6	3,9
11	-0,7	-0,3	0,3	3,8
12	0,3	0,6	0,2	3,3
13	0,3	-0,5	0,3	2,1
14	-0,9	-2,3	0,4	2,5
15	-0,8	-0,6	-0,5	1,6
16	-2,4	-2,4	-1,3	0,6

Table C.5.5 C80 for the big box measurement in the 4 Baffle configuration

Measurement position	500 Hz	1 kHz	2 kHz	4 kHz
1	12,0	13,9	14,2	19,6
2	10,3	11,5	11,3	16,8
3	8,4	9,2	9,1	14,3
4	6,3	8,1	7,0	12,2
5	5,5	6,7	5,6	10,9
6	5,1	5,7	5,0	10,0
7	3,3	4,0	3,5	8,1
8	2,1	3,4	2,3	6,5
9	1,7	2,3	1,9	5,8
10	0,1	0,4	1,4	4,6
11	-0,3	0,7	1,6	4,3
12	1,6	1,4	1,1	3,9
13	1,5	0,3	1,2	2,6
14	0,1	-1,2	1,2	2,9
15	-0,4	0,2	0,4	2,4
16	-1,1	-1,3	-0,7	1,4

Table C.5.6 C80 for the small box measurement in the 0 Baffle configuration

Measurement position	500 Hz	1 kHz	2 kHz	4 kHz
1	8,7	11,6	13,8	17,9
2	6,6	8,4	11,6	15,1
3	4,7	6,0	9,1	11,9
4	2,5	3,1	6,4	9,0
5	0,8	1,1	3,9	7,1
6	-0,2	0,0	2,8	5,4
7	-0,9	-0,8	1,7	4,0
8	-2,4	-2,3	0,2	2,5
9	-2,4	-2,3	0,2	2,5
10	-3,4	-2,5	-0,8	1,5
11	-3,5	-3,9	-1,8	0,5
12	-5,7	-4,4	-1,9	-0,1
13	-3,7	-3,4	-2,0	-0,8
14	-3,9	-4,6	-2,7	-0,7
15	-5,3	-5,6	-1,9	-0,3
16	-4,1	-5,1	-2,9	-0,9
17	-5,2	-6,0	-4,2	-2,4

Table C.5.7 C80 for the small box measurement in the 1 Baffle configuration

Measurement position	500 Hz	1 kHz	2 kHz	4 kHz
1	10,7	13,3	15,5	19,4
2	8,7	10,4	13,5	16,6
3	6,6	7,5	10,3	12,9
4	4,4	4,6	7,6	10,1
5	2,5	2,6	5,6	8,0
6	1,7	1,8	4,3	6,6
7	1,1	1,2	3,2	5,4
8	-0,3	-0,4	1,8	4,1
9	-1,7	-0,6	0,9	2,5
10	-2,0	-2,2	-0,4	1,7
11	-3,5	-3,2	-0,7	0,9
12	-4,0	-2,8	-0,3	1,1
13	-2,1	-2,1	-0,7	1,0
14	-2,3	-3,2	-1,8	0,1
15	-3,6	-4,7	-1,2	-0,3
16	-2,3	-3,0	-2,1	-0,1
17	-3,8	-4,5	-2,3	-0,5

Table C.5.8 C80 for the small box measurement in the 2 Baffle configuration

Measurement position	500 Hz	1 kHz	2 kHz	4 kHz
1	11,8	14,3	16,1	19,9
2	9,6	10,7	13,7	16,7
3	7,9	8,6	11,1	13,8
4	6,2	6,1	8,6	11,1
5	4,3	3,9	6,6	8,6
6	3,3	2,9	5,2	7,2
7	2,8	2,1	4,2	6,1
8	1,2	0,5	2,9	4,5
9	-0,5	0,2	1,7	3,4
10	-0,8	-1,0	0,8	2,5
11	-1,6	-1,5	-0,1	1,6
12	-2,2	-1,4	0,7	1,8
13	-0,7	-0,9	0,2	1,4
14	-0,9	-2,0	-1,1	0,8
15	-2,3	-3,7	-0,3	0,2
16	-1,1	-1,9	-1,1	0,5
17	-2,6	-3,6	-1,7	0,2

Appendix C Measurement results

Table C.5.9 C80 for the small box measurement in the 3 Baffle configuration

Measurement position	500 Hz	1 kHz	2 kHz	4 kHz
1	12,8	15,6	17,1	21,0
2	-2,5	-1,5	-1,0	0,8
3	9,2	9,7	12,0	14,8
4	7,2	7,0	9,5	11,6
5	5,5	5,3	7,6	9,9
6	4,2	4,1	6,3	8,1
7	3,7	3,5	5,2	7,1
8	2,0	1,9	3,9	5,5
9	0,5	1,2	2,8	4,1
10	0,8	-0,2	1,3	3,5
11	-1,1	-1,0	0,9	2,5
12	-1,2	-0,6	1,5	2,7
13	0,0	-0,1	1,0	2,7
14	0,0	-1,0	-0,1	1,3
15	-0,8	-2,7	0,6	1,4
16	0,0	-1,0	-0,2	1,2
17	-1,9	-2,9	-0,9	1,2

Table C.5.10 C80 for the small box measurement in the 4 Baffle configuration

Measurement position	500 Hz	1 kHz	2 kHz	4 kHz
1	13,5	16,8	18,1	21,3
2	11,4	13,5	15,7	18,4
3	9,5	10,7	12,9	15,1
4	7,2	7,5	10,2	12,3
5	5,7	6,0	8,1	10,3
6	4,8	4,7	7,1	8,9
7	4,4	3,9	5,8	7,7
8	3,1	2,4	4,3	5,9
9	1,9	1,8	3,2	4,7
10	1,6	0,7	2,2	4,2
11	-0,1	-0,4	1,8	3,3
12	-0,9	-0,2	2,0	3,3
13	1,5	0,7	1,8	3,4
14	1,3	-0,6	0,9	1,4
15	0,2	-1,5	1,5	2,4
16	0,4	-0,3	0,4	1,6
17	-1,4	-1,6	-0,5	1,4

C.6 Centre time (T_S)

Table C.6.1 TS for the big box measurement in the 0 Baffle configuration

Measurement position	500 Hz	1 kHz	2 kHz	4 kHz
1	66,9	40,8	30,8	7,0
2	87,5	68,1	56,7	12,7
3	121,2	105,0	88,7	22,9
4	166,0	140,3	119,9	32,9
5	192,8	165,4	143,8	42,3
6	211,5	182,7	156,6	52,2
7	247,8	207,8	185,7	72,5
8	264,4	238,8	202,8	92,0
9	282,7	252,5	218,2	105,6
10	296,8	269,8	233,8	115,2
11	304,6	276,7	234,6	120,4
12	277,5	265,8	221,3	129,8
13	283,1	279,8	225,3	139,2
14	313,5	309,2	233,6	138,1
15	290,4	289,2	241,2	144,2
16	285,0	309,4	245,6	160,5

Table C.6.2 TS for the big box measurement in the 1 Baffle configuration

Measurement position	500 Hz	1 kHz	2 kHz	4 kHz
1	38,3	26,0	19,7	5,1
2	49,2	40,6	36,9	9,1
3	71,7	63,4	58,3	15,3
4	105,0	87,2	82,2	23,3
5	127,0	105,7	98,8	30,0
6	138,2	115,6	107,2	35,3
7	159,8	137,2	137,5	54,3
8	184,4	158,9	149,9	69,1
9	197,0	171,7	160,0	81,2
10	210,3	196,3	172,5	90,2
11	215,8	196,8	173,9	96,0
12	196,1	188,7	168,8	104,0
13	198,3	196,7	169,8	112,8
14	219,6	220,8	178,0	112,4
15	198,7	206,0	180,5	116,9
16	190,8	226,0	198,4	143,5

Table C.6.3 TS for the big box measurement in the 2 Baffle configuration

Measurement position	500 Hz	1 kHz	2 kHz	4 kHz
1	24,1	16,9	13,6	3,8
2	32,2	29,1	27,0	7,0
3	49,4	46,6	44,9	13,0
4	72,2	63,2	61,3	18,4
5	87,6	76,1	76,5	24,7
6	96,1	87,9	87,8	31,3
7	115,8	103,3	110,5	43,9
8	134,0	118,4	119,3	57,3
9	147,5	138,3	133,9	69,2
10	156,8	152,7	140,0	77,8
11	168,9	152,0	140,2	81,6
12	152,5	149,1	138,9	88,5
13	150,0	161,2	142,4	97,5
14	172,3	183,0	145,9	100,5
15	156,2	165,8	154,1	100,7
16	164,0	183,5	156,6	124,7

Table C.6.4 TS for the big box measurement in the 3 Baffle configuration

Measurement position	500 Hz	1 kHz	2 kHz	4 kHz
1	20,1	13,7	11,1	3,3
2	26,9	21,9	20,6	5,7
3	37,1	33,5	32,8	9,7
4	53,5	46,2	48,2	15,0
5	70,1	61,4	63,8	20,8
6	77,3	71,2	72,1	25,8
7	96,8	83,0	86,6	34,8
8	115,5	96,3	99,1	48,4
9	118,9	117,8	112,8	55,6
10	130,5	129,3	116,8	66,2
11	141,0	130,5	121,0	70,3
12	130,2	123,0	120,1	76,6
13	128,6	135,2	121,5	85,7
14	142,7	158,1	124,0	81,6
15	135,4	142,8	130,0	91,0
16	146,7	161,6	140,2	108,2

Table C.6.5 TS for the big box measurement in the 4 Baffle configuration

Measurement position	500 Hz	1 kHz	2 kHz	4 kHz
1	15,8	10,4	8,8	2,9
2	21,5	17,5	16,7	5,1
3	30,9	27,5	26,2	8,4
4	45,5	36,5	38,6	13,1
5	56,2	45,8	48,9	16,8
6	62,4	56,2	57,3	20,1
7	80,3	67,5	72,7	29,7
8	92,0	79,4	85,7	40,5
9	94,2	95,1	93,1	48,0
10	108,0	107,0	99,7	57,8
11	121,6	108,2	100,4	61,4
12	105,6	102,6	103,0	67,0
13	106,1	114,0	102,6	76,1
14	119,5	132,3	107,2	74,2
15	114,6	120,5	109,7	79,5
16	123,8	134,5	122,0	96,8

Table C.6.6 TS for the small box measurement in the 0 Baffle configuration

Measurement position	500 Hz	1 kHz	2 kHz	4 kHz
1	50,9	27,9	14,4	4,9
2	75,1	48,4	22,7	8,8
3	100,8	81,7	37,8	17,2
4	135,6	131,4	64,7	31,3
5	176,8	178,2	94,6	45,6
6	208,1	200,1	115,7	60,3
7	230,3	222,4	134,8	75,2
8	261,9	241,2	163,2	95,3
9	262,3	241,5	164,4	95,1
10	265,9	255,7	184,9	115,7
11	271,9	271,7	191,1	127,5
12	311,1	286,4	210,0	135,0
13	280,1	273,1	213,8	147,9
14	283,1	289,0	219,5	151,5
15	307,9	315,1	212,8	143,0
16	276,8	294,4	222,5	150,9
17	279,8	304,8	247,2	169,9

Appendix C Measurement results

Table C.6.7 TS for the small box measurement in the 1 Baffle configuration

Measurement position	500 Hz	1 kHz	2 kHz	4 kHz
1	26,9	16,5	8,7	3,4
2	39,7	27,6	13,3	6,0
3	55,9	51,4	25,7	12,6
4	80,8	82,1	43,8	23,2
5	114,3	117,4	61,8	34,9
6	135,0	133,7	79,2	45,7
7	145,6	143,4	93,3	55,5
8	168,2	168,4	115,7	71,6
9	189,3	178,3	132,7	92,2
10	196,6	199,3	147,0	101,2
11	213,1	208,0	154,5	110,8
12	222,9	202,3	158,4	110,7
13	195,7	200,7	159,6	115,4
14	203,4	208,7	170,3	121,7
15	223,5	230,1	166,3	125,0
16	194,6	206,9	174,9	126,0
17	197,7	228,0	182,2	136,4

Table C.6.8 TS for the small box measurement in the 2 Baffle configuration

Measurement position	500 Hz	1 kHz	2 kHz	4 kHz
1	19,7	11,7	7,0	2,8
2	29,1	22,5	11,3	5,4
3	38,7	36,5	18,8	9,9
4	52,0	57,1	32,5	17,8
5	79,0	86,5	47,6	28,7
6	98,4	99,6	60,2	37,1
7	105,8	110,2	74,2	47,1
8	123,0	131,7	91,9	61,4
9	147,5	140,5	105,5	76,5
10	156,5	158,7	122,0	87,2
11	166,1	159,5	128,7	96,5
12	172,9	161,5	129,9	96,2
13	151,0	156,9	130,2	101,1
14	155,3	172,1	143,6	104,6
15	175,0	187,5	138,0	111,3
16	149,5	164,7	145,5	110,1
17	163,7	190,0	152,3	119,7

Table C.6.9 TS for the small box measurement in the 3 Baffle configuration

Measurement position	500 Hz	1 kHz	2 kHz	4 kHz
1	14,7	8,3	5,3	2,3
2	151,4	147,3	134,4	108,0
3	27,5	26,4	14,6	7,5
4	38,5	43,8	25,3	15,0
5	55,6	61,7	35,6	22,2
6	72,5	75,1	46,8	29,8
7	81,1	85,5	57,9	36,6
8	101,7	101,4	74,7	50,3
9	119,5	111,8	87,7	64,4
10	117,9	132,0	100,9	72,4
11	130,4	135,0	107,6	81,5
12	139,0	131,7	106,8	80,9
13	122,3	131,3	109,6	83,1
14	129,5	142,6	119,9	95,4
15	139,5	162,0	112,6	95,0
16	124,9	141,1	123,0	95,7
17	138,1	162,5	131,4	104,0

Table C.6.10 TS for the small box measurement in the 4 Baffle configuration

Measurement position	500 Hz	1 kHz	2 kHz	4 kHz
1	12,3	6,4	4,3	2,1
2	17,6	11,2	6,6	3,6
3	24,6	20,4	11,8	6,8
4	36,5	38,0	20,8	12,8
5	50,8	52,1	31,1	19,0
6	62,8	63,1	38,5	25,4
7	69,1	73,8	48,7	31,3
8	84,4	86,5	64,1	44,3
9	96,9	97,1	75,8	56,7
10	95,6	112,0	87,1	64,3
11	111,9	117,0	91,8	71,8
12	126,1	119,7	94,3	71,0
13	106,7	112,0	98,9	75,1
14	109,4	123,8	104,3	87,3
15	121,1	134,1	99,3	80,3
16	111,3	122,3	107,9	88,5
17	126,7	138,8	116,9	95,4

Over the last ten years, research performed on room in room acoustics has been done at the Eindhoven University of Technology. Room in room acoustics is the study of the effects of room acoustics on the intended (perceived) acoustics of reproduced sound. The effects occur most notably when a recording made in a reverberant environment is reproduced in a similar environment, the case where the playback environment is more reverberant is not taken into account. This follows after conclusions in the literature that a sound field can only be reproduced in a less reverberant environment.

The primary focus of earlier publications and reports is on effects the reproduction has on signals recorded under diffuse field conditions. Little is known when the recorded signal is measured with a certain amount of direct sound. The most notable literature conclusions are that the effects of room in room acoustics can be decreased with two methods. The first is decreasing the reverberation time in the listening room; the second is increasing the direct sound level in the listening room.

The study presented in this thesis aims to give insight on the combined effects of direct sound levels and diffuse sound fields in both recording room and listening room. Specifically, room acoustical parameter deviations were investigated. An analytical presentation of the impulse response is proposed to find these deviations. An extensive set of measurements was conducted to successfully validate the model (within bounds of its application). With this analytical impulse response, acoustical parameters and their deviations as a result of the room in room acoustics scenario are collected.

By convolving two room impulse responses a room in room impulse response is created. The two impulse responses used to create this response represent the recording and listening room. Contrary to the literature, measurements indicate that calculating reverberation time from the room in room impulse response can be done equally accurate as from a single room impulse response. This conclusion is reached after comparing the Curvature Parameter of room in room impulse responses with single room impulse responses.

Parameters calculated from the analytical model show that reproducing reverberation times within an accuracy of the just noticeable difference can be done when the reverberation time in the listening room is 1.2 times lower than that in the recording room. The Initial Drop in the room in room scenario was found to be an energetic subtraction of the initial drop in the recording and listening room. This drop can never be larger than the lower of the two involved initial drops. Because the direct sound level indicated by the Initial Drop is an energetic subtraction, reproduction within 1 dB accuracy is achieved when the Initial Drop in the listening room is at least 6 dB higher than in the recording room.

Furthermore, it is shown that reproduction of the Reverberation Time is primarily dependent on the ratio of the reverberation times in listening and recording rooms. For Clarity, the deviations are primarily depending on the difference of direct sound levels, with the little notion that for higher C_{80} the deviations are also higher. Centre time deviations are found to be depending on both the reverberation time ratio and difference of direct sound level.